POLINA SHPARTKO

ANALYTICAL AND NUMERICAL STUDY OF DRIFT-DIFFUSION MODELS FOR SPIN-TRANSPORT IN SEMICONDUCTORS

DISSERTATION

ANALYTICAL AND NUMERICAL STUDY OF DRIFT-DIFFUSION MODELS FOR SPIN-TRANSPORT IN SEMICONDUCTORS

Ausgeführt zum Zwecke der Erlangung des akademischen Grades einer Doktorin der technischen Wissenschaften unter der Leitung von

Univ.-Prof. Dr. Ansgar Jüngel
E101 - Institut für Analysis und Scientific Computing

eingereicht an der Technischen Universität Wien

Fakultät für Mathematik und Geoinformation

von
POLINA SHPARTKO
1326460
Wiedner Hauptstrasse 8, 1040 Wien

Wien, am

Polina Shpartko: *Analytical and numerical study of drift-diffusion models for spin-transport in semiconductors,* PhD thesis, © April 2016

ABSTRACT

The thesis is devoted to mathematical investigation of spin-transport in semiconductor material. The main object of the study is a spinorial matrix drift-diffusion model describing evolution of charge and spin densities. The model consists of parabolic balance equations for the densities incorporated with the Poisson equation for the electric potential. The system is fully coupled and nonlinear.

The work is composed of three parts. The first two parts consider analytical and numerical aspects of the model respectively. The key idea of the analysis is a usage of different reformulations: in spin-up and spin-down as well as parallel and perpendicular variables. The first part considers analysis of the model. We show that the system has a unique bounded solution. The proof of the global-in-time existence is based on the Leray-Schauder fixed-point theorem. Stampacchia and Moser techniques are used to prove the boundedness. Dissipation of the free energy is also shown.

The second part presents an implicit Euler finite-volume scheme for the model. The charge and spin fluxes are approximated by a Scharfetter-Gummel discretization. Existence of numerical solution is proven by means of the fixed-point theorem of Brouwer. It is shown that with a restriction on the time step the scheme features nonnegativity and boundedness of densities as well as the discrete free energy decay. As an illustration to the analysis numerical results for a diode in 1D and for a metal-semiconductor field-effect transistor (MESFET) in 2D are presented, some simple experiments on different variation of material properties (magnetic properties, doping) are performed.

The third part of the thesis considers the extension of the system to a spinorial energy-transport drift-diffusion model where along with the balance of charge and spin densities the balance of energy is considered. The derivation of the model is based on the spinorial matrix Boltzmann equation with energy conserving collision operator and exploits entropy maximization. The straightforward version of the model is implicit. To obtain an explicit formulation some simplifying assumptions are used. Numerical results are presented for the illustration.

CONTENTS

LIST OF FIGURES

LIST OF TABLES

KEYWORDS

Spinor drift-diffusion equations, semiconductors, spin transport, existence of bounded weak solutions, Stampacchia truncation, Moser iteration, finite volumes, energy dissipation, field-effect transistor, energy-transport equations, entropy inequalities.

Part I

INTRODUCTION

1 INTRODUCTION

1.1 SPIN IN SEMICONDUCTOR PHYSICS

According to quantum theory an electron additionally to its charge possesses an intrinsic angular momentum, or spin [33]. If there is a predetermined space direction the measurement of spin with respect to this direction gives one of two values. It is either $1/2$ or $-1/2$. In the first case one can name the electron "spin-up", or directed along the chosen axis, in the second – "spin-down", or opposite to the axis.

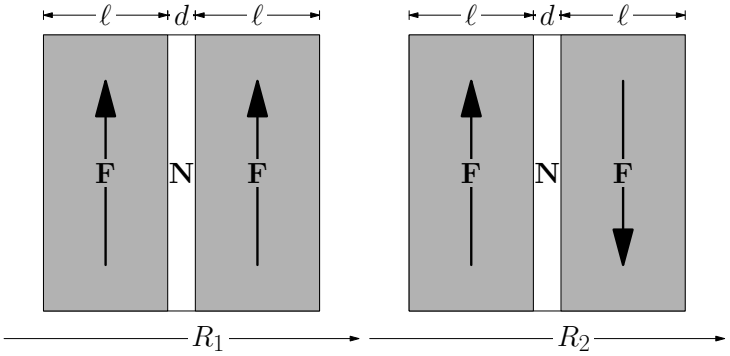

Figure 1: Giant magnetoresistance ($R_1 \ll R_2$) could be observed in the thin-layer structures when ferromagnetic layers (F) are separated by a nonmagnetic layer (N), preferably $d \ll \ell$.

The crucial discoveries involving the electron's spin degree of freedom were made in 1980s. That time the Giant Magnetoresistance (GMR) was first observed and it gave a strong impulse to development of spintronics, a research area studying spin and opportunities of its control and exploitation. The GMR effect takes place in the thin-layer-structures (see Figure 1). If two ferromagnetic layers are separated by a non-magnetic one and the magnetisation of ferromagnetic layers is parallel (spins of the electrons in both layers are parallel) the resistance of the structure can be much lower than when the magnetisation of the layers is antiparallel. Nowadays the GMR effect is widely and actively used in computer memory. Thanks to such a successful application in the last decades spintronics became a booming branch of microelectronics. Though the investigations of spintronics are not restricted only to GMR and ferromagnetic materials.

Semiconductor spintronics being widely investigated and highly promising still does not have any real application. The one of the most known possible semiconductor spin devices is a spin transistor. It has various modifications proposed but still lacks demonstrations in realistic physical conditions. One of the pioneering works on spin transistor was published in 1990 by S. Datta and B. Das [14]. They proposed a scheme of a spin field-effect transistor (SFET). The source and drain are made of ferromagnetic material, the first one plays a

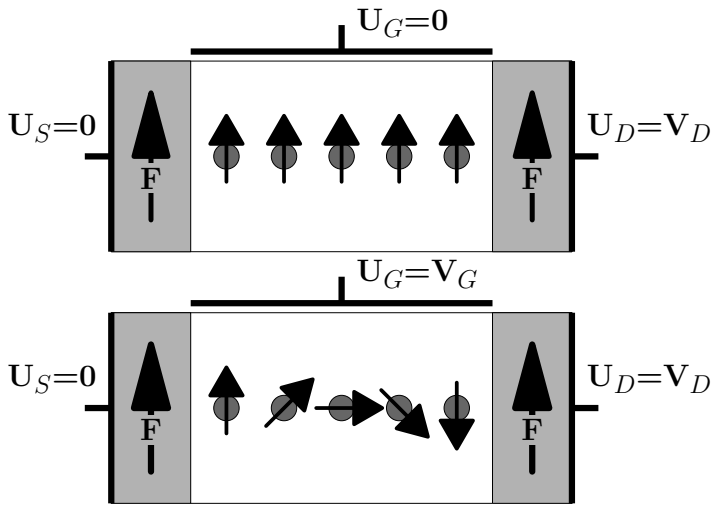

Figure 2: Principle of the spin transistor operation

role of a spin polarizer, when the second is a spin analyser. The channel between them should be a two-dimensional electron gas, which means that the electrons are free to move in two dimensions and confined in the third one. The work of the device is based on the spin orbit interaction of Bychov-Rashba type [16, 19]. Due to this effect, moving electrons confined in 2D and subjected to asymmetry of the potential experience an effective magnetic field which forces the spin of electrons to rotate (see Figure 2). The gate potential regulates the strength of the spin-orbit interaction and the respective rotation of the spin on the way of the electron from the polarizer to the analyser. If there is no potential applied to the gate the electrons do not change their spin and enter the analyser (open state). If the gate potential and the respective effective field are big enough to rotate the spin of polarized electrons by π the electrons will bounce from the analyser which will increase the resistance of the device (close state). This scheme was sensational when it was published. However, it does not take into account spin relaxation or the problem of effective spin polarization and other difficulties which one encounters trying to implement such a device [6, 9]. Later in 90s and 2000s more and more different modifications containing metallic and insulating regions or exploiting pure spin current were proposed [34, 43, 50]. Though, despite the fact that theoretically the spin transistor could be more effective than the classical one, practically there is still no real device implemented.

In the current work we consider the models which take into account only a part of all effects related to spin physics but even with this restricted case the mathematical problems behind becomes really complicated. Resolving this complicity helps to clarify some aspects of spin modelling in semiconductors.

1.2 THE CUTTING EDGE OF SPIN MODELLING

In the literature, several models have been proposed to describe the spin-polarized transport in semiconductor structures [19, 50]. Drift-

diffusion approximations are widely employed [35, 39, 49], since they do not require large computational resources but still describe the main transport phenomena. The existing drift-diffusion models can be classified into two main groups. The first group is given by two-component drift-diffusion equations for the spin-up and spin-down densities. Some versions of this model were rigorously derived from the spinor Boltzmann equation in the diffusion limit with strong spin-orbit coupling (compared to the mean-free path) in [23] and in [27]. Two-component models are well known in the physical community; see Formulas (II.39)-(II.40) in [19]. They are parabolic equations which are only weakly coupled through spin-flip interaction terms. The existence, uniqueness, and boundedness of weak solutions to such models (for spin-polarized electrons and holes) was proved by A. Glitzky in two space dimensions [25]. In three space dimensions, the well-posedness of the stationary system was shown in [23]. A quantum correction of Bohm potential type was derived in [7].

The second group consists of spin-vector drift-diffusion models in which the spin variable is a vector quantity. Combining the charge density with the spin-vector density, we can define the electron density matrix which solves a spinorial matrix drift-diffusion system. These models can be derived from the spinor Boltzmann equation by assuming a moderate spin-orbit coupling [27], [36]. Projecting the spin-vector density in the direction of the precession vector, we recover the two-component drift-diffusion system as a special case. In [27], the scattering rates are supposed to be scalar quantities. Assuming that the scattering rates are positive definite Hermitian matrices, a more general matrix drift-diffusion model was derived in [36]. We consider the system from [36] completed with the Poisson equation for potential. Because of the strong coupling of the model equations and the quadratic-type nonlinearity of the drift term, there are no analytical results available for spin-vector drift-diffusion systems like this. This thesis fills this lacuna.

In the second part we analyze an implicit Euler finite-volume approximation of the spinorial matrix drift-diffusion model and present some numerical simulations in two space dimensions. One of the features of the presented scheme is the simultaneous approximation of the diffusive and convective part of the fluxes by using a Scharfetter-Gummel discretization. These fluxes were introduced by Il'in [30] and Scharfetter and Gummel [40] for the classical drift-diffusion model (without spin coupling). The dissipativity with an implicit Euler discretization was shown in [21]. The discrete steady states were proved to be bounded [23]. Discrete entropy (free energy) estimates and/or the exponential decay of the free energy along trajectories towards the global equilibrium were investigated in [11, 26] but still without any spin coupling.

In the current work we consider magnetic field as a given function. We do not study the opportunity of incorporation of self-consistent magnetization in our system, though theoretically there could be some methods for that ([38, 46]). For example, in [38] the Landau-Lifshitz-Gilbert equation (LLG) was incorporated with the spin sta-

tionary drift-diffusion equation. A finite-element scheme for a spin-vector equation coupled to LLG (but with given electron current density) was analyzed in [5] and simulated in [4].

In the last part of the thesis we investigate the situation when hot electron thermalization has to be taken into account. Then the carrier transport needs to be described by higher-order moment equations including energy transport. This leads to semiclassical energy-transport equations in semiconductors, see, e.g., [1, 2, 12, 13, 32]. A spinorial energy-transport model was derived in [3], but the equations are not explicit and their structure is not easy to analyze. We present the derivation and the analysis of the explicit versions of this model.

1.3 THE MODEL EQUATIONS

The spin-vector model of [36], which is analyzed in this work, consists of the scaled drift-diffusion equation for the (Hermitian) electron density matrix $N \in \mathbb{C}^{2\times 2}$ and the current density matrix $J \in \mathbb{C}^{2\times 2}$,

$$\partial_t N + \operatorname{div} J + i\gamma[N, \vec{m}\cdot\vec{\sigma}] = \frac{1}{\tau}\left(\frac{1}{2}\operatorname{tr}(N)\sigma_0 - N\right), \tag{1}$$

$$J = -D_0 P^{-1/2}(\nabla N + N\nabla V)P^{-1/2} \quad \text{in } \Omega,\ t > 0, \tag{2}$$

where $[A, B] = AB - BA$ is the commutator of two matrices A and B and $\Omega \subset \mathbb{R}^2$ is a bounded domain. The scaled physical parameters are the strength of the effective magnetic field, $\gamma > 0$, the (normalized) direction of the precession vector $\vec{m} = (m_1, m_2, m_3) \in \mathbb{R}^3$, the spin-flip relaxation time $\tau > 0$, and the diffusion coefficient $D_0 > 0$. The precession vector plays the role of the local direction of the magnetization in the ferromagnet.

In the analytic part of this work, we assume for technical reasons that the precession vector $\vec{m}$ is constant. The triple $\vec{\sigma} = (\sigma_1, \sigma_2, \sigma_3)$ are the Pauli matrices and σ_0 is the unit matrix in $\mathbb{C}^{2\times 2}$:

$$\sigma_0 = \begin{pmatrix} 1 & 0 \\ 0 & 1 \end{pmatrix}, \quad \sigma_1 = \begin{pmatrix} 0 & 1 \\ 1 & 0 \end{pmatrix}, \quad \sigma_2 = \begin{pmatrix} 0 & -i \\ i & 0 \end{pmatrix}, \quad \sigma_3 = \begin{pmatrix} 1 & 0 \\ 0 & -1 \end{pmatrix},$$

where i is the imaginary unit. Furthermore, $\operatorname{tr}(N)$ denotes the trace of the matrix N and $P = \sigma_0 + p\vec{m}\cdot\vec{\sigma}$, where $p \in [0, 1)$ represents the spin polarization of the scattering rates. The product $\vec{m}\cdot\vec{\sigma}$ equals $m_1\sigma_1 + m_2\sigma_2 + m_3\sigma_3$. System (1)-(2) is solved in the bounded cylinder $\Omega \times [0, T) \subset \mathbb{R}^3 \times [0, \infty)$, supplemented with the boundary and initial conditions

$$N = \frac{1}{2}n_D\sigma_0 \quad \text{on } \partial\Omega,\ t > 0, \quad N(0) = N^0 \quad \text{in } \Omega. \tag{3}$$

The electric potential V is self-consistently given by the Poisson equation

$$-\lambda_D^2 \Delta V = \operatorname{tr}(N) - C(x) \quad \text{in } \Omega, \tag{4}$$

where $\lambda_D > 0$ is the scaled Debye length and $C(x) \geqslant 0$ denotes the doping profile in the n-doped semiconductor [32].

Equations (1)-(2) describe the time evolution of the density matrix of the electrons, coupling the charge and spin degrees of freedom. The coupling is linear in the polarization p of the scattering states. The commutator $[N, \vec{m} \cdot \vec{\sigma}]$ in (1) models the precession of the spin polarization on the macroscopic level. Furthermore, the right-hand side in (1) describes the relaxation of the spin density to an equilibrium density due to so-called spin-flip processes.

The above model was derived in [36] from a matrix Boltzmann equation involving the precession of the spin polarization in the diffusion limit. In this derivation, the scattering operator is assumed to consist of a (dominant) symmetric collision operator from the Stone model and a spin-flip operator with the relaxation time $\tau > 0$. Generally, D_0 is a diffusion matrix in $\mathbb{R}^{3\times 3}$. However, under the assumption that the scattering rate in the Stone model is smooth and invariant under isometric transformations, Proposition 1 in [37] shows that D_0 is a multiple of the identity matrix with a positive factor which is identified with the positive number D_0.

Remark 1. In the semiconductor literature (e.g. [32, 41]), the sign of the electric potential is opposite. We have chosen the above sign convention in order to be close to the notation of [36]. It does not affect the analytical results. □

Remark 2. Equations (1)-(2) are scaled using the time scale τ_s and the length scale L, where $L > 0$ is a typical length (e.g. the device size). In the numerical part, we choose τ_s to be equal to the physical spin-relaxation time τ^* such that $\tau = \tau^*/\tau_s = 1$. The density matrix and the doping profile are scaled by $\sup_\Omega C$, and $D_0 = D^*\tau_s/L^2$, $\gamma = \gamma^*\tau_s/\hbar$, where $D^* > 0$ is the physical diffusion coefficient, $\gamma^* > 0$ the physical strength of the effective magnetic field, and $\hbar$ the reduced Planck constant. The density matrix is scaled by $\sup_\Omega C$ and the electric potential by the thermal voltage $U_T = 0.026\,V$ (at room temperature). □

1.4 VARIOUS FORMULATIONS

The key idea of the continuous as well as the discrete analysis is to work with different transformations of the variables which make the diffusion matrix diagonal and thus reduce the level of coupling.

1.4.1 *Charge and spin-vector densities*

First of all, we investigate a scalar form of equations (1)-(2). For this, we develop N and J in the Pauli basis via $N = \frac{1}{2}n_0\sigma_0 + \vec{n} \cdot \vec{\sigma}$ and $J = \frac{1}{2}j_0\sigma_0 + \vec{j} \cdot \vec{\sigma}$, where n_0 is the electron charge density and $\vec{n}$ the spin-vector density. Setting $\vec{n} = (n_1, n_2, n_3)$ and $\vec{j} = (j_1, j_2, j_3)$ and

defining $\eta = \sqrt{1-p^2}$, system (1)-(2) can be written equivalently (see [36, Remark 1]) as

$$\partial_t n_0 + \operatorname{div} j_0 = 0, \tag{5}$$

$$\partial_t n_\ell + \operatorname{div} j_\ell - 2\gamma(\vec{n}\times\vec{m})_\ell = -\frac{n_\ell}{\tau}, \quad \ell = 1,2,3, \tag{6}$$

$$j_0 = \frac{D_0}{\eta^2}(J_0 - 2p\vec{J}\cdot\vec{m}), \tag{7}$$

$$j_\ell = \frac{D_0}{\eta^2}\left(\eta J_\ell + (1-\eta)(\vec{J}\cdot\vec{m})m_\ell - \frac{p}{2}J_0 m_\ell\right), \quad \ell = 1,2,3, \tag{8}$$

$$J_0 = -\nabla n_0 - n_0\nabla V, \tag{9}$$

$$\vec{J} = (J_1,J_2,J_3) = -\nabla\vec{n} - \vec{n}\nabla V \quad \text{in } \Omega,\ t>0. \tag{10}$$

Moreover, the Poisson equation (4) rewrites

$$-\lambda_D^2\Delta V = n_0 - C(x) \quad \text{in } \Omega. \tag{11}$$

System (5)-(11) is strongly coupled due to the cross-diffusion terms in (7)-(8) and nonlinear due to the Poisson coupling. Note that any solution $(n_0,\vec{n})$ to (5)-(10) defines a solution N to (1)-(2) and vice versa.

In the simplest physical configuration boundary and initial data could be given as follows

$$n_0 = n_D, \quad \vec{n} = 0 \quad \text{on } \partial\Omega,\ t>0, \quad n_0(0) = n_0^0, \quad \vec{n}(0) = \vec{n}^0 \quad \text{in } \Omega. \tag{12}$$

This configuration we use in the continuous analysis (Chapter 2).

In Chapter 3 devoted to numerical analysis we assume that the boundary $\partial\Omega = \Gamma^D \cup \Gamma^N$ consists of the union of contacts Γ^D and the isolating boundary part Γ^N. Then the boundary and initial data are given by

$$n_0 = n^D, \quad \vec{n} = 0, \quad V = V^D \quad \text{on } \Gamma^D,\ t>0, \tag{13}$$

$$\nabla n_0\cdot\nu = \nabla n_\ell\cdot\nu = \nabla V\cdot\nu = 0 \quad \text{on } \Gamma^N,\ t>0,\ \ell = 1,2,3, \tag{14}$$

$$n_0(0) = n_0^0, \quad \vec{n}(0) = \vec{n}^0 \quad \text{in } \Omega, \tag{15}$$

where ν is the exterior unit normal vector to $\partial\Omega$.

1.4.2 *Spin-up and spin-down densities*

The other transformation is defined by the spin-up and spin-down densities $n_\pm = \frac{1}{2}n_0 \pm \vec{n}\cdot\vec{m}$. Indeed, multiplying (6) by $\vec{m}$, some terms cancel, and combining the resulting expression with (5), we find that (n_+,n_-) solves

$$\partial_t n_+ + \operatorname{div}\left(D_0(1+p)(-\nabla n_+ - n_+\nabla V)\right) = -\frac{1}{2\tau}(n_+ - n_-), \tag{16}$$

$$\partial_t n_- + \operatorname{div}\left(D_0(1-p)(-\nabla n_- - n_-\nabla V)\right) = -\frac{1}{2\tau}(n_- - n_+) \tag{17}$$

and the boundary conditions (13), (14) imply

$$n_\pm = \frac{n^D}{2} \text{ on } \Gamma^D \quad \text{and} \quad \nabla n_\pm \cdot \nu = 0 \text{ on } \Gamma^N,\ t > 0. \tag{18}$$

This formulation is only possible if the precession vector $\vec{m}$ is constant. Its advantage is that the above system is only coupled in the source terms (and through the electric potential) so that we can apply a maximum principle. We observe that (5)-(10) implies (16)-(17) but not vice versa. Physically this is clear since the spin-up and spin-down densities contain less information than the full density matrix N. In fact, drift-diffusion equations similar to (16)-(17) have been thoroughly investigated in, e.g., [22].

1.4.3 *Parallel and perpendicular densities*

For the proof of the boundedness of $\vec{n}$, we employ a third formulation, the decomposition in the parallel and perpendipular components of $\vec{n}$ with respect to $\vec{m}$. For this, let $\vec{n}_\parallel = (\vec{n}\cdot\vec{m})\vec{m}$ and $\vec{n}_\perp = \vec{n} - (\vec{n}\cdot\vec{m})\vec{m}$. Then an elementary computation, using that $\vec{m}$ is constant, shows that $(\vec{n}_\parallel, \vec{n}_\perp)$ solves

$$\partial_t \vec{n}_\parallel - \operatorname{div}\left(\frac{D}{\eta^2}\left((\vec{J}\cdot\vec{m})\vec{m} - \frac{p}{2}J_0\vec{m}\right)\right) = -\frac{\vec{n}_\parallel}{\tau}, \tag{19}$$

$$\partial_t \vec{n}_\perp - \operatorname{div}\left(\frac{D}{\eta}(\nabla\vec{n}_\perp + \vec{n}_\perp\nabla V)\right) - 2\gamma(\vec{n}_\perp\times\vec{m}) = -\frac{\vec{n}_\perp}{\tau}. \tag{20}$$

The second equation depends on $\vec{n}_\perp$ only, which makes the application of a maximum principle possible.

1.5 LIST OF THE MAIN RESULTS AND THE THESIS STRUCTURE

Here we shortly list the main results and the exploited methods to give the reader a clearer structure of the work.

Chapter 2 is devoted to the continuous analysis of the spinorial drift-diffusion model (1)-(4). For the existence of the weak solution we use Leray-Schauder fixed point theorem [24], the proof of nonnegativity and boundedness of the charge density n_0 is based on the Stampacchia method, for boundedness of $\vec{n}$ we exploit the Moser iteration technique. Moreover, we present the free energy of the system and demonstrate the numerical solution in 1D. Thus, the main results of this chapter are:

- global-in-time existence and uniqueness of the weak solution $(n_0, \vec{n}, V)$
- nonnegativity and boundedness of the charge density n_0
- boundedness of potential V and spin density $\vec{n}$
- monotonicity of the free energy
- numerical solution in 1D

In Chapter 3 we present an implicit Euler finite volume scheme for the model (1)-(4), the analysis of the numerical solution and the numerical results obtained for the scheme in 2D. The existence proof is based on the fixed-point theorem of Brouwer [17] could be accomplished only with some restriction on the time step. Also for the boundedness of the numerical counterpart of $\vec{n}$ we need a restriction on the relaxation time. Numerical experiments show that the last restriction is likely to be technical. Summing this up, the main achievements of the chapter devoted to the numerical solution are:

- finite volume numerical scheme for 2D (3D)
- existence of the numerical solution
- nonnegativity and boundedness of the discrete charge density
- boundedness of discrete potential and spin densities
- monotonicity of the discrete free energy
- numerical solution in 2D

The last part (Chapter 4) expands the drift-diffusion model (1)-(4) to the spinorial energy-transport model. Exploiting the implicit model for spin-dependent energy transport proposed in [3] we derive an explicit version obtained with some simplifying assumption. The derivation is based on the entropy maximization principle and the energy conserving collision operator. The results presented in the third chapter are:

- derivation of an explicit energy-transport model
- monotonicity of the free energy
- numerical solution in 1D

Part II

SPINORIAL DRIFT-DIFFUSION MODEL

2

CONTINUOUS ANALYSIS

In this chapter we study the properties of the matrix drift-diffusion model (1)-(4). First in Section 2.1 we shortly present (in the form of theorems) the main results including existence of a unique bounded weak solution (Theorem 1) and monotonicity of the free energy (Proposition 2). Theorem 1 is proven in Section 2.2. Proposition 2 and formula (25) are shown in Section 2.3. Some numerical results for a one-dimensional ballistic diode in a multilayer structure using a finite-volume scheme are presented in Section 2.4.

2.1 MAIN RESULTS

Our first result is the global-in-time existence of weak solutions to (1)-(4) (or equivalently, (4)-(12)) under the assumption that the diffusion coefficient D and the spin polarization p are constant. We introduce the space

$$W^{1,2}(0,T;H^1_0,L^2) = H^1(0,T;H^{-1}(\Omega)) \cap L^2(0,T;H^1_0(\Omega)).$$

Recall that $\vec{m}$ is assumed to be a constant vector.

Theorem 1 (Existence of bounded weak solutions I). *Let $T > 0$ and let $\Omega \subset \mathbb{R}^3$ be a bounded domain with $\partial\Omega \in C^{1,1}$. Furthermore, let λ_D, γ, $D > 0$, $0 \leqslant p < 1$, and $\vec{m} \in \mathbb{R}^3$ with $|\vec{m}| = 1$. The data satisfies $C \in L^\infty(\Omega)$ and*

$$0 \leqslant n_D \in H^1(\Omega) \cap L^\infty(\Omega), \quad V_D \in W^{2,q_0}(\Omega), \quad q_0 > 3,$$
$$n_0^0,\ \vec{n}^0 \cdot \vec{m} \in L^\infty(\Omega), \quad \frac{1}{2}n_0^0 \pm \vec{n}^0 \cdot \vec{m} \geqslant 0.$$

Then there exists a unique solution (N,V) to (1)-(4) such that $N = \frac{1}{2}n_0\sigma_0 + \vec{n}\cdot\vec{\sigma}$ satisfies

$$n_0,\ n_k \in W^{1,2}(0,T;H^1_0,L^2), \quad V \in L^\infty(0,T;W^{2,q_0}(\Omega)), \quad q_0 > 3,$$
$$0 \leqslant \frac{1}{2}n_0 \pm \vec{n}\cdot\vec{m} \in L^\infty(0,T;L^\infty(\Omega)), \quad k = 1,2,3.$$

Moreover, n_0 and $\vec{n}\cdot\vec{m}$ are bounded uniformly in $t > 0$. If additionally $|\vec{n}^0| \in L^\infty(\Omega)$, then $|\vec{n}| \in L^\infty(0,T;L^\infty(\Omega))$.

For simplicity, the boundary data is assumed to be independent of time. The general situation can also be treated but is more technical; see, e.g., [47]. The proof is based on the Leray-Schauder fixed-point theorem. The key idea is to employ the variables $(n_0, \vec{n}\cdot\vec{m})$ for the ellipticity argument. More precisely, consider the main part of the

differential operator in its weak formulation (Equation (5) is divided by four),

$$\begin{aligned} I = \frac{D}{\eta^2}\int_\Omega \Big(&\frac{1}{4}\nabla n_0\cdot\nabla\phi_0 - \frac{p}{2}\nabla(\vec{n}\cdot\vec{m})\cdot\nabla\phi_0 + \eta\nabla\vec{n}:\nabla\vec{\phi} \\ &+ (1-\eta)\nabla(\vec{n}\cdot\vec{m})\cdot\nabla(\vec{\phi}\cdot\vec{m}) - \frac{p}{2}\nabla n_0\cdot\nabla(\vec{\phi}\cdot\vec{m})\Big)dx, \end{aligned}$$

where $(\phi_0, \vec{\phi})$ is some test function. Then, choosing $\phi_0 = n_0$, $\vec{\phi} = \vec{n}$ and using $\eta(1-\eta/2)\|\nabla\vec{n}\|^2 \geqslant \eta(1-\eta/2)|\nabla\vec{n}\cdot\vec{m}|^2$, the above integral can be estimated by

$$\begin{aligned} I &= \frac{D}{\eta^2}\int_\Omega \Big(\frac{1}{4}|\nabla n_0|^2 - p\nabla(\vec{n}\cdot\vec{m})\cdot\nabla n_0 \\ &\quad + \eta\Big(1-\frac{\eta}{2}\Big)\|\nabla\vec{n}\|^2 + \frac{\eta^2}{2}\|\nabla\vec{n}\|^2 + (1-\eta)|\nabla(\vec{n}\cdot\vec{m})|^2\Big)dx \\ &\geqslant \frac{D}{\eta^2}\int_\Omega \begin{pmatrix}\nabla n_0 \\ \nabla(\vec{n}\cdot\vec{m})\end{pmatrix}^\top \begin{pmatrix}1/4 & -p/2 \\ -p/2 & 1-\eta^2/2\end{pmatrix}\begin{pmatrix}\nabla n_0 \\ \nabla(\vec{n}\cdot\vec{m})\end{pmatrix} dx \\ &\quad + \frac{D}{2}\int_\Omega \|\nabla\vec{n}\|^2 dx. \end{aligned} \tag{21}$$

The 2×2 matrix on the right-hand side is positive definite (see the discussion after (32)), which allows us to apply the Lax-Milgram lemma. Although the matrix is positive definite in the variables $(n_0, \vec{n}\cdot\vec{m})$ only, we achieve gradient estimates also for $\vec{n}$. This is the key estimate. Note that the assumption that $\vec{m}$ is constant is crucial here.

The positivity and boundedness of n_0 is proved by applying a Stampacchia truncation argument to system (16)-(17) in the variables $n_\pm = \frac{1}{2}n_0 \pm \vec{n}\cdot\vec{m}$. The boundedness of $\vec{n}$ does not follow from this argument. The idea is to prove the boundedness of $\vec{n}_\perp = \vec{n} - (\vec{n}\cdot\vec{m})\vec{m}$, since it satisfies the decoupled drift-diffusion equation (20). Then, because of $\vec{n}\cdot\vec{m} \in L^\infty$, we infer that $|\vec{n}| \in L^\infty$. A standard Stampacchia truncation method cannot be employed here since the term $\vec{n}\times\vec{m}$ mixes the components of $\vec{n}$. Therefore, we use a Moser-type iteration method, i.e., we derive L^q estimates for $\vec{n}_\perp$ uniform in $q < \infty$ and pass to the limit $q\to\infty$.

Our second result is the existence of an entropy (more precisely, free energy) [1] for the spinorial drift-diffusion system. This result holds also for nonconstant diffusion coefficients $D(x)$ and spin polarizations $p(x)$. We assume that there exists $\delta_0 > 0$ such that

$$D, p \in L^\infty(\Omega), \quad D(x) \geqslant \delta_0 > 0,\ 0 \leqslant p(x) \leqslant 1-\delta_0 \quad \text{for } x\in\Omega. \tag{22}$$

The entropy is formulated in terms of the solution to (16)-(17):

$$\begin{aligned} H_0(t) &= \int_\Omega \left(h(n_+) + h(n_-) + \frac{\lambda_D^2}{2}|\nabla(V-V_D)|^2\right)dx, \\ h(n_\pm) &= \int_{n_D/2}^{n_\pm} (\log s - \log(n_D/2))ds. \end{aligned} \tag{23}$$

1 In contrast to the physical notation, the mathematical entropy is defined here as the negative physical entropy.

The first two terms in the definition of $H_0(t)$ describe the internal energy of the two spin components and the last term is the electric energy, relative to the boundary values. From the results on the standard drift-diffusion model (see, e.g., [22]), it is not surprising that the entropy H_0 is nonincreasing in time if the initial data are in thermal equilibrium. We say that (n_{th}, V_{th}) is a thermal equilibrium state if $n_{th} = \rho\exp(-V_{th})$ for some constant $\rho > 0$ and V_{th} is the unique solution to

$$-\lambda_D^2\Delta V_{th} = \rho e^{-V_{th}} - C(x) \quad \text{in } \Omega, \quad V_{th} = V_D \quad \text{on } \partial\Omega.$$

For given (n_D, V_D), defined on $\partial\Omega$ and satisfying $\log(n_D/2) + V_D = c \in \mathbb{R}$ on $\partial\Omega$, we extend these functions to Ω by setting $n_D = n_{th}$, $V_D = V_{th}$ and $\rho = 2\exp(c)$. Then $\log(n_D/2) + V_D = c$ in Ω. The following result holds.

Proposition 2 (Monotonicity of H_0). *Let* (22) *hold,* $\log(n_D/2) + V_D =$ const. *in* Ω, *and* $n_D \in W^{1,\infty}(\Omega)$ *with* $n_D \geqslant n_* > 0$ *in* Ω. *Let* (n_+, n_-, V) *be a weak solution to* (4), (16)-(18) *in the sense of Theorem 1. Then* $t \mapsto H_0(t)$ *is nonincreasing for* $t > 0$.

Using the techniques of [22], it is possible to infer the exponential decay of $(n_+(t), n_-(t))$ to equilibrium as $t \to \infty$. Since the proof is very similar to that of [22], we omit it. However, later in Section 2.4 we give a numerical example which illustrates the exponential decay.

One may ask if the quantum or von-Neumann entropy (or free energy)

$$H_Q(t) = \int_\Omega \Big(\mathrm{tr}[N(\log N - \log N_D - 1) + N_D] + \frac{\lambda_D^2}{2}|\nabla(V - V_D)|^2 \Big)\,dx, \tag{24}$$

where $N_D = \frac{1}{2}n_D\sigma_0$ (see (3)), is also nonincreasing in time. Since the eigenvalues of N are given by $\frac{1}{2}n_0 \pm |\vec{n}|$, we need to suppose that $\frac{1}{2}n_0 > |\vec{n}|$ to have well-posedness of the expression $\log N$. Because of the drift-diffusion structure of (1), such a functional would be a natural candidate for an entropy. A formal computation, detailed in Remark 3, shows that

$$\begin{aligned}\frac{dH_Q}{dt} &= \\ &= -\int_\Omega Dn_0 \sum_{j=1}^3 \mathrm{tr}\left[P^{-1/2}(\partial_j N + N\partial_j V)P^{-1/2}\partial_j(\log N + V\sigma_0)\right] dx \\ &\quad - \frac{1}{\tau}\int_\Omega |\vec{n}| \log\frac{\frac{1}{2}n_0 + |\vec{n}|}{\frac{1}{2}n_0 - |\vec{n}|}\,dx. \end{aligned} \tag{25}$$

Clearly, the second integral is nonnegative. However, it seems to be difficult to determine the sign of the entropy dissipation in the general case. If $\vec{m} = (0,0,1)^\top$ and $\vec{n}_0 = (0,0,n_3^0)^\top$, which we assume in our numerical simulations in Section 2.4, the spin-vector density only depends on the

third component, $\vec{n}(t) = (0, 0, n_3(t))^\top$ for all $t > 0$. In this situation, H_Q is nonincreasing. Indeed, we can write H_Q equivalently as

$$\begin{aligned} H_Q(t) = \int_\Omega \Big(&(\tfrac{1}{2}n_0 + |\vec{n}|)\big(\log(\tfrac{1}{2}n_0 + |\vec{n}|) - 1\big) \\ &+ (\tfrac{1}{2}n_0 - |\vec{n}|)\big(\log(\tfrac{1}{2}n_0 - |\vec{n}|) - 1\big) \\ &+ n_D - n_0 \log(\tfrac{1}{2}n_D) + \frac{\lambda_D^2}{2}|\nabla(V - V_D)|^2\Big)\,dx. \end{aligned}$$

This formulation follows from spectral theory and the fact that the eigenvalues of N are given by $\frac{1}{2}n_0 \pm |\vec{n}|$; see Section 2 in [36] We recall that for any continuous function $f : \mathbb{R} \to \mathbb{R}$ and any Hermitian matrix A with (real) eigenvalues λ_j, it holds that $\mathrm{tr}[f(A)] = \sum_j f(\lambda_j)$. Now, $\frac{1}{2}n_0 \pm |\vec{n}| = \frac{1}{2}n_0 \pm n_3 = n_\pm$, and consequently, H_Q coincides with H_0, which is monotone by Proposition 2.

2.2 EXISTENCE OF A SOLUTION

The existence proof is based on the Leray-Schauder fixed-point theorem and a truncation argument. It is divided into several steps.

Step 1: Reformulation. We introduce the variable $w_0 = n_0 - n_D(x)$ whose trace vanishes on $\partial\Omega$. Then equations (5)-(10) are equivalent to

$$\frac{1}{4}\partial_t w_0 - \frac{D}{4\eta^2}\,\mathrm{div}(J_w - 2p\vec{J}\cdot\vec{m}) = \frac{D}{4\eta^2}\,\mathrm{div}(\nabla n_D + n_D\nabla V), \tag{26}$$

$$\begin{aligned} &\partial_t n_k - \frac{D}{\eta^2}\,\mathrm{div}\Big(\eta J_k + (1-\eta)(\vec{J}\cdot\vec{m})m_k - \frac{p}{2}J_w m_k\Big) - 2\gamma(\vec{n}\times\vec{m})_k \\ &\quad = -\frac{n_k}{\tau} - \frac{Dp}{2\eta^2}\,\mathrm{div}\big((\nabla n_D + n_D\nabla V)m_k\big), \quad k = 1,2,3, \end{aligned} \tag{27}$$

where $J_w = \nabla w_0 + w_0\nabla V$. The boundary and initial conditions are given by

$$w_0 = n_k = 0 \quad \text{on } \partial\Omega,\ k = 1,2,3, \quad w_0(\cdot,0) = n_0^0 - n_D,\ \vec{n}(0) = \vec{n}^0 \quad \text{in } \Omega. \tag{28}$$

Step 2: Definition of the fixed-point operator. The idea is to fix a density $(\rho_0, \vec{\rho})$, to solve the Poisson equation including ρ_0 on its right-hand side, and finally to solve a linearized version of (26)-(27) for the density $(w_0, \vec{w})$, where $\vec{w} = (w_1, w_2, w_3)$. The fixed-point operator is then defined by the mapping $(\rho_0, \vec{\rho}) \mapsto V \mapsto (w_0, \vec{w})$. More precisely, let $\rho = (\rho_0, \vec{\rho}) \in L^2(0,T;L^2(\Omega))^4$ and $\delta \in [0,1]$ be given and introduce the truncation $[x] = \max\{0, \min\{x, 2M\}\}$ for $x \in \mathbb{R}$, where

$$M = \max\Big\{\sup_{\partial\Omega} n_D,\ \sup_\Omega\Big(\frac{1}{2}n_0^0 + |\vec{n}^0\cdot\vec{m}|\Big),\ \sup_\Omega C\Big\}.$$

Let $V(t) \in H^1(\Omega)$ be the unique solution to

$$-\lambda^2\Delta V(t) = [\rho_0(t) + n_D] - C(x) \quad \text{in } \Omega, \quad V(t) = V_D \quad \text{on } \partial\Omega. \tag{29}$$

Then $t \mapsto V(t)$ is Bochner measurable and $V \in L^2(0,T;H^1(\Omega))$. In fact, by elliptic regularity and $\partial\Omega \in C^{1,1}$, $V(t) \in W^{2,q_0}(\Omega)$ for $q_0 > 3$. Since the right-hand side of (29) is an element of $L^\infty(0,T;L^\infty(\Omega))$, $V \in L^\infty(0,T;W^{2,q_0}(\Omega))$. This implies, because of the Sobolev embedding $W^{2,q_0}(\Omega) \hookrightarrow W^{1,\infty}(\Omega)$ in dimensions $d \leqslant 3$, that $|\nabla V| \in L^\infty(0,T;L^\infty(\Omega))$.

Next, we define the bilinear form $a(\cdot,\cdot;t) : H_0^1(\Omega)^4 \times H_0^1(\Omega)^4 \to \mathbb{R}$ for all $w = (w_0, \vec{w}) = (w_0, w_1, w_2, w_3)$, $\phi = (\phi_0, \vec{\phi}) = (\phi_0, \phi_1, \phi_2, \phi_3) \in H_0^1(\Omega)^4$ by

$$a(w, \phi; t) = a_0(w, \phi) + a_V(w, \phi; t) + a_1(w, \phi) + a_2(w, \phi), \tag{30}$$

where

$$\begin{aligned}
a_0(w,\phi) &= \frac{D}{\eta^2}\int_\Omega \Big(\frac{1}{4}\nabla w_0\cdot\nabla\phi_0+\eta\nabla\vec{w}:\nabla\vec{\phi}\\
&\quad+(1-\eta)\nabla(\vec{w}\cdot\vec{m})\cdot\nabla(\vec{\phi}\cdot\vec{m})-\frac{p}{2}\nabla(\vec{w}\cdot\vec{m})\cdot\nabla\phi_0\\
&\quad-\frac{p}{2}\nabla w_0\cdot\nabla(\vec{\phi}\cdot\vec{m})\Big)dx,\\
a_V(w,\phi;t) &= \frac{D\delta}{\eta^2}\int_\Omega \nabla V(t)\cdot\Big(\frac{1}{4}w_0\nabla\phi_0+\eta\nabla\vec{\phi}\cdot\vec{w}\\
&\quad+(1-\eta)(\vec{w}\cdot\vec{m})\nabla(\vec{\phi}\cdot\vec{m})-\frac{p}{2}(\vec{w}\cdot\vec{m})\nabla\phi_0\\
&\quad-\frac{p}{2}w_0\nabla(\vec{\phi}\cdot\vec{m})\Big)dx,\\
a_1(w,\phi) &= -2\gamma\delta\int_\Omega(\vec{w}\times\vec{m})\cdot\vec{\phi}dx,\\
a_2(w,\phi) &= \frac{1}{\tau}\int_\Omega \vec{w}\cdot\vec{\phi}dx,
\end{aligned}$$

and $\nabla\vec{w}:\nabla\vec{\phi}=\sum_{k=1}^3\nabla w_k\cdot\nabla\phi_k$, and the linear mapping $F(\cdot;t):H_0^1(\Omega)^4\to\mathbb{R}$ by

$$\begin{aligned}
F(\phi;t) &= -\frac{D\delta}{4\eta^2}\int_\Omega(\nabla n_D+n_D\nabla V)\cdot\nabla\phi_0\\
&\quad+\frac{D\delta p}{2\eta^2}\int_\Omega(\nabla n_D+n_D\nabla V)\cdot\nabla(\vec{\phi}\cdot\vec{m})dx.
\end{aligned}$$

Then the weak formulation of (26)-(28) (for $\delta=1$) reads as

$$\frac{d}{dt}\int_\Omega w(t)\cdot\phi dx+a(w,\phi;t)=F(\phi;t)\quad\text{for }\phi\in H_0^1(\Omega),\ t>0. \tag{31}$$

Since $|\nabla V|\in L^\infty(0,T;L^\infty(\Omega))$, an elementary estimation shows that a and F are bounded in the sense

$$a(w,\phi;t)\leqslant K_0\|w\|_{H_0^1(\Omega)}\|\phi\|_{H_0^1(\Omega)},\quad |F(\phi;t)|\leqslant K_0\|\phi\|_{H_0^1(\Omega)}$$

for all $w,\phi\in H_0^1(\Omega)^4$, where $K_0>0$ depends on the $L^\infty(0,T;L^\infty(\Omega))$ norm of ∇V (and hence on M) but is independent of $t>0$. We claim that a satisfies an abstract Gårding inequality, i.e., there exist $K_1,K_2>0$ such that for all $w\in H_0^1(\Omega)^4$,

$$a(w,w)\geqslant K_1\|w\|^2_{H_0^1(\Omega)}-K_2\|w\|^2_{L^2(\Omega)}.$$

To this end, we estimate the forms a_0, a_V, a_1, and a_2. The first form equals

$$\begin{aligned}
a_0(w,w) &= \frac{D}{\eta^2}\int_\Omega\Big(\frac{1}{4}|\nabla w_0|^2+\frac{\eta^2}{2}\|\nabla\vec{w}\|^2+\eta\Big(1-\frac{\eta}{2}\Big)\|\nabla\vec{w}\|^2\\
&\quad+(1-\eta)|\nabla(\vec{w}\cdot\vec{m})|^2-p\nabla w_0\cdot\nabla(\vec{w}\cdot\vec{m})\Big)dx.
\end{aligned}$$

Estimate (21) in the introduction shows that

$$\begin{aligned}
a_0(w,w) &\geqslant \frac{D}{\eta^2}\int_\Omega\begin{pmatrix}\nabla w_0\\ \nabla\vec{w}\cdot\vec{m}\end{pmatrix}^\top\begin{pmatrix}1/4 & -p/2\\ -p/2 & 1-\eta^2/2\end{pmatrix}\begin{pmatrix}\nabla w_0\\ \nabla\vec{w}\cdot\vec{m}\end{pmatrix}dx\\
&\quad+\frac{D}{2}\int_\Omega\|\nabla\vec{w}\|^2dx.
\end{aligned}\tag{32}$$

The above symmetric matrix is positive definite because its eigenvalues

$$\lambda_\pm=\frac{1}{8}(5-2\eta^2)\pm\frac{1}{8}\sqrt{(5-2\eta^2)^2-8\eta^2}$$

are real (since $\eta \leqslant 1$) and positive (since $\eta > 0$). This leads to

$$\begin{aligned} a_0(w,w) &\geqslant \frac{D}{\eta^2}\int_\Omega \Big(\lambda_-|\nabla w_0|^2 + \lambda_-|\nabla(\vec{w}\cdot\vec{m})|^2 + \frac{\eta^2}{2}\|\nabla\vec{w}\|^2\Big)\,dx \\ &\geqslant K_1\|w\|^2_{H^1_0(\Omega)}, \end{aligned}$$

where $K_1 = \min\{\lambda_-, \eta^2/2\}$.

In order to estimate the second form $a_V(w,w)$, we employ the Poisson equation:

$$\begin{aligned} a_V(w,w) &= \frac{D\delta}{2\eta^2}\int_\Omega \nabla V\cdot\nabla\Big(\frac{1}{4}w_0^2 + \eta|\vec{w}|^2 + (1-\eta)(\vec{w}\cdot\vec{m})^2 \\ &\quad - pw_0(\vec{w}\cdot\vec{m})\Big)\,dx = \frac{D\delta}{2\eta^2\lambda_D^2}\int_\Omega ([\rho_0+n_D]-C(x))\Big(\frac{1}{4}w_0^2+\eta|\vec{w}|^2 \\ &\quad + (1-\eta)(\vec{w}\cdot\vec{m})^2 - pw_0(\vec{w}\cdot\vec{m})\Big)\,dx. \end{aligned}$$

Observing that

$$\begin{aligned} &\frac{1}{4}w_0^2 + \eta|\vec{w}|^2 + (1-\eta)(\vec{w}\cdot\vec{m})^2 - pw_0(\vec{w}\cdot\vec{m}) \\ &\qquad = \Big(\frac{1}{2}w_0 - p\vec{w}\cdot\vec{m}\Big)^2 + \eta\big(|\vec{w}|^2 - (\vec{w}\cdot\vec{m})^2\big) + \eta^2(\vec{w}\cdot\vec{m})^2 \geqslant 0 \end{aligned}$$

and employing the Cauchy-Schwarz inequality, it follows that

$$\begin{aligned} a_V(w,w) &\geqslant -\frac{D}{2\eta^2\lambda_D^2}\int_\Omega |C(x)|\Big(\frac{1}{4}w_0^2+\eta|\vec{w}|^2 + (1-\eta)(\vec{w}\cdot\vec{m})^2 \\ &\quad - pw_0(\vec{w}\cdot\vec{m})\Big)\,dx \geqslant -K_2\|w\|^2_{L^2(\Omega)}, \end{aligned}$$

where K_2 depends on $\|C\|_{L^\infty(\Omega)}$ and the parameters D, p, and λ_D but not on M or ρ. Finally, the third form vanishes, $a_1(w,w) = 0$, and the fourth form is nonnegative, $a_2(w,w) \geqslant 0$. This shows the claim.

By Corollary 23.26 in [48], there exists a unique solution $w \in W^{1,2}(0,T;H^1_0, L^2)^4$ to (31) satisfying $w(0) = (n_0^0 - n_D, \vec{n}^0)$. This defines the fixed-point operator $S : L^2(0,T;L^2(\Omega))^4 \times [0,1] \to L^2(0,T;L^2(\Omega))^4$, $S(\rho,\delta) = w$. By construction, $S(\rho,0) = 0$. Furthermore, standard arguments show that S is continuous. By the Aubin lemma, the space $W^{1,2}(0,T;H^1_0, L^2)^4$ embeddes compactly into $L^2(0,T;L^2(\Omega))^4$. Consequently, S is compact. It remains to prove some uniform estimates for all fixed points of $S(\cdot,\delta)$ in $L^2(0,T;L^2(\Omega))^4$. Let $w \in W^{1,2}(0,T;H^1_0,L^2)^4$ be such a fixed point. Employing $w = (w_0,\vec{w})$ as a test function in (31), the above estimates show that

$$\begin{aligned} &\frac{1}{2}\|w(\cdot,T)\|^2_{L^2(\Omega)} + K_1\|w\|^2_{L^2(0,T;H^1_0(\Omega))} \\ &\quad \leqslant K_2\|w\|^2_{L^2(0,T;L^2(\Omega))} + K_0\|w\|_{L^2(0,T;H^1_0(\Omega))} \\ &\quad \leqslant K_2\|w\|^2_{L^2(0,T;L^2(\Omega))} + \frac{K_1}{2}\|w\|^2_{L^2(0,T;H^1_0(\Omega))} + \frac{K_0^2}{2K_1}. \end{aligned}$$

Absorbing the second summand on the right-hand side by the corresponding term on the left-hand side and applying Gronwall's lemma, we achieve the bound $\|w\|_{L^2(0,T;L^2(\Omega))} \leqslant K$ for some $K > 0$ uniform in ρ and δ. By the Leray-Schauder fixed-point theorem, there exists a fixed point of $S(\cdot,1)$, i.e. a solution to (26)-(29) with $[\rho(t)+n_D]$ replaced by $[w(t)+n_D]$.

Step 3: Lower and upper bounds. We show that $0 \leqslant n_0 := w + n_D \leqslant 2M$ in $\Omega\times(0,T)$ which allows us to remove the truncation in the Poisson equation. For this, we consider the variables $n_\pm = \frac{1}{2}n_0 \pm \vec{n}\cdot\vec{m}$. We claim that $n_\pm \geqslant 0$. Indeed, with the test functions $[n_\pm]^- = \min\{0, n_\pm\}$, which satisfy

$[n_\pm]^- = 0$ on $\partial\Omega$ and $[n_\pm(0)]^- = 0$, in the weak formulation of (16) and (17), respectively, it follows from $n_\pm \nabla V \cdot \nabla [n_\pm]^- = [n_\pm]^- \nabla V \cdot \nabla [n_\pm]^- = \frac{1}{2} \nabla V \cdot \nabla ([n_\pm]^-)^2$ that

$$\begin{aligned}
&\frac{1}{2}\int_\Omega ([n_\pm(t)]^-)^2 dx + D(1\pm p)\int_0^t\int_\Omega |\nabla [n_\pm]^-|^2 dx\,ds \\
&\quad = -D(1\pm p)\int_0^t\int_\Omega [n_\pm]^- \nabla V \cdot \nabla [n_\pm]^- dx\,ds \\
&\qquad \mp \frac{1}{2\tau}\int_0^t\int_\Omega (n_+ - n_-)[n_\pm]^- dx\,ds \\
&\quad = -\frac{D(1\pm p)}{2\lambda_D^2}\int_0^t\int_\Omega ([n_0] - C(x))([n_\pm]^-)^2 dx\,ds \\
&\qquad \mp \frac{1}{2\tau}\int_0^t\int_\Omega (n_+ - n_-)[n_\pm]^- dx\,ds.
\end{aligned}$$

In the last step we have integrated by parts and employed the Poisson equation. We add both equations and neglect the integrals involving $|\nabla [n_\pm]^-|^2$ to obtain

$$\begin{aligned}
&\frac{1}{2}\int_\Omega \big(([n_+(t)]^-)^2 + ([n_-(t)]^-)^2\big) dx \\
&\leqslant -\frac{D}{2\lambda_D^2}\int_0^t\int_\Omega ([n_0] - C(x))\big((1+p)([n_+]^-)^2 + (1-p)([n_-]^-)^2\big) dx\,ds \\
&\quad - \frac{1}{2\tau}\int_0^t\int_\Omega (n_+ - n_-)([n_+]^- - [n_-]^-) dx\,ds \\
&\leqslant \frac{D}{2\lambda_D^2}\|C\|_{L^\infty(\Omega)}\int_0^t\int_\Omega \big(([n_+]^-)^2 + ([n_-]^-)^2\big) dx\,ds,
\end{aligned}$$

using the fact that $x \mapsto [x]^-$ is nondecreasing. Gronwall's lemma shows that $[n_\pm(t)]^- = 0$ in Ω for any $t > 0$ and hence, $n_\pm \geqslant 0$ in $\Omega \times (0,T)$.

For the proof of the upper bound, we employ the test function $[n_\pm - M]^+ = \max\{0, n_\pm - M\}$, which is admissible since $M \geqslant \frac{1}{2}\sup_{\Omega\times(0,T)} n_D$, and which satisfies $[n_\pm(0) - M]^+ = 0$, in (16) and (17), respectively, and add both equations:

$$\begin{aligned}
&\frac{1}{2}\int_\Omega \big(([n_+(t) - M]^+)^2 + ([n_-(t) - M]^+)^2\big) dx \\
&+ D\int_0^t\int_\Omega \big((1+p)|\nabla [n_+ - M]^+|^2 + (1-p)|\nabla [n_- - M]^+|^2\big) dx\,ds \\
&= -D\int_0^t\int_\Omega \big((1+p)(n_+ - M)\nabla V \cdot \nabla [n_+ - M]^+ \\
&+ (1-p)(n_- - M)\nabla V \cdot \nabla [n_- - M]^+\big) dx\,ds \\
&- DM\int_0^t\int_\Omega \nabla V \cdot \big((1+p)\nabla [n_+ - M]^+ + (1-p)\nabla [n_- - M]^+\big) dx\,ds \\
&- \frac{1}{2\tau}\int_0^t\int_\Omega (n_+ - n_-)\big([n_+ - M]^+ - [n_- - M]^+\big) dx\,ds.
\end{aligned}$$

Observing that $(n_\pm - M)\nabla V \cdot \nabla [n_\pm - M]^+ = \frac{1}{2}\nabla V \cdot \nabla ([n_\pm - M]^+)^2$, integrating by parts, and employing the Poisson equation, we find that

$$\begin{aligned}
&\frac{1}{2}\int_\Omega \big(([n_+(t) - M]^+)^2 + ([n_-(t) - M]^+)^2\big)\,dx \\
&\quad \leqslant -\frac{D}{2\lambda_D^2}\int_0^t \int_\Omega ([n_0] - C(x))\big((1+p)([n_+ - M]^+)^2 \\
&\qquad + (1-p)([n_- - M]^+)^2\big)\,dx\,ds \\
&\qquad - \frac{DM}{\lambda_D^2}\int_0^t \int_\Omega ([n_0] - C(x))\big((1+p)[n_+ - M]^+ \\
&\qquad + (1-p)[n_- - M]^+\big)\,dx\,ds.
\end{aligned}$$

The last integral is nonnegative since $[n_0] - C(x) = [n_+ + n_-] - C(x) \geqslant 0$ on $\{n_\pm \geqslant M\}$ by definition of M. Then Gronwall's lemma gives $[n_\pm - M]^+ = 0$ and $n_\pm \leqslant M$ in $\Omega \times (0,T)$. We have shown that $n_0 = n_+ + n_- \leqslant 2M$, $\vec{n}\cdot\vec{m} = \frac{1}{2}(n_+ - n_-) \leqslant \frac{1}{2}n_+ \leqslant \frac{1}{2}M$, and $\vec{n}\cdot\vec{m} \geqslant -\frac{1}{2}n_- \geqslant -\frac{1}{2}M$. Thus, we can remove the truncation in the Poisson equation, since $[n_0] = n_0$.

Step 4: Uniqueness of solutions. Let (w, V) and (w^*, V^*) with $w = (w_0, \vec{w})$ and $w^* = (w_0^*, \vec{w}^*)$ be two weak solutions to (29) and (31) on $(0, T^*)$, where $0 < T^* < T$. Taking the difference of the equations (31) for w and w^*, respectively, and employing the admissible test function $w - w^*$, we obtain

$$\begin{aligned}
&\frac{1}{2}\|(w-w^*)(T^*)\|_{L^2(\Omega)}^2 + \int_0^{T^*} \big(a(w, w-w^*; t) - a^*(w^*, w-w^*; t)\big)\,dt \\
&\quad = \int_0^{T^*} (F(w-w^*;t) - F^*(w-w^*;t))\,dt,
\end{aligned}$$

where a^* and F^* denote the forms with V replaced by V^*. The Cauchy-Schwarz and Young inequalities and the elliptic estimate $\|\nabla(V - V^*)\|_{L^2(\Omega)} \leqslant K\|w_0 - w_0^*\|_{L^2(\Omega)}$ yield

$$\begin{aligned}
&\int_0^{T^*} (F(w-w^*;t) - F^*(w-w^*;t))\,dt \\
&\quad = -\frac{D}{4\eta^2}\int_0^{T^*}\int_\Omega n_D \nabla(V - V^*)\cdot\nabla(w_0 - w_0^*)\,dx\,dt \\
&\qquad + \frac{Dp}{2\eta^2}\int_0^{T^*}\int_\Omega n_D \nabla(V - V^*)\cdot\nabla((\vec{w} - \vec{w}^*)\cdot\vec{m})\,dx\,dt \\
&\quad \leqslant \varepsilon\|\nabla(w - w^*)\|_{L^2(0,T^*;L^2(\Omega))}^2 + K(\varepsilon)\|w_0 - w_0^*\|_{L^2(0,T^*;L^2(\Omega))}^2,
\end{aligned}$$

where here and in the following, $K > 0$ denotes a generic constant and $\varepsilon > 0$.

Next, we consider the difference $a(w, w-w^*; t) - a^*(w^*, w-w^*; t)$. As in Step 2, we find that

$$\begin{aligned}
&\int_0^{T^*} a_0(w-w^*, w-w^*)\,dt \\
&\geqslant K\int_0^{T^*}\int_\Omega \big(|\nabla(w_0 - w_0^*)|^2 + \|\nabla(\vec{w} - \vec{w}^*)\|^2\big)\,dx\,dt, \\
&\int_0^{T^*} a_1(w-w^*, w-w^*)\,dt = 0, \\
&\int_0^{T^*} a_2(w-w^*, w-w^*)\,dt = \frac{1}{\tau}\int_0^{T^*}\int_\Omega |\vec{w} - \vec{w}^*|^2\,dx\,dt \geqslant 0.
\end{aligned}$$

The remaining difference involving the electric potentials becomes

$$\begin{aligned}
&\int_0^{T^*} \big(a_V(w, w-w^*; t) - a_{V^*}(w^*, w-w^*; t)\big)\,dt \\
&\quad = \frac{D}{2\eta^2}\int_0^{T^*}\int_\Omega \nabla V\cdot\nabla\Big(\frac{1}{4}(w_0-w_0^*)^2 + \eta|\vec{w}-\vec{w}^*|^2 \\
&\qquad + (1-\eta)((\vec{w}-\vec{w}^*)\cdot\vec{m})^2 - \frac{p}{2}(w_0-w_0^*)(\vec{w}-\vec{w}^*)\cdot\vec{m}\Big)\,dx\,dt \\
&\qquad + \frac{D}{\eta^2}\int_0^{T^*}\int_\Omega \nabla(V-V^*)\cdot\Big(\frac{1}{4}w_0^*\nabla(w_0-w_0^*) + \eta\vec{w}^*\nabla(\vec{w}-\vec{w}^*) \\
&\qquad + (1-\eta)(\vec{w}^*\cdot\vec{m})\nabla((\vec{w}-\vec{w}^*)\cdot\vec{m}) \\
&\qquad - \frac{p}{2}(\vec{w}^*\cdot\vec{m})\nabla(w_0-w_0^*) - \frac{p}{2}w_0^*\nabla((\vec{w}-\vec{w}^*)\cdot\vec{m})\Big)\,dx\,dt \\
&\quad =: I_1 + I_2.
\end{aligned}$$

Integrating by parts in the first integral on the right-hand side and employing the Poisson equation shows that the first integral can be estimated as

$$\begin{aligned}
I_1 &\leqslant K\big(\|w_0-w_0^*\|^2_{L^2(0,T^*;L^2(\Omega))} + \|\vec{w}-\vec{w}^*\|^2_{L^2(0,T^*;L^2(\Omega))} \\
&\quad + \|(\vec{w}-\vec{w}^*)\cdot\vec{m}\|^2_{L^2(0,T^*;L^2(\Omega))}\big) \\
&\leqslant K\big(\|w_0-w_0^*\|^2_{L^2(0,T^*;L^2(\Omega))} + \|\vec{w}-\vec{w}^*\|^2_{L^2(0,T^*;L^2(\Omega))}\big),
\end{aligned}$$

where $K > 0$ depends on the $L^\infty(0,T^*;L^\infty(\Omega))$ norm of w_0. We take into account the L^∞ norms of w_0^* and $\vec{w}^*\cdot\vec{m}$ to estimate the second integral according to

$$\begin{aligned}
I_2 &\leqslant K\|\nabla(V-V^*)\|_{L^2(0,T^*;L^2(\Omega))} \\
&\quad \times \big(\|\nabla(w_0-w_0^*)\|_{L^2(0,T^*;L^2(\Omega))} + \|\nabla(\vec{w}-\vec{w}^*)\cdot\vec{m}\|_{L^2(0,T^*;L^2(\Omega))}\big) \\
&\quad + \|\nabla(V-V^*)\|_{L^2(0,T^*;L^\infty(\Omega))}\|\vec{w}^*\|_{L^\infty(0,T^*;L^2(\Omega))} \\
&\quad \times \|\nabla(\vec{w}-\vec{w}^*)\|_{L^2(0,T^*;L^2(\Omega))}.
\end{aligned} \tag{33}$$

Using the elliptic estimate $\|\nabla(V-V^*)\|_{L^2(\Omega)} \leqslant K\|w_0-w_0^*\|_{L^2(\Omega)}$ and Young's inequality, the first term is estimated from above by

$$\begin{aligned}
&\frac{\varepsilon}{2}\|\nabla(w_0-w_0^*)\|^2_{L^2(0,T^*;L^2(\Omega))} + \frac{\varepsilon}{2}\|\nabla(\vec{w}-\vec{w}^*)\cdot\vec{m}\|^2_{L^2(0,T^*;L^2(\Omega))} \\
&\qquad\qquad + K(\varepsilon)\|w_0-w_0^*\|^2_{L^2(0,T^*;L^2(\Omega))}.
\end{aligned}$$

For the second term in (33), we observe that, in view of the continuous embedding $W^{1,2}(0,T^*;H^1_0,L^2) \hookrightarrow L^\infty(0,T^*;L^2(\Omega))$, $\vec{w}^*$ is bounded in $L^\infty(0,T^*;L^2(\Omega))$. Let $3 < p < 6$. By elliptic regularity and the Gagliardo-Nirenberg inequality, it follows that

$$\begin{aligned}
\|\nabla(V-V^*)\|_{L^2(0,T^*;L^\infty(\Omega))} &\leqslant K\|V-V^*\|_{L^2(0,T^*;W^{2,p}(\Omega))} \\
&\leqslant K\|w_0-w_0^*\|_{L^2(0,T^*;L^p(\Omega))} \\
&\leqslant K\|\nabla(w_0-w_0^*)\|^\theta_{L^2(0,T^*;L^2(\Omega))}\|w_0-w_0^*\|^{1-\theta}_{L^2(0,T^*;L^2(\Omega))},
\end{aligned}$$

where $\theta = 3/2 - 3/p \in (0,1)$. Inserting this and the above estimate into (33) and employing Young's inequality again, we obtain

$$\begin{aligned}
I_2 &\leqslant \varepsilon\|\nabla(w_0-w_0^*)\|^2_{L^2(0,T^*;L^2(\Omega))} + \varepsilon\|\nabla(\vec{w}-\vec{w}^*)\|^2_{L^2(0,T^*;L^2(\Omega))} \\
&\quad + K(\varepsilon)\|w_0-w_0^*\|^2_{L^2(0,T^*;L^2(\Omega))}.
\end{aligned}$$

Summarizing the above estimates, we infer that

$$\begin{aligned}&\|(w-w^*)(T^*)\|^2_{L^2(\Omega)}+(K-\varepsilon)\big(\|\nabla(w_0-w_0^*)\|^2_{L^2(0,T^*;L^2(\Omega))}\\&\quad+\|\nabla(\vec{w}-\vec{w}^*)\|^2_{L^2(0,T^*;L^2(\Omega))}\big)\\&\leqslant K(\varepsilon)\big(\|w_0-w_0^*\|^2_{L^2(0,T^*;L^2(\Omega))}+\|\vec{w}-\vec{w}^*\|^2_{L^2(\Omega)}\big).\end{aligned}$$

Thus, choosing $\varepsilon>0$ sufficiently small and employing Gronwall's lemma, we infer that $w=w^*$ in Ω, $t>0$.

Step 5: L^∞ *bound for* $\vec{n}$. Let $q\geqslant 1$. Since $|\vec{n}_\perp|^q\vec{n}_\perp$ is not an admissible test function, we need to regularize. For this, set $g_\varepsilon(y)=y^q/(1+\varepsilon y^q)$ and $G_\varepsilon(y)=\int_0^y g_\varepsilon(z)dz$ for $y\geqslant 0$ and $\varepsilon>0$. Then $g_\varepsilon(|\vec{n}_\perp|^2)\vec{n}_\perp$ is an admissible test function in the weak formulation of (20) (since $\vec{n}=0$ on $\partial\Omega$):

$$\begin{aligned}&\int_0^t\langle\partial_t\vec{n}_\perp,g_\varepsilon(|\vec{n}_\perp|^2)\vec{n}_\perp\rangle ds+\frac{D}{\eta}\int_0^t\int_\Omega(\nabla\vec{n}_\perp+\nabla V\vec{n}_\perp)\\&:\nabla(g_\varepsilon(|\vec{n}_\perp|^2)\vec{n}_\perp)dx\,ds=2\gamma\int_0^t\int_\Omega g_\varepsilon(|\vec{n}_\perp|^2)(\vec{n}_\perp\times\vec{m})\cdot\vec{n}_\perp dx\,ds\\&-\frac{1}{\tau}\int_0^t\int_\Omega g_\varepsilon(|\vec{n}_\perp|^2)|\vec{n}_\perp|^2dx\,ds\leqslant 0,\end{aligned}\tag{34}$$

since the first integral on the right-hand side vanishes and the second one is nonnegative. Here, $\langle\cdot,\cdot\rangle$ denotes the dual product between $H^{-1}(\Omega)$ and $H^1_0(\Omega)$. Taking into account a variant of Prop. 23.20 in [48], the first integral on the left-hand side of (34) equals

$$\langle\partial_t\vec{n}_\perp,g_\varepsilon(|\vec{n}_\perp|^2)\vec{n}_\perp\rangle=\frac12\frac{d}{dt}\int_\Omega G_\varepsilon(|\vec{n}_\perp|^2)dx.$$

Setting $F_\varepsilon(y)=\int_0^y g'_\varepsilon(z)zdz$ and employing the Poisson equation (4), the second integral in (34) can be estimated as

$$\begin{aligned}&\frac{D}{\eta}\int_0^t\int_\Omega\Big(\frac14 g'_\varepsilon(|\vec{n}_\perp|^2)\big|\nabla(|\vec{n}_\perp|^2)\big|^2+g_\varepsilon(|\vec{n}_\perp|^2)\|\nabla\vec{n}_\perp\|^2\\&+g'_\varepsilon(|\vec{n}_\perp|^2)|\vec{n}_\perp|^2\nabla(|\vec{n}_\perp|^2)\cdot\nabla V+\frac12 g_\varepsilon(|\vec{n}_\perp|^2)\nabla(|\vec{n}_\perp|^2)\cdot\nabla V\Big)dx\,ds\\&\geqslant\frac{D}{2\eta}\int_0^t\int_\Omega\nabla\big(2F_\varepsilon(|\vec{n}_\perp|^2)+G_\varepsilon(|\vec{n}_\perp|^2)\big)\cdot\nabla V dx\,ds\\&=\frac{D}{2\eta\lambda_D^2}\int_0^t\int_\Omega\big(2F_\varepsilon(|\vec{n}_\perp|^2)+G_\varepsilon(|\vec{n}_\perp|^2)\big)(n_0-C(x))dx\,ds\\&\geqslant-\frac{D}{2\eta\lambda_D^2}\|C\|_{L^\infty(\Omega)}\int_0^t\int_\Omega\big(2F_\varepsilon(|\vec{n}_\perp|^2)+G_\varepsilon(|\vec{n}_\perp|^2)\big)dx\,ds.\end{aligned}$$

We have proved that

$$\frac{d}{dt}\int_\Omega G_\varepsilon(|\vec{n}_\perp|^2)dx\leqslant\frac{D}{\eta\lambda_D^2}\|C\|_{L^\infty(\Omega)}\int_0^t\int_\Omega\big(2F_\varepsilon(|\vec{n}_\perp|^2)+G_\varepsilon(|\vec{n}_\perp|^2)\big)dx\,ds.$$

Elementary estimations show that $F_\varepsilon(y)\leqslant qG_\varepsilon(y)$ for all $y\geqslant 0$, yielding

$$\frac{d}{dt}\int_\Omega G_\varepsilon(|\vec{n}_\perp|^2)dx\leqslant K(2q+1)\int_\Omega G_\varepsilon(|\vec{n}_\perp|^2)dx,\quad K=\frac{D}{\eta\lambda_D^2}\|C\|_{L^\infty(\Omega)}.$$

Then Gronwall's lemma and the assumption $|\vec{n}_\perp(0)|\in L^\infty(\Omega)$ give for all $t>0$,

$$\begin{aligned}\int_\Omega G_\varepsilon(|\vec{n}_\perp(t)|^2)dx&\leqslant e^{K(2q+1)t}\int_\Omega G_\varepsilon(|\vec{n}_\perp(0)|^2)dx\\&\leqslant e^{K(2q+1)t}\int_\Omega|\vec{n}_\perp(0)|^{2q}dx.\end{aligned}$$

By dominated convergence, we can pass to the limit $\varepsilon \to 0$. Then, taking the $2q$-th root,

$$\|\vec{n}_\perp(t)\|_{L^{2q}(\Omega)} \leqslant e^{2Kt}\|\vec{n}_\perp(0)\|_{L^{2q}(\Omega)}, \quad t > 0.$$

The right-hand side is bounded uniformly in $q < \infty$. Therefore, the limit $q \to \infty$ leads to

$$\|\vec{n}_\perp(t)\|_{L^\infty(\Omega)} \leqslant e^{2Kt}\|\vec{n}_\perp(0)\|_{L^\infty(\Omega)}, \quad t > 0,$$

which ends the proof. □

2.3 MONOTONICITY OF THE ENTROPY

In this section, we prove Proposition 2 and formula (25).

Proof of Proposition 2. The idea is to employ $(\log(n_+/\widetilde{n}_D) + V - V_D, \log(n_-/\widetilde{n}_D) + V - V_D)$ as a test function in (16)-(17), where $\widetilde{n}_D = \frac{1}{2}n_D$. Since the logarithm may be undefined, we need to regularize. We set

$$\begin{aligned}
H_\delta(t) &= \int_\Omega \left(h_\delta(n_+) + h_\delta(n_-) + \frac{\lambda_D^2}{2}|\nabla(V - V_D)|^2 \right) dx, \quad \delta > 0, \\
h_\delta(n_\pm) &= \int_{\widetilde{n}_D}^{n_\pm} \big(\log(s+\delta) - \log(\widetilde{n}_D + \delta) \big) ds \\
&= (n_\pm + \delta)(\log(n_\pm + \delta) - 1) - (\widetilde{n}_D + \delta)(\log(\widetilde{n}_D + \delta) - 1) \\
&\quad - (n_\pm - \widetilde{n}_D)\log(\widetilde{n}_D + \delta).
\end{aligned}$$

Then the pointwise convergence $h_\delta(n_\pm) \to h(n_\pm)$, where $h(n_\pm)$ is defined in (23), as $\delta \to 0$ holds. Since $n_\pm = \frac{1}{2}n_D = \widetilde{n}_D$ on $\partial\Omega$ and $-\lambda_D^2 \partial_t \Delta V = \partial_t(n_+ + n_-) \in L^2(0,T;H^{-1}(\Omega))$, we can differentiate H_δ to obtain

$$\begin{aligned}
\frac{dH_\delta}{dt} &= \langle \partial_t n_+, \log(n_+ + \delta) - \log(\widetilde{n}_D + \delta) \rangle \\
&\quad + \langle \partial_t n_-, \log(n_- + \delta) - \log(\widetilde{n}_D + \delta) \rangle + \lambda_D^2 \langle \partial_t \nabla V, \nabla(V - V_D) \rangle,
\end{aligned}$$

where $\langle \cdot, \cdot \rangle$ is the duality pairing between $H^{-1}(\Omega)$ and $H_0^1(\Omega)$. Observing that

$$\lambda_D^2 \langle \partial_t \nabla V, \nabla(V - V_D) \rangle = -\lambda_D^2 \langle \partial_t \Delta V, V - V_D \rangle = \langle \partial_t(n_+ + n_-), V - V_D \rangle,$$

it follows that

$$\begin{aligned}
\frac{dH_\delta}{dt} &= \langle \partial_t n_+, \log(n_+ + \delta) + V - \log(\widetilde{n}_D + \delta) - V_D \rangle \\
&\quad + \langle \partial_t n_-, \log(n_- + \delta) + V - \log(\widetilde{n}_D + \delta) - V_D \rangle \\
&= I_1 + I_2.
\end{aligned}$$

After inserting the evolution equation (16) for n_+, setting $J_+ = D_+(\nabla n_+ + n_+ \nabla V)$ with $D_\pm = D(1 \pm p)$, and integrating by parts, we find that the first term I_1 equals

$$\begin{aligned}
I_1 &= -\int_\Omega \big(J_+ \cdot \nabla(\log(n_+ + \delta) + V) - J_+ \cdot \nabla(\log(\widetilde{n}_D + \delta) + V_D) \big) dx \\
&\quad - \int_\Omega \frac{n_+ - n_-}{\tau} \big(\log(n_+ + \delta) + V - \log(\widetilde{n}_D + \delta) - V_D \big) dx.
\end{aligned}$$

By Young's inequality, the first integral becomes

$$\begin{aligned}
&\int_\Omega \left(-\frac{J_+}{n_+ + \delta}\cdot(\nabla n_+ + (n_+ + \delta)\nabla V)\right)dx \\
&\quad + \int_\Omega J_+ \cdot \nabla(\log(\widetilde{n}_D + \delta) + V_D)\,dx \\
&= \int_\Omega \left(-\frac{|J_+|^2}{D_+(n_+ + \delta)} - \frac{\delta J_+ \cdot \nabla V}{D_+(n_+ + \delta)}\right)dx \\
&\quad + \int_\Omega J_+ \cdot \nabla(\log(\widetilde{n}_D + \delta) + V_D)\,dx \\
&\leqslant -\int_\Omega \frac{|J_+|^2}{2D_+(n_+ + \delta)}\,dx + \delta^2 \int_\Omega \frac{|\nabla V|^2}{D_+(n_+ + \delta)}\,dx \\
&\quad + \int_\Omega (n_+ + \delta)|\nabla(\log(\widetilde{n}_D + \delta) + V_D)|^2\,dx \\
&\leqslant -\int_\Omega \frac{|J_+|^2}{2D_+(n_+ + \delta)}\,dx + \delta \int_\Omega \frac{|\nabla V|^2}{D_+}\,dx \\
&\quad + \int_\Omega (n_+ + \delta)|\nabla(\log(\widetilde{n}_D + \delta) + V_D)|^2\,dx.
\end{aligned}$$

The integral I_2 can be estimated in a similar way, eventually leading to

$$\begin{aligned}
\frac{dH_\delta}{dt} &\leqslant -\int_\Omega \left(\frac{|J_+|^2}{2D_+(n_+ + \delta)} + \frac{|J_-|^2}{2D_-(n_- + \delta)}\right)dx \\
&\quad + \delta \int_\Omega \left(\frac{1}{D_+} + \frac{1}{D_-}\right)|\nabla V|^2\,dx \\
&\quad + \int_\Omega \big((n_+ + \delta) + (n_- + \delta)\big)|\nabla(\log(\widetilde{n}_D + \delta) + V_D)|^2\,dx \\
&\quad - \int_\Omega \frac{n_+ - n_-}{\tau}\big(\log(n_+ + \delta) - \log(n_- + \delta)\big)\,dx.
\end{aligned}$$

The last integral is nonnegative since $x \mapsto \log(x + \delta)$ is an increasing function. Therefore,

$$\begin{aligned}
H_\delta(t) &\leqslant H_\delta(0) + \delta \int_0^t \int_\Omega \left(\frac{1}{D_+} + \frac{1}{D_-}\right)|\nabla V|^2\,dx\,dt \\
&\quad + \int_0^t \int_\Omega \big((n_+ + \delta) + (n_- + \delta)\big)|\nabla(\log(\widetilde{n}_D + \delta) + V_D)|^2\,dx\,ds.
\end{aligned} \tag{35}$$

Since $\log \widetilde{n}_D + V_D = \text{const.}$ and $n_D \geqslant n_* > 0$, the gradient term in the last integral can be estimated by

$$\begin{aligned}
&|\nabla(\log(\widetilde{n}_D + \delta) + V_D)|^2 \\
&= \big|\nabla(\log \widetilde{n}_D + V_D) + \nabla(\log(\widetilde{n}_D + \delta) - \log \widetilde{n}_D)\big|^2 \leqslant \frac{\delta^2 |\nabla \widetilde{n}_D|^2}{\frac{1}{2}n_*(\frac{1}{2}n_* + \delta)},
\end{aligned}$$

and the right-hand side is bounded in $L^\infty(\Omega)$ uniformly in δ.

Therefore, the last two integrals in (35) can be bounded from above by a multiple of H_δ. Then Gronwall's lemma shows that H_δ is bounded uniformly in $\delta \in (0, 1)$. By dominated convergence, we can pass to the limit $\delta \to 0$ in the integrals, leading to $H_\delta(t) \leqslant H_0(0)$ for $t > 0$, where we used that $\nabla(\log \widetilde{n}_D + V_D) = 0$. This finishes the proof. □

Remark 3. We prove formula (25). For this, we first observe that $\partial_t \operatorname{tr}[N(\log N - \log N_D - 1)] = \operatorname{tr}[\partial_t N(\log N - \log N_D)]$ holds for smooth positive definite Hermitian matrices N; see the proof of Theorem 3 in [42]. We assume that $\log(n_D/2) + V_D = c \in \mathbb{R}$ in Ω (thermal equilibrium). Then $\log N_D + V_D \sigma_0 =$

$c\sigma_0$ in Ω. Now, using the Poisson equation (4), a formal computation leads to

$$\begin{aligned}\frac{dH_Q}{dt} &= \int_\Omega \big(\operatorname{tr}[\partial_t N(\log N - \log N_D)] + \lambda_D^2 \partial_t \nabla V \cdot \nabla(V - V_D)\big)\,dx \\ &= \int_\Omega \big(\operatorname{tr}[\partial_t N(\log N - \log N_D)] + \partial_t(\operatorname{tr}(N) - C(x))(V - V_D)\big)\,dx \\ &= \int_\Omega \operatorname{tr}\left[\partial_t N(\log N - \log N_D + (V - V_D)\sigma_0)\right]dx.\end{aligned}$$

Then, with the evolution equation (1) for N, an integration by parts, and the property $\log N_D + V_D\sigma_0 = c\sigma_0$ in Ω, we obtain

$$\begin{aligned}\frac{dH_Q}{dt} &= -\int_\Omega \sum_{j=1}^3 D(x)\operatorname{tr}\left[P^{-1/2}(\partial_j N + N\partial_j V)P^{-1/2}\partial_j(\log N + V\sigma_0)\right]dx \\ &\quad - i\gamma\int_\Omega \operatorname{tr}\left[[N, \vec{m}\cdot\vec{\sigma}](\log N + V\sigma_0)\right]dx \\ &\quad + \frac{1}{\tau}\int_\Omega \operatorname{tr}\left[\left(\frac{1}{2}\operatorname{tr}(N)\sigma_0 - N\right)(\log N + V\sigma_0)\right]dx \\ &= I_1 + I_2 + I_3.\end{aligned}$$

We compute the three integrals term by term. Employing the invariance of the trace under cyclic permutations and the commutativity relation $\log(N)N = N\log(N)$ gives

$$\operatorname{tr}\left[[N, \vec{m}\cdot\vec{\sigma}]\log N\right] = \operatorname{tr}\left[\vec{m}\cdot\vec{\sigma}\log(N)N - \vec{m}\cdot\vec{\sigma}N\log(N)\right] = 0,$$

which shows that $I_2 = 0$. For the integral I_3, the spectral property $\operatorname{tr}[f(A)] = \sum_j f(\lambda_j)$ for any continuous function f and any Hermitian matrix A with (real) eigenvalues λ_j, we have

$$\begin{aligned}\operatorname{tr}\left[\left(\frac{1}{2}\operatorname{tr}(N)\sigma_0 - N\right)(\log N + V\sigma_0)\right] &= \frac{1}{2}\operatorname{tr}[N]\operatorname{tr}[\log N] - \operatorname{tr}[N\log N] \\ &= \frac{1}{2}n_0\left(\log\left(\frac{1}{2}n_0 + |\vec{n}|\right) + \log\left(\frac{1}{2}n_0 - |\vec{n}|\right)\right) \\ &\quad - \left(\frac{1}{2}n_0 + |\vec{n}|\right)\log\left(\frac{1}{2}n_0 + |\vec{n}|\right) - \left(\frac{1}{2}n_0 - |\vec{n}|\right)\log\left(\frac{1}{2}n_0 - |\vec{n}|\right) \\ &= -|\vec{n}|\left(\log\left(\frac{1}{2}n_0 + |\vec{n}|\right) - \log\left(\frac{1}{2}n_0 - |\vec{n}|\right)\right) \leqslant 0.\end{aligned}$$

Hence, $I_3 \leqslant 0$. The integral I_1 remains unchanged. This proves (25). □

2.4 NUMERICAL SIMULATIONS

In this section, we solve equations (5)-(12) numerically for a one-dimensional ballistic diode in a multilayer structure. The aim is twofold: First, we present simulations of the stationary state and detail the differences between the numerical solutions with and without Poisson equation. Second, we show numerically that the entropy (23) decreases exponentially fast in time.

The multilayer consists of a ferromagnetic layer sandwiched between two nonmagnetic layers. More precisely, let $\Omega = (0, L)$. The nonmagnetic layers $(0, \ell_1)$ and (ℓ_2, L) are characterized by $\vec{m} = 0$, $p = 0$ and a high doping concentration, $C(x) = C_{max}$ for $x \in (0, \ell_1) \cup (\ell_2, L)$, whereas the magnetic layer (ℓ_1, ℓ_2) features a nonvanishing precession vector, $\vec{m} = (0, 0, 1)^\top$ and $p > 0$, and a low doping, $C(x) = C_{min}$ for $x \in (\ell_1, \ell_2)$. This multilayer structure was numerically solved in [36] but for constant electric fields only and without doping.

The boundary conditions read as

$$n_0(0,t) = n_0(L,t) = C_{max}, \quad \vec{n}(0,t) = \vec{n}(L,t) = 0, \quad V(0,t) = 0,\ V(L,t) = U$$

for all $t > 0$, and the initial conditions are $n_0(x) = 1$, $\vec{n}(x) = 0$, and $V(x) = Ux/L$ for $x \in \Omega$ and for some $U > 0$. We choose $C_{max} = 10^{21}\,m^{-3}$ and $C_{min} = 0.4 \cdot 10^{19}\,m^{-3}$. This corresponds to an overall low-doping situation. With larger doping concentrations, we observed numerical problems in the Poisson equation due to the smallness of the scaled Debye length λ_D. This problem is well known and can be solved by employing more sophisticated numerical methods.

We choose the same physical parameters as in [36]: the diffusion coefficient $D = 10^{-3}\,m^2s^{-1}$, the thermal voltage $V_{th} = 0.0259\,V$, the spin-flip relaxation time $\tau = 10^{-12}\,s$, the strength of the pseudo-exchange field $\gamma = 2\hbar/\tau$, and the applied potential $U = 1\,V$. Typically, the spin-flip relaxation time is of the order of a few to 100 picoseconds.[20] The layers have the same length of $0.4\,\mu m$ such that the device length equals $L = 1.2\,\mu m$.

2.4.1 *Implementation*

The equations are discretized in time by the implicit Euler approximation and in space by a node-centered finite-volume method. This method is conservative and is able to deal with discontinuous coefficients. We choose a uniform grid of M points $x_i = i\triangle x$ with step size $\triangle x > 0$, containing the interface points ℓ_1 and ℓ_2, and uniform time steps $t_k = k\triangle t$ with step size $\triangle t > 0$. We also introduce the cell-center points $x_{i+1/2} = (i+1/2)\triangle x$. Denoting by $n_{\ell,i}^k$ an approximation of $(\triangle x)^{-1}\int_{x_{i-1/2}}^{x_{i+1/2}} n_\ell(x,t_k)dx$ for $\ell = 0,1,2,3$ (the index of the spin component), the discretization of (5)-(6) reads as follows:

$$\frac{1}{\triangle t}(n_{0,i}^k - n_{0,i}^{k-1}) + \frac{1}{\triangle x}(j_{0,i+1/2}^k - j_{0,i-1/2}^k) = 0, \tag{36}$$

$$\frac{1}{\triangle t}(n_{\ell,i}^k - n_{\ell,i}^{k-1}) + \frac{1}{\triangle x}(j_{\ell,i+1/2}^k - j_{\ell,i-1/2}^k) - \frac{2\gamma}{\hbar}(\vec{n}_i^k \times \vec{m}_i)_\ell + \frac{1}{\tau}n_{\ell,i}^k = 0, \tag{37}$$

where $\ell = 1,2,3$, $\vec{n}_i^k = (n_{1,i}^k, n_{2,i}^k, n_{3,i}^k)$, $\vec{m}_i = (m_{1,i}, m_{2,i}, m_{3,i}) = \vec{m}(x_i)$, and

$$\begin{aligned}
j_{0,i+1/2}^k &= -\frac{D}{\eta_{i+1/2}^2}\left(J_{0,i+1/2}^k - 2p_{i+1/2}\vec{J}_{i+1/2}^k \cdot \vec{m}_{i+1/2}\right),\\
j_{\ell,i+1/2}^k &= -\frac{D}{\eta_{i+1/2}^2}\left(\eta_{i+1/2}J_{\ell,i+1/2}^k + (1-\eta_{i+1/2})\right.\\
&\qquad \left.\times(\vec{J}_{i+1/2}^k \cdot \vec{m}_{i+1/2})m_{\ell,i+1/2} - \frac{p_{i+1/2}}{2}J_{0,i+1/2}^k m_{\ell,i+1/2}\right),\\
J_{\ell,i+1/2}^k &= \frac{1}{\triangle x}\left((n_{\ell,i+1}^k - n_{\ell,i}^k) + \frac{1}{2}(n_{\ell,i+1}^k + n_{\ell,i}^k)(V_{i+1}^k - V_i^k)\right),\\
&\qquad \ell = 0,1,2,3.
\end{aligned}$$

where $\vec{J}_{i+1/2}^k = (J_{\ell,i+1/2}^k)_{\ell=1,2,3}$. The discrete electric potential V_i^k, which is scaled by the thermal voltage V_{th}, is obtained from the Poisson equation, discretized by central finite differences. The nonlinear discrete system is solved by the Gummel method, i.e., given $(n_{\ell,i}^{k-1}, V_i^{k-1})$ and setting $\rho_i = n_{0,i}^{k-1}\exp(-V_i^{k-1})$, we solve first the nonlinear system

$$-\lambda_D^2(V_{i+1}^k - 2V_i^k + V_{i-1}^k) = \rho_i e^{V_i^k} - C(x_i),$$

by Newton's method. Then, using the updated potential (V_i^k), the discrete system (36)-(37) is solved for $n_{\ell,i}^k$, and the procedure is iterated. For details on the Gummel method, we refer to [31]. We have chosen 60 grid points in each layer (i.e. $M = 180$) and the time step size $\triangle t = 0.005\tau$. These values are chosen in such a way that further refinement did not change the results.

2.4.2 *Numerical simulations*

We compute the solution to the above numerical scheme for "large" time until the steady state is approximately reached. We compare the numerical results for the case of a fixed linear potential (i.e. without Poisson equation, as in [36]) and for the self-consistent case (with Poisson equation).

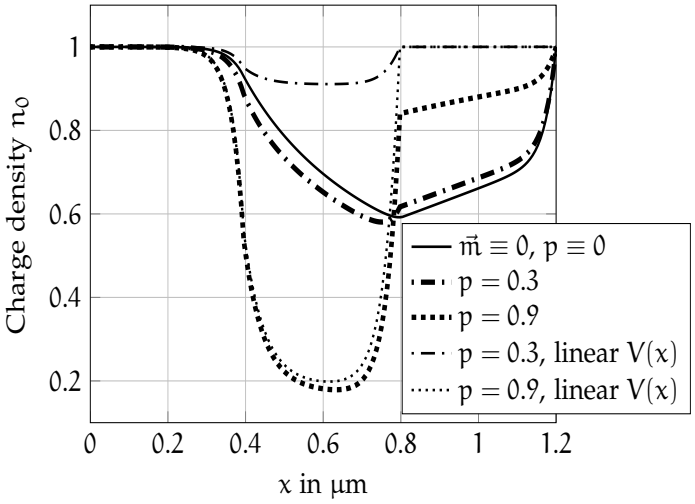

Figure 3: Charge density n_0 in the three-layer structure with different spin polarizations p.

The (scaled) stationary charge density n_0 and spin-vector density $\vec{n} = (0, 0, n_3)$ in both cases are presented in Figure 3 and Figure 4. With linear potential, the charge density (Figure 3) becomes significantly smaller in the ferromagnetic region but the decrease is similar at the left and right interface. In contrast, the self-consistent simulations show a decrease of the charge density in the right layer. This can be explained by the rather small doping concentration and large voltage, which causes the electrons to drift to the right contact. For small values of the spin polarization p, the charge density is similar to the charge density computed with vanishing precession vector. When the spin polarization p increases, the charge density is reduced in the ferromagnetic layer and increases in the right nonmagnetic region.

In Figure 4, we present the simulations of the spin density in the self-consistent case. The plot demonstrates the local nonequilibrium spin concentration on the interfaces between non- and ferromagnetic materials, which exponentially decays diffusing inside the layers. This behavior is in a good correspondence with the literature (e.g. [36], [45]). The results with linear potential are similar, but the self-consistent potential leads to a slight reduction of the peaks of the spin density.

Our numerical results correspond to those in [36, Figure 1] except for the values of the charge density n_0 in the right layer. Possanner and Negulescu found that n_0 is strictly smaller than the doping concentration and that there is a small boundary layer at $x = L$.

In order to understand this difference, we have implemented the scheme of [36], which consists of a standard Crank-Nicolson discretization in each

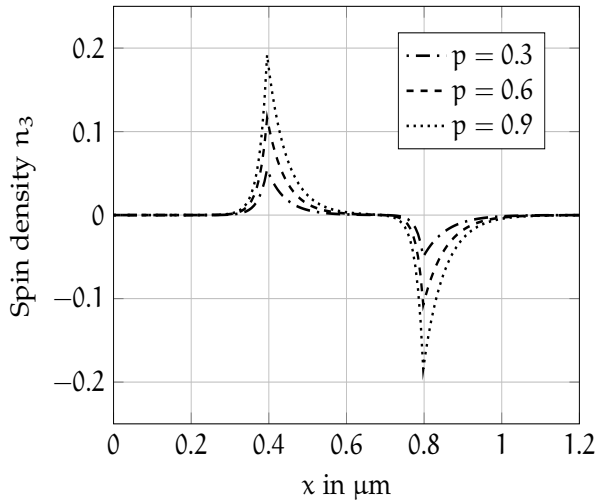

Figure 4: Spin density n_3 in the three-layer structure with different spin polarizations p. The potential is computed self-consistently.

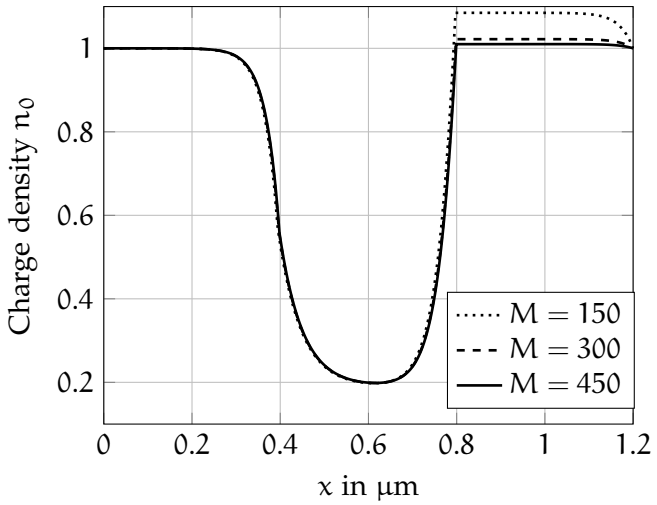

Figure 5: Charge density n_0 computed from the scheme in [36] (without Poisson equation) for different grid point numbers M.

of the layers, together with continuity conditions for n_0, $\vec{n}$, j_0, and $\vec{j} = (j_1, j_2, j_3)$ at the interfaces $x = \ell_1$ and $x = \ell_2$. The numerical result for n_0 is shown in Figure 5. This does not correspond exactly to the outcome of [36] since our charge density is strictly *larger* than the doping in the right layer. Refining the mesh, however, we see that n_0 becomes closer to the doping and to the behavior shown in Figure 3 (linear $V(x)$). This supports the validity of the numerical results computed from the finite-volume scheme.

Next, we consider a smaller device with length $L = 0.4\,\mu m$ and a higher level of doping, $C_{max} = 9 \cdot 10^{21}\ m^{-3}$. With these parameters, the scaled Debye length is the same as in the previous case. As a consequence, the charge density with vanishing precession vector does not change. The influence of the spin polarization is similar as in the previous test case (see Figure 6), but the charge density is larger in the ferromagnetic layer due to the reduced size.

Our final example is concerned with a transient simulation. As initial data, we choose $V = 0$, $n_0 = 1$, and $\vec{n} = 0$. Figure 7 presents the time decay of the entropy (free energy) H_0, defined in (23). It turns out that $H_0(t)$ is decaying exponentially fast with approximate decay rate 0.12. For times $t > 270\,ps$,

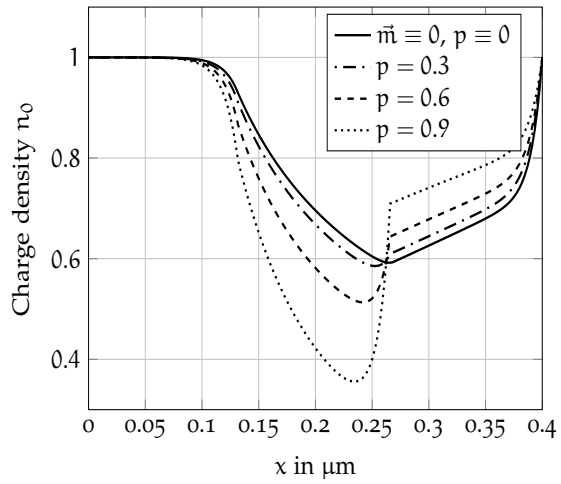

Figure 6: Charge density n_0 in the three-layer structure with self-consistent potential and smaller device length $L = 0.4\,\mu m$.

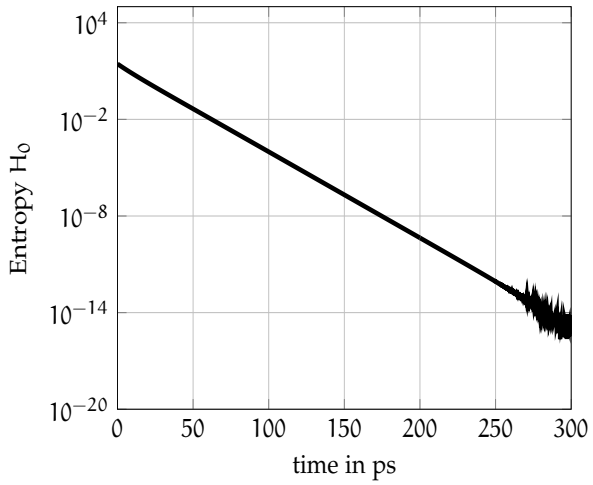

Figure 7: Semilogarithmic plot of the entropy $H_0(t)$ versus time.

the equilibrium state is almost attained, and since we reached the computer precision of about 10^{-16}, we observe some oscillations in the values for H_0. We recall that in the one-dimensional case, the entropies H_0 and H_Q, defined in (24), coincide.

3

FINITE VOLUME SCHEME

We design a numerical scheme for the system (5)-(11), (13)-(15) which preserves some qualitative properties of the continuous model, in particular preservation of the positivity of the charge density, boundedness of the density matrix, and dissipation of the free energy.

The chapter is organized as follows. In Section 3.1, we detail the numerical scheme and present the main results, in particular the existence of discrete solutions (Theorem 3) and the dissipativity of the discrete free energy (Theorem 4). The proofs are given in Sections 3.2 and 3.3. Some numerical tests are presented in Section 3.4.

3.1 NUMERICAL METHOD AND MAIN RESULTS

3.1.1 *Notations*

Before we state the numerical scheme, we need to define the mesh of the domain Ω and to introduce some notation. We consider the two-dimensional case only but the scheme can be generalized in a straightforward way to higher dimensions.

Let $\Omega \subset \mathbb{R}^2$ be an open bounded polygonal set. The mesh $\mathcal{M} = (\mathcal{T}, \mathcal{E}, \mathcal{P})$ is given by a family $\mathcal{T}$ of open polygonal control volumes or cells, a family $\mathcal{E}$ of edges, and a family $\mathcal{P} = (x_K)_{K\in\mathcal{T}}$ of points. We assume that the mesh is admissible in the sense of Definition 9.1 in [18]. This definition implies that the straight line between two neighboring centers of cell (x_K, x_L) is orthogonal to the edge $\sigma = K|L$ between two control volumes K and L and therefore collinear to the unit normal vector $\nu_{K,\sigma}$ to σ outward to K. For instance, triangular meshes satisfy the admissibility condition if all angles of the triangles are smaller than $\pi/2$ [18, Example 9.1]. Voronoi meshes are also admissible meshes [18, Example 9.2].

Each edge $\sigma \in \mathcal{E}$ is either an internal edge, $\sigma = K|L$, or an exterior edge, $\sigma \subset \partial\Omega$, and we set $\mathcal{E} = \mathcal{E}_{int} \cup \mathcal{E}_{ext}$. We assume that each exterior edge is an element of either the Dirichlet or Neumann boundary such that we can set $\mathcal{E}_{ext} = \mathcal{E}_{ext}^D \cup \mathcal{E}_{ext}^N$. For a given control volume $K \in \mathcal{T}$, we define the set $\mathcal{E}_K$ of the edges of K, which can be written as the union of $\mathcal{E}_{K,int}$, $\mathcal{E}_{K,ext}^D$, and $\mathcal{E}_{K,ext}^N$. For every $\sigma \in \mathcal{E}$, there exists at least one cell $K \in \mathcal{T}$ satisfying $\sigma \in \mathcal{E}_K$, and we denote this cell by K_σ. When σ is an interior edge with $\sigma = K|L$, we have $K_\sigma = K$ or $K_\sigma = L$.

For $K \in \mathcal{T}$ and $\sigma \in \mathcal{E}_K$, we denote by $d_{K,\sigma}$ the distance $d_{K,\sigma} = d(x_K, \sigma)$. Then, for $\sigma \in \mathcal{E}_{int}$, $\sigma = K|L$, we define $d_\sigma = d_{K,\sigma} + d_{L,\sigma} = d(x_K, x_L)$ and for $\sigma \in \mathcal{E}_{ext}$ with $\sigma \in \mathcal{E}_K$, $d_\sigma = d_{K,\sigma}$. Furthermore, the measure of $\sigma \in \mathcal{E}$ or a set $\omega \subset \Omega$ is denoted by $m(\sigma)$ or $m(\omega)$, respectively. In the numerical scheme, we need the so-called transmissibility coefficient $\tau_\sigma = m(\sigma)/d_\sigma$ for $\sigma \in \mathcal{E}$. We assume that the mesh satisfies the regularity constraint

$$\exists \xi > 0 : \ \forall K \in \mathcal{T} : \ \forall \sigma \in \mathcal{E}_K : \ d(x_K, \sigma) \geqslant \xi \mathrm{diam}(K). \tag{38}$$

The finite-volume scheme for a conservation law with unknown u provides a vector $u_\mathcal{T} = (u_K)_{K\in\mathcal{T}}$ of approximate values and the associated piecewise constant function, still denoted by $u_\mathcal{T}$, $u_\mathcal{T} = \sum_{K\in\mathcal{T}} u_K \mathbf{1}_K$, which approximates the unknown u. Here, $\mathbf{1}_K$ denotes the characteristic function of the cell K. The approximate values of the Dirichlet boundary provide a vector $u_{\mathcal{E}^D} = (u_\sigma)_{\sigma\in\mathcal{E}_{ext}^D}$. The vector containing the approximate values

in the control volumes and at the Dirichlet boundary edges is denoted by $u_{\mathcal{M}} = (u_{\mathcal{T}}, u_{\mathcal{E}_D})$.

The numerical scheme can be formulated in a compact form by introducing the following notation. For any vector $u_{\mathcal{M}} = (u_{\mathcal{T}}, u_{\mathcal{E}_D})$, we define, for all $K \in \mathcal{T}$ and $\sigma \in \mathcal{E}_K$,

$$u_{K,\sigma} = \begin{cases} u_L & \text{if } \sigma = K|L, \\ u_\sigma & \text{if } \sigma = \mathcal{E}_{K,\text{ext}}^D, \\ u_K & \text{if } \sigma = \mathcal{E}_{K,\text{ext}}^N, \end{cases}$$

and we set $Du_{K,\sigma} = u_{K,\sigma} - u_K$. We remark that the definition of $u_{K,\sigma}$ ensures that $Du_{K,\sigma} = 0$ on the Neumann boundary edges. Then the discrete H^1 seminorm for $u_{\mathcal{M}}$ can be defined by

$$|u_{\mathcal{M}}|_{1,\mathcal{M}} = \left(\sum_{\sigma \in \mathcal{E}} \tau_\sigma |Du_{K,\sigma}|^2 \right)^{1/2},$$

where the summation is over all edges $\sigma \in \mathcal{E}$ with $K = K_\sigma$. The L^p norm of $u_{\mathcal{T}}$ reads as

$$\|u_{\mathcal{T}}\|_p = \left(\sum_{K \in \mathcal{T}} m(K) |u_K|^p \right)^{1/p} \quad \text{for } 1 \leqslant p < \infty$$
$$\text{and} \quad \|u_{\mathcal{T}}\|_\infty = \max_{K \in \mathcal{T}} |u_K|.$$

When formulating a finite-volume scheme, we have to define some numerical fluxes $J_{K,\sigma}$ which are consistent approximations of the exact fluxes through the edges $\int_\sigma J \cdot \nu_{K,\sigma} ds$. We impose the conservation of the numerical fluxes $J_{K,\sigma} + J_{L,\sigma}$ for $\sigma = K|L$, requiring that they vanish on the Neumann boundary edges, $J_{K,\sigma} = 0$ for $\sigma \in \mathcal{E}_{K,\text{ext}}^N$. Then the discrete integration-by-parts formula becomes

$$\sum_{K \in \mathcal{T}} \sum_{\sigma \in \mathcal{E}_K} J_{K,\sigma} u_K = - \sum_{\sigma \in \mathcal{E}} J_{K,\sigma} Du_{K,\sigma} + \sum_{\sigma \in \mathcal{E}_{\text{ext}}^D} J_{K,\sigma} u_{K,\sigma}. \tag{39}$$

3.1.2 *Numerical scheme*

At each time step $k \geqslant 0$, we define the approximate solution $u_{\mathcal{T}}^k = (u_K^k)_{K \in \mathcal{T}}$ for $u \in \{n_0, \vec{n}, V\}$ and the approximate values at the Dirichlet boundary, $u_{\mathcal{E}_D}^k = (u_\sigma^k)_{\sigma \in \mathcal{E}_{\text{ext}}^D}$ (which in fact does not depend on k since the boundary data is time-independent). We first define the initial and boundary conditions corresponding to (15) and (13). We set

$$(n_{0,K}^0, \vec{n}_K^0) = \frac{1}{m(K)} \int_K (n_0^0, \vec{n}^0) dx \quad \text{for all } K \in \mathcal{T}, \tag{40}$$
$$(n_{0,\sigma}^D, \vec{n}_\sigma^D, V_\sigma^D) = \frac{1}{m(\sigma)} \int_\sigma (n^D, \vec{0}, V^D) ds \quad \text{for all } \sigma \in \mathcal{E}_{\text{ext}}^D.$$

Note that $\vec{n}_\sigma^D = 0$ for $\sigma \in \mathcal{E}_{\text{ext}}^D$. We may define similarly the quantities $\vec{m}_K, C_K, D_{0,K}, p_K$ for a given $K \in \mathcal{T}$.

We consider a temporal implicit Euler and spatial finite-volume discretization. The scheme for (5), (6), (11) writes, for all $K \in \mathcal{T}$ and $k \geqslant 1$, as

$$m(K)\frac{n_{0,K}^k - n_{0,K}^{k-1}}{\triangle t} + \sum_{\sigma\in\mathcal{E}_K} j_{0,K,\sigma}^k = 0, \tag{41}$$

$$m(K)\frac{\vec{n}_K^k - \vec{n}_K^{k-1}}{\triangle t} + \sum_{\sigma\in\mathcal{E}_K} \vec{j}_{K,\sigma}^k - 2\gamma\, m(K)(\vec{n}_K^k \times \vec{m}_K) = -\frac{m(K)}{\tau}\vec{n}_K^k, \tag{42}$$

$$-\lambda_D^2 \sum_{\sigma\in\mathcal{E}_K} \tau_\sigma DV_{K,\sigma}^k = m(K)(n_{0,K}^k - C_K), \tag{43}$$

where the discrete counterpart to (8) is, for all $K \in \mathcal{T}$, $\sigma \in \mathcal{E}_K$, $k \geqslant 0$,

$$j_{0,K,\sigma}^k = \frac{D_\sigma}{\eta_\sigma^2}\left(J_{0,K,\sigma}^k - 2p_\sigma \vec{J}_{K,\sigma}^k \cdot \vec{m}_\sigma\right), \tag{44}$$

$$\vec{j}_{K,\sigma}^k = \frac{D_\sigma}{\eta_\sigma^2}\left(\eta_\sigma \vec{J}_{K,\sigma}^k + (1-\eta_\sigma)(\vec{J}_{K,\sigma}^k \cdot \vec{m}_\sigma)\vec{m}_\sigma - \frac{p_\sigma}{2} J_{0,K,\sigma}^k \vec{m}_\sigma\right). \tag{45}$$

The numerical fluxes $J_{0,K,\sigma}^k$ and $J_{\ell,K,\sigma}^k$ are approximations of the integrals $\int_\sigma J_0 \cdot \nu_{K,\sigma} ds$ and $\int_\sigma J_\ell \cdot \nu_{K,\sigma} ds$ at time $k\triangle t$, and we set $\vec{J}_{K,\sigma}^k = (J_{\ell,K,\sigma}^k)_{\ell=1,2,3}$. We recall that J_0 and $\vec{J}$ are defined by (9). We use a Scharfetter-Gummel approximation for the definition of the numerical fluxes. For given $K \in \mathcal{T}$ and $\sigma \in \mathcal{E}_K$, we set

$$J_{\ell,K,\sigma}^k = \tau_\sigma\left(B(DV_{K,\sigma}^k)n_{\ell,K}^k - B(-DV_{K,\sigma}^k)n_{\ell,K,\sigma}^k\right), \quad \ell = 0,1,2,3, \tag{46}$$

where B is the Bernoulli function defined by

$$B(x) = \frac{x}{\exp(x)-1} \text{ for } x \neq 0 \quad \text{and} \quad B(0) = 1.$$

It remains to define the quantities D_σ, $\vec{m}_\sigma$, p_σ and η_σ appearing in (44) and (45). We use a weighted harmonic average on the interior edges and a classical mean value on the boundary edges,

$$D_\sigma = \frac{d_\sigma D_{0,K} D_{0,L}}{d_{K,\sigma} D_{0,L} + d_{L,\sigma} D_{0,K}} \text{ for } \sigma \in \mathcal{E}_{\text{int}},\ \sigma = K|L,$$

$$D_\sigma = \frac{1}{m(\sigma)}\int_\sigma D_0(s)ds \text{ for } \sigma \in \mathcal{E}_{\text{ext}}^D,$$

and similar definitions for $\vec{m}_\sigma$ and p_σ. Furthermore, we set $\eta_\sigma = \sqrt{1-p_\sigma^2}$.

Finally, the boundary conditions are

$$n_{0,\sigma}^k = n_{0,\sigma}^D, \quad \vec{n}_\sigma^k = 0, \quad V_\sigma^k = V_\sigma^D \quad \text{for } \sigma \in \mathcal{E}_{\text{ext}}^D, \tag{47}$$

$$Dn_{\ell,K,\sigma}^k = DV_{K,\sigma}^k = 0 \quad \text{for } \sigma \in \mathcal{E}_{K,\text{ext}}^N,\ \ell = 0,1,2,3,\ k \geqslant 0. \tag{48}$$

We remark that they imply $J_{l,K,\sigma}^k = 0$ for $\sigma \in \mathcal{E}_{K,\text{ext}}^N$, $\ell = 0,1,2,3$, and $k \geqslant 0$.

For later use, we note that, using the elementary property $B(x) - B(-x) = -x$ for $x \in \mathbb{R}$, the numerical fluxes can be reformulated in two different manners:

$$J_{\ell,K,\sigma}^k = \tau_\sigma\left(-DV_{K,\sigma}^k n_{\ell,K}^k - B(-DV_{K,\sigma}^k)Dn_{\ell,K,\sigma}^k\right) \tag{49}$$

$$= \tau_\sigma\left(-DV_{K,\sigma}^k n_{\ell,K,\sigma}^k - B(DV_{K,\sigma}^k)Dn_{\ell,K,\sigma}^k\right), \quad \ell = 0,1,2,3, \tag{50}$$

and adding these expressions leads to a third formulation:

$$J_{\ell,K,\sigma}^k = \tau_\sigma\left(-\frac{1}{2}(n_{\ell,K}^k + n_{\ell,K,\sigma}^k)DV_{K,\sigma}^k - B^s(DV_{K,\sigma}^k)Dn_{\ell,K,\sigma}^k\right), \tag{51}$$

where

$$B^s(x) = \frac{x}{2}\coth\left(\frac{x}{2}\right) = \frac{B(x)+B(-x)}{2}. \tag{52}$$

3.1.3 *Main results*

We impose the following assumptions on the domain and the data:

$$\Omega \subset \mathbb{R}^2 \text{ bounded domain, } \partial\Omega = \Gamma^D \cup \Gamma^N,\ \Gamma^D \cap \Gamma^N = \emptyset, \quad (53)$$
$$m(\Gamma^D) > 0,\ \Gamma^N \text{ open,}$$
$$D_0,\ p,\ \lambda_D,\ \vec{m} \text{ are constant and } |\vec{m}| = 1,\ C \in L^\infty(\Omega),\ C(x) \geqslant 0, \quad (54)$$
$$n_0^0,\ \vec{n}^0,\ n^D \in L^\infty(\Omega),\ \frac{1}{2}n_0^0 \pm \vec{n}^0 \cdot m \geqslant 0,\ n^D \geqslant 0,\ n^D, \quad (55)$$
$$V^D \in H^1(\Omega),$$
$$\mathcal{M} = (\mathcal{T}, \mathcal{E}, \mathcal{P}) \text{ is an admissible mesh satisfying (38).} \quad (56)$$

We first remark that if $(n_{0,\mathcal{T}}^k, \vec{n}_{\mathcal{T}}^k, V_{\mathcal{T}}^k)$ is a solution to scheme (41)-(48) for a given $k \geqslant 1$ ($(n_{0,\mathcal{T}}^0, \vec{n}_{\mathcal{T}}^0)$ are defined as the discretization of the initial conditions), we can define $n_{\pm,\mathcal{T}}^k = \frac{1}{2}n_{0,\mathcal{T}}^k \pm \vec{n}_{\mathcal{T}}^k \cdot \vec{m}$, $\vec{n}_{\perp,\mathcal{T}}^k = \vec{n}_{\mathcal{T}}^k - (\vec{n}_{\mathcal{T}}^k \cdot \vec{m})\vec{m}$. Moreover, as n^D and V^D are defined on the whole domain Ω, we can define $n_{\mathcal{T}}^D$ and $V_{\mathcal{T}}^D$ by taking the mean value of n^D and V^D on each control volume $K \in \mathcal{T}$.

Then the following existence result holds.

Theorem 3 (Existence of a solution to the numerical scheme and L^∞ bounds)**.** *Let assumptions (53)-(56) hold. We impose the following constraints:*

$$\triangle t \leqslant \frac{1}{\alpha} := \frac{\lambda_D^2}{D_0(1+p)\|C\|_\infty}, \quad \tau \leqslant \frac{\eta\lambda_D^2}{D_0\|C\|_\infty}. \quad (57)$$

Then for $k \geqslant 1$, there exists a solution $(n_{0,\mathcal{T}}^k, \vec{n}_{\mathcal{T}}^k, V_{\mathcal{T}}^k)$ to scheme (41)-(48) satisyfing

$$0 \leqslant n_{0,\mathcal{T}}^k \leqslant 2M^0, \quad 0 \leqslant n_{\pm,\mathcal{T}}^k \leqslant M^0, \quad |\vec{n}_{\mathcal{T}}^k| \leqslant 2M^k \quad \text{in } \Omega,$$

where $M^k = M^0(1-\alpha\triangle t)^{-k}$ and

$$M^0 = \max\left(\frac{1}{2}\sup_{\partial\Omega} n^D,\ \sup_\Omega\left(\frac{1}{2}n_0^0 + |\vec{n}^0 \cdot \vec{m}|\right),\ \sup|\vec{n}_\perp^0|,\ \sup_\Omega C\right).$$

In the continuous case, similar L^∞ bounds for the spin-up and spin-down densities, and therefore for the electron charge density, are shown in Chapter 2. These bounds do not depend on time. The mixing of the spin-vector components prevents the use of the monotonicity argument for $\vec{n}_\perp$, solving (20). Therefore, both in the continuous and discrete situations, the L^∞ bound for the spin-vector density depends on time.

The constraint on $\triangle t$ is needed in the definition of M^k. Furthermore, the condition on τ is necessary to prove the L^∞ bound for $\vec{n}_{\perp,\mathcal{T}}^k$. The numerical results presented in Section 3.4 indicate that the latter restriction is technical. We stress the fact that our scheme is unconditionally stable if the semiconductor is undoped, i.e. $C = 0$. In this situation, $\triangle t$ and τ can be chosen arbitrarily.

Let us discuss the conditions under which the constraint on τ in (57) is satisfied. Choosing $\tau_s = \tau^*$ (see Remark 2) and observing that the scaled doping profile satisfies $\|C\|_\infty = 1$, we obtain

$$\frac{D^*\tau^*}{L^2} = D_0 \leqslant \eta\lambda_D^2 = \frac{\eta\varepsilon_r\varepsilon_0 U_T}{q_e L^2 \sup_\Omega C},$$

where ε_r is the relative permittivity of the material, ε_0 the permittivity of vacuum, and q_e the elementary charge. This gives a bound on the spin-flip relaxation time or the maximal physical doping value:

$$\tau^* \sup_\Omega C \leqslant \frac{\eta\varepsilon_r\varepsilon_0 U_T}{q_e D^*}.$$

For silicon at room temperature and with the choice $D^* = 10^{-3}\,m^2 s^{-1}$ (see Section 3.4), we obtain $\tau^* \sup_\Omega C \leqslant 10^7 \eta\, m^3 s$. With the relaxation time $\tau^* = 10^{-12}\,s$, a small spin polarization (such that $\eta \approx 1$), the above bound is satisfied for lowly doped semiconductors, $\sup_\Omega C \lesssim 10^{19}\,m^{-3}$.

We note that Stampacchia's method applied to the discrete Poisson equation (43) gives an L^∞ bound for the electric potential $V_\mathcal{T}^k$. This bound depends on M^0 and is uniform in time. The proof follows the lines of the proof for the continuous equation; see e.g. [44, Section 2.3].

Next, we prove that the scheme dissipates the discrete free energy. Using the notation $\sum_\pm a_\pm = a_+ + a_-$, the continuous (relative) free energy $H_0(t)$ (23) for the system (16)-(18) can be reformulated as

$$H_0(t) = E(t) = \sum_\pm \int_\Omega \left(n_\pm(\log n_\pm - 1) - n_\pm \log \frac{n^D}{2} + \frac{n^D}{2} \right) dx + \frac{\lambda_D^2}{2} \int_\Omega |\nabla(V - V^D)|^2 dx. \tag{58}$$

Thus, the discrete free energy could be defined by

$$E^k = \sum_\pm \sum_{K\in\mathcal{T}} m(K) \left(n_{\pm,K}^k (\log n_{\pm,K}^k - 1) - n_{\pm,K}^k \log \frac{n_K^D}{2} + \frac{n_K^D}{2} \right) + \frac{\lambda_D^2}{2} \sum_{\sigma\in\mathcal{E}} \tau_\sigma (D(V^k - V^D)_{K,\sigma})^2. \tag{59}$$

Theorem 4 (Dissipation of the discrete free energy)**.** *Let assumptions* (53)-(56) *hold and let* $(n_{0,\mathcal{T}}^k, \vec{n}_\mathcal{T}^k, V_\mathcal{T}^k)_{k\geqslant 0}$ *be a solution to scheme* (41)-(48) *satisfying* $0 \leqslant n_{\pm,\mathcal{T}}^k \leqslant M^0$. *We further assume that* $n^D \geqslant n_* > 0$ *and that* $\log(n^D/2) + V^D$ *is constant in* $\overline{\Omega}$. *Then the mapping* $k \mapsto E^k$ *is nonincreasing, i.e., the scheme dissipates the free energy* (59)*:*

$$E^k + \frac{\triangle t}{2} \sum_\pm D_0(1 \pm p) \sum_{\sigma\in\mathcal{E}} \tau_\sigma \min\{n_{\pm,K}^k, n_{\pm,K,\sigma}^k\} \big(D(\log n_\pm^k + V^k)_{K,\sigma}\big)^2 \leqslant E^{k-1}, \quad k \geqslant 1. \tag{60}$$

The above dissipation inequality for the free energy is the discrete counterpart of the continuous estimate (35) for the free energy (58):

$$E(t_2) + \frac{1}{2} \int_{t_1}^{t_2} \int_\Omega \sum_\pm D_0(1 \pm p) n_\pm |\nabla(\log n_\pm + V)|^2 dx ds \leqslant E(t_1), \quad 0 \leqslant t_1 \leqslant t_2.$$

The energy dissipation vanishes if $\log n_\pm + V = \text{const.}$. This equation coincides with the definition of the thermodynamic equilibrium (together with $\vec{n} = 0$ and V solving (43)). Consequently, the assumption $\log(n^D/2) + V^D = \text{const.}$ in Theorem 4, imposed on the Dirichlet boundary, means that we require that the Dirichlet boundary data is compatible with the thermodynamic equilibrium.

Since our estimates are local in time, we may also use nonconstant time step sizes $\triangle t^k$ as long as condition (57) is satisfied.

One may ask if the discrete solution converges to the continuous one when the approximation parameters tend to zero. However, it seems to be difficult to extract a discrete gradient estimate for $n_{\pm,\mathcal{T}}^k$ from the discrete free energy estimate in Theorem 4 since we do not have a suitable discrete version of the chain rule $n_\pm |\nabla \log n_\pm|^2 = 4|\nabla \sqrt{n_\pm}|^2$.

3.2 PROOF OF THEOREM 3

The proof of Theorem 3 will be presented in two subsections. We first establish the existence of a solution $(n_{0,\mathcal{T}}^k, \vec{n}_{\mathcal{T}}^k, V_{\mathcal{T}}^k)$ at each time step $k \geqslant 1$ by an induction argument. The proof is based on the fixed-point theorem of Brouwer. In this subsection, we also show L^∞ bounds on $n_{0,\mathcal{T}}^k$ and $n_{\pm,\mathcal{T}}^k$ which depend on k. Then, in the second subsection, we prove that these bounds are in fact uniform with respect to k.

3.2.1 *Existence of a solution to the scheme*

We first note that the initial condition $(n_{0,\mathcal{T}}^0, \vec{n}_{\mathcal{T}}^0)$ is well-defined by (40). Moreover, the definition of M^0 ensures that $|n_{\perp,\mathcal{T}}^0| \leqslant M^0$, $0 \leqslant n_{\pm,\mathcal{T}}^0 \leqslant M^0$ and therefore $0 \leqslant n_{0,\mathcal{T}}^0 \leqslant 2M^0$ and $|\vec{n}_{\pm,\mathcal{T}}^0| \leqslant 2M^0$.

The proof is done by induction. Let $k \geqslant 1$. Assuming that $(n_{0,\mathcal{T}}^{k-1}, \vec{n}_{\mathcal{T}}^{k-1}, V_{\mathcal{T}}^{k-1})$ is given and verifies $|n_{\perp,\mathcal{T}}^{k-1}| \leqslant M^{k-1}$, $0 \leqslant n_{\pm,\mathcal{T}}^{k-1} \leqslant M^{k-1}$, we will prove the existence of $(n_{0,\mathcal{T}}^k, \vec{n}_{\mathcal{T}}^k, V_{\mathcal{T}}^k)$, solution to (41)-(48), satisfying these bounds with k instead of $k-1$. Scheme (41)-(48) is a nonlinear system of equations. We prove the existence of a solution by using a fixed-point theorem. Let us denote by θ the cardinality of the mesh $\mathcal{T}$ (the number of control volumes) and let $\mu > 0$. We define an application $F_\mu^k : \mathbb{R}^{4\theta} \to \mathbb{R}^{4\theta}$ such that $F_\mu^k(\rho_{\mathcal{T}}) = n_{\mathcal{T}}$, where $\rho_{\mathcal{T}} = (\rho_{0,\mathcal{T}}, \vec{\rho}_{\mathcal{T}})$ and $n_{\mathcal{T}} = (n_{0,\mathcal{T}}, \vec{n}_{\mathcal{T}})$. It is based on a linearization of the scheme and defined in two steps:

- First, we define $V_{\mathcal{T}} \in \mathbb{R}^\theta$ as the solution to the linear system

$$-\lambda_D^2 \sum_{\sigma\in\mathcal{E}_K} \tau_\sigma DV_{K,\sigma} = m(K)(\rho_{0,K} - C_K) \quad \text{for } K \in \mathcal{T}, \tag{61}$$
$$V_\sigma = V_\sigma^D \text{ for } \sigma \in \mathcal{E}_{ext}^D, \quad DV_{K,\sigma} = 0 \text{ for } \sigma \in \mathcal{E}_{K,ext}^N.$$

- Second, we construct $n_{\mathcal{T}} = (n_{0,\mathcal{T}}, \vec{n}_{\mathcal{T}}) \in \mathbb{R}^{4\theta}$ as the solution to

$$\frac{m(K)}{\triangle t}(n_{0,K} - n_{0,K}^{k-1}) + \mu\frac{m(K)}{\triangle t}(n_{0,K} - \rho_{0,K}) \tag{62}$$
$$+ \sum_{\sigma\in\mathcal{E}_K} j_{0,K,\sigma} = 0 \quad \text{for } K \in \mathcal{T},$$
$$\frac{m(K)}{\triangle t}(n_{\ell,K} - n_{\ell,K}^{k-1}) + \mu\frac{m(K)}{\triangle t}(n_{\ell,K} - \rho_{\ell,K}) + \sum_{\sigma\in\mathcal{E}_K} j_{\ell,K,\sigma} \tag{63}$$
$$-2\gamma\, m(K)(\vec{n}_K \times \vec{m})_\ell = -\frac{m(K)}{\tau} n_{\ell,K} \quad \text{for } K \in \mathcal{T},\ \ell = 1,2,3,$$

  where $j_{0,K,\sigma}$ and $j_{\ell,K,\sigma}$ are defined in (44) and (45), with $J_{\ell,K,\sigma}$ defined in (46), but without the superindex k. The boundary conditions read as

$$n_{0,\sigma} = n_\sigma^D,\ n_{\ell,\sigma} = 0 \quad \text{for } \sigma \in \mathcal{E}_{ext}^D,\ \ell = 1,2,3, \tag{64}$$
$$Dn_{\ell,K,\sigma} = 0 \quad \text{for } \sigma \in \mathcal{E}_{K,ext}^N,\ K \in \mathcal{T},\ \ell = 0,1,2,3. \tag{65}$$

The parameter $\mu > 0$ allows us to prove unconditional stability for the linearized problem; see e.g. [8]. The corresponding term vanishes for fixed points $\rho_{\mathcal{T}} = n_{\mathcal{T}}$, so that a fixed point for F_μ^k is a solution to scheme (41)-(48). We choose

$$\mu \geqslant \frac{D_0\|C\|_\infty}{\lambda_D^2} \max\left\{\frac{1}{\eta^2}, \frac{1+p}{2}\right\} \triangle t. \tag{66}$$

The existence and uniqueness of $V_{\mathcal{T}}$, solution to (61), are obvious since the corresponding matrix is positive definite. As this matrix does not depend on $\rho_{\mathcal{T}}$ and the right-hand side is continuous with respect to $\rho_{\mathcal{T}}$, the first mapping $\rho_{\mathcal{T}} \mapsto V_{\mathcal{T}}$ is continuous from $\mathbb{R}^{4\theta}$ to $\mathbb{R}^{\theta}$. This property is not so obvious for the second mapping, based on the linear system of equations (62)-(65). We will prove this property below (Step 1), in order to guarantee that the mapping F_μ^k is well-defined and continuous.

Then, in order to apply Brouwer's fixed-point theorem, we will prove that F_μ^k preserves the set

$$\mathcal{S}^k = \left\{ n_{\mathcal{T}} = (n_{0,\mathcal{T}}, \vec{n}_{\mathcal{T}}) \in \mathbb{R}^{4\theta} : \ 0 \leqslant n_{\pm,\mathcal{T}} \leqslant M^k, \ |\vec{n}_{\perp,\mathcal{T}}| \leqslant M^k \right\}. \quad (67)$$

It is a bounded set because each element $n_{\mathcal{T}} \in \mathcal{S}^k$ verifies $0 \leqslant n_{0,\mathcal{T}} \leqslant 2M^k$ and $|\vec{n}_{\mathcal{T}}| \leqslant 2M^k$. This part of the proof is the most challenging one. Given $\rho_{\mathcal{T}} \in \mathcal{S}^k$ and $n_{\mathcal{T}} = F_\mu^k(\rho_{\mathcal{T}})$, we will first establish the nonnegativity of $n_{\pm,\mathcal{T}}$ (Step 2), then the upper bounds for $n_{\pm,\mathcal{T}}$ (Step 3), and finally the L^∞ bound for $\vec{n}_{\perp,\mathcal{T}}$ (Step 4).

Step 1: Existence and uniqueness of solutions to (62)-(65). The linear system of equations (62)-(65) is a square system of size 4θ. The existence of a solution is equivalent to the uniqueness of a solution and to the invertibility of the corresponding matrix. Therefore, we just have to prove that if the right-hand side to the system is zero then the solution is zero. Thus, we may work with the original linear system assuming homogeneous Dirichlet boundary conditions and setting $n_{0,K}^{k-1} = \rho_{0,K} = 0$ and $\vec{n}_K^{k-1} = \vec{\rho}_K = 0$, in order to set the right-hand side to zero.

We multiply the corresponding equation (62) by $\frac{1}{4} n_{0,K}$ and (63) by $n_{\ell,K}$, sum these four equations, and sum over all control volumes $K \in \mathcal{T}$:

$$\begin{aligned}
0 &= (1+\mu) \sum_{K\in\mathcal{T}} \frac{m(K)}{4\triangle t} n_{0,K}^2 + (1+\mu) \sum_{K\in\mathcal{T}} \frac{m(K)}{\triangle t} |\vec{n}_K|^2 \\
&\quad + \frac{1}{4} \sum_{K\in\mathcal{T}} \sum_{\sigma\in\mathcal{E}_K} j_{0,K,\sigma} n_{0,K} + \sum_{K\in\mathcal{T}} \sum_{\sigma\in\mathcal{E}_K} \vec{j}_{K,\sigma} \cdot \vec{n}_K \\
&\quad - 2\gamma \sum_{K\in\mathcal{T}} m(K) (\vec{n}_K \times \vec{m}) \cdot \vec{n}_K + \frac{1}{\tau} \sum_{K\in\mathcal{T}} m(K) |\vec{n}_K|^2 \\
&= T_1 + \cdots + T_6.
\end{aligned}$$

Note that $T_5 = 0$ and T_1, T_2, and T_6 are nonnegative. Thus, it remains to estimate the terms T_3 and T_4. By discrete integration by parts (note that the problem is homogeneous) and the definitions (44)-(45) of $j_{\ell,K,\sigma}$ (omitting the superindex k),

$$\begin{aligned}
T_3 &= -\frac{D_0}{4\eta^2} \sum_{\sigma\in\mathcal{E}} (J_{0,K,\sigma} - 2p\vec{J}_{K,\sigma} \cdot \vec{m}) D n_{0,K,\sigma} =: T_{31} + T_{32}, \\
T_4 &= -\frac{D_0}{\eta^2} \sum_{\sigma\in\mathcal{E}} \left(\eta \vec{J}_{K,\sigma} + (1-\eta)(\vec{J}_{K,\sigma} \cdot \vec{m}) \vec{m} - \frac{p}{2} J_{0,K,\sigma} \vec{m} \right) \cdot D\vec{n}_{K,\sigma} \\
&=: T_{41} + T_{42} + T_{43}.
\end{aligned}$$

With formulation (51), definition (52) of B^s, and the discrete chain rule $(n_{\ell,K} + n_{\ell,K,\sigma}) \times Dn_{\ell,K,\sigma} = D(n_\ell^2)_{K,\sigma}$, we have

$$\begin{aligned}
T_{31} &= \frac{D_0}{8\eta^2} \sum_{\sigma\in\mathcal{E}} \tau_\sigma \left(2B^s(DV_{K,\sigma})(Dn_{0,K,\sigma})^2 + D(n_0^2)_{K,\sigma} DV_{K,\sigma}\right),\\
T_{32} &= -\frac{pD_0}{4\eta^2} \sum_{\sigma\in\mathcal{E}} \tau_\sigma \big(2B^s(DV_{K,\sigma}) D\vec{n}_{K,\sigma} \cdot \vec{m}\\
&\quad + (\vec{n}_K + \vec{n}_{K,\sigma}) \cdot \vec{m} DV_{K,\sigma}\big) Dn_{0,K,\sigma},\\
T_{41} &= \frac{D_0}{2\eta} \sum_{\sigma\in\mathcal{E}} \tau_\sigma \left(2B^s(DV_{K,\sigma}) |D\vec{n}_{K,\sigma}|^2 + D(|\vec{n}|^2)_{K,\sigma} DV_{K,\sigma}\right),\\
T_{42} &= \frac{(1-\eta)D_0}{2\eta^2} \sum_{\sigma\in\mathcal{E}} \tau_\sigma \big(2B^s(DV_{K,\sigma}) (D\vec{n}_{K,\sigma} \cdot \vec{m})^2\\
&\quad + D((\vec{n} \cdot \vec{m})^2)_{K,\sigma} DV_{K,\sigma}\big),\\
T_{43} &= -\frac{pD_0}{4\eta^2} \sum_{\sigma\in\mathcal{E}} \tau_\sigma \big(2B^s(DV_{K,\sigma}) Dn_{0,K,\sigma}\\
&\quad + (n_{0,K} + n_{0,K,\sigma}) DV_{K,\sigma}\big) D\vec{n}_{K,\sigma} \cdot \vec{m}.
\end{aligned}$$

We collect all terms from $T_3 + T_4$ involving the function B^s:

$$\begin{aligned}
I_1 &:= \frac{D_0}{\eta^2} \sum_{\sigma\in\mathcal{E}} \tau_\sigma B^s(DV_{K,\sigma}) \bigg(\frac{1}{4}(Dn_{0,K,\sigma})^2 + \eta |D\vec{n}_{K,\sigma}|^2\\
&\quad + (1-\eta)(D\vec{n}_{K,\sigma} \cdot \vec{m})^2 - pDn_{0,K,\sigma} D\vec{n}_{K,\sigma} \cdot \vec{m}\bigg)\\
&= \frac{D_0}{\eta^2} \sum_{\sigma\in\mathcal{E}} \tau_\sigma B^s(DV_{K,\sigma}) \bigg[\begin{pmatrix} Dn_{0,K,\sigma} \\ D\vec{n}_{K,\sigma} \cdot \vec{m}\end{pmatrix}^\top \begin{pmatrix} 1/4 & -p/2 \\ -p/2 & 1-\eta^2/2\end{pmatrix}\\
&\quad \times \begin{pmatrix} Dn_{0,K,\sigma} \\ D\vec{n}_{K,\sigma} \cdot \vec{m}\end{pmatrix} + \frac{\eta^2}{2} |D\vec{n}_{K,\sigma}|^2\\
&\quad + \eta\left(1 - \frac{\eta}{2}\right)\left(|D\vec{n}_{K,\sigma}|^2 - |D\vec{n}_{K,\sigma} \cdot \vec{m}|^2\right)\bigg].
\end{aligned}$$

The eigenvalues of the 2×2 matrix appearing in I_1 are

$$\lambda_\pm = \frac{1}{8}(5 - 2\eta^2) \pm \frac{1}{8}\sqrt{(5-2\eta^2)^2 - 8\eta^2} \geqslant \frac{1}{4} > 0.$$

Then, using the inequalities $B^s(z) \geqslant 1$ for all $z \in \mathbb{R}$ and $|D\vec{n}_{K,\sigma}|^2 \geqslant |D\vec{n}_{K,\sigma} \cdot \vec{m}|^2$ (since $|\vec{m}|^2 = 1$), it follows that

$$\begin{aligned}
I_1 &\geqslant \frac{D_0}{\eta^2} \sum_{\sigma\in\mathcal{E}} \tau_\sigma \left(\lambda_- \big((Dn_{0,K,\sigma})^2 + (D\vec{n}_{K,\sigma} \cdot \vec{m})^2\big) + \frac{\eta^2}{2} |D\vec{n}_{K,\sigma}|^2\right)\\
&\geqslant 0.
\end{aligned}$$

Next, we collect in I_2 the remaining terms from $T_3 + T_4$ involving the discrete gradient $DV_{K,\sigma}$. Taking into account that

$$(\vec{n}_K + \vec{n}_{K,\sigma}) \cdot \vec{m} Dn_{0,K,\sigma} + (n_{0,K} + n_{0,K,\sigma}) D\vec{n}_{K,\sigma} \cdot \vec{m} = 2D((\vec{n} \cdot \vec{m}) n_0)_{K,\sigma},$$

integrating by parts, and employing the discrete Poisson equation (61), we infer that

$$\begin{aligned} I_2 &:= \frac{D_0}{2\eta^2} \sum_{\sigma\in\mathcal{E}} \tau_\sigma DV_{K,\sigma} \bigg(\frac{1}{4} D(n_0^2)_{K,\sigma} + \eta D(|\vec{n}|^2)_{K,\sigma} \\ &\quad + (1-\eta) D((\vec{n}\cdot\vec{m})^2)_{K,\sigma} - p D((\vec{n}\cdot\vec{m})n_0)_{K,\sigma} \bigg) \\ &= \frac{D_0}{2\eta^2\lambda_D^2} \sum_{K\in\mathcal{T}} m(K)(\rho_{0,K} - C_K) \bigg(\frac{1}{4} n_{0,K}^2 + \eta|\vec{n}_K|^2 \\ &\quad + (1-\eta)(\vec{n}_K\cdot\vec{m})^2 - p(\vec{n}_K\cdot\vec{m})n_{0,K} \bigg). \end{aligned}$$

The sum of the terms in the brackets is nonnegative since

$$\begin{aligned} &\frac{1}{4} n_{0,K}^2 + \eta|\vec{n}_K|^2 + (1-\eta)(\vec{n}_K\cdot\vec{m})^2 - p(\vec{n}_K\cdot\vec{m})n_{0,K} \\ &\qquad = \bigg(\frac{1}{2} n_{0,K} - p\vec{n}_K\cdot\vec{m} \bigg)^2 + \eta^2(\vec{n}_K\cdot\vec{m})^2 \\ &\qquad\quad + \eta\big(|\vec{n}_K|^2 - (\vec{n}_K\cdot\vec{m})^2 \big) \geqslant 0. \end{aligned}$$

Therefore, the term involving $\rho_{0,K} \geqslant 0$ can be omitted, giving

$$\begin{aligned} I_2 &\geqslant -\frac{D_0}{2\eta^2\lambda_D^2} \sum_{K\in\mathcal{T}} m(K) C_K \bigg(\frac{1}{4} n_{0,K}^2 + \eta|\vec{n}_K|^2 \\ &\quad + (1-\eta)(\vec{n}_K\cdot\vec{m})^2 - p(\vec{n}_K\cdot\vec{m})n_{0,K} \bigg) \\ &\geqslant -\frac{D_0}{2\eta^2\lambda_D^2} \|C\|_\infty \sum_{K\in\mathcal{T}} m(K) \bigg(\frac{1}{2} n_{0,K}^2 + 2|\vec{n}_K|^2 \bigg) \\ &= -\frac{D_0}{\eta^2\lambda_D^2} \|C\|_\infty \bigg(\frac{1}{4} \|n_{0,\mathcal{T}}\|_2^2 + \|\vec{n}_\mathcal{T}\|_2^2 \bigg). \end{aligned}$$

This shows finally that

$$T_3 + T_4 \geqslant -\frac{D_0\|C\|_\infty}{\eta^2\lambda_D^2} \bigg(\frac{1}{4} \|n_{0,\mathcal{T}}\|_2^2 + \|\vec{n}_\mathcal{T}\|_2^2 \bigg),$$

and summarizing the estimates for $T_1, \ldots, T_6$, we conclude that

$$\bigg(\frac{1+\mu}{\triangle t} - \frac{D_0\|C\|_\infty}{\eta^2\lambda_D^2} \bigg) \bigg(\frac{1}{4} \|n_{0,\mathcal{T}}\|_2^2 + \|\vec{n}_\mathcal{T}\|_2^2 \bigg) \leqslant 0.$$

Hence, choosing μ as in (66), the first bracket is positive, showing that $n_{0,\mathcal{T}} = 0$ and $\vec{n}_\mathcal{T} = 0$, which proves the invertibility of the linear system of equations (62)-(65). The second step involved in the definition of F_μ^k, $(V_\mathcal{T}, \rho_\mathcal{T}) \to n_\mathcal{T}$, is a well-defined mapping. Moreover, the matrix and the right-hand side of the linear system of equations are continuous with respect to $(V_\mathcal{T}, \rho_\mathcal{T})$ so that the mapping is continuous.

Step 2: Nonnegativity of $n_{\pm,\mathcal{T}}$. We will prove that $n_{\pm,K} \geqslant 0$ for all $K \in \mathcal{T}$. Multiplying (63) by $\vec{m}$ and adding or subtracting it from (62), multiplied by $\frac{1}{2}$, we find that

$$\begin{aligned} &\frac{m(K)}{\triangle t}(n_{\pm,K} - n_{\pm,K}^{k-1}) + \mu\frac{m(K)}{\triangle t}(n_{\pm,K} - \rho_{\pm,K}) \\ &\qquad + D_0(1\pm p) \sum_{\sigma\in\mathcal{E}_K} J_{\pm,K,\sigma} = \mp\frac{m(K)}{2\tau}(n_{+,K} - n_{-,K}), \end{aligned} \tag{68}$$

where $\rho_{\pm,K} = \frac{1}{2}\rho_{0,K} \pm \vec{\rho}_K \cdot \vec{m}_K$ and $J_{\pm,K,\sigma} = \frac{1}{2}J_{0,K,\sigma} \pm \vec{J}_{K,\sigma} \cdot \vec{m}$, i.e.

$$J_{\pm,K,\sigma} = \tau_\sigma\big(B(DV_{K,\sigma})n_{\pm,K} - B(-DV_{K,\sigma})n_{\pm,K,\sigma}\big). \tag{69}$$

Then, multiplying (68) by $n^-_{\pm,K} = \min\{0, n_{\pm,K}\}$, summing over all control volumes $K \in \mathcal{T}$, and adding both equations, it follows that

$$\begin{aligned}
0 &= \sum_\pm \sum_{K\in\mathcal{T}} \frac{m(K)}{\triangle t}(n_{\pm,K} - n_{\pm,K}^{k-1})n^-_{\pm,K} \\
&\quad + \mu \sum_\pm \sum_{K\in\mathcal{T}} \frac{m(K)}{\triangle t}(n_{\pm,K} - \rho_{\pm,K})n^-_{\pm,K} \\
&\quad + D_0 \sum_\pm (1\pm p) \sum_{K\in\mathcal{T}} \sum_{\sigma\in\mathcal{E}_K} J_{\pm,K,\sigma} n^-_{\pm,K} \\
&\quad + \sum_{K\in\mathcal{T}} \frac{m(K)}{2\tau}(n_{+,K} - n_{-,K})(n^-_{+,K} - n^-_{-,K}) \\
&=: T_7 + T_8 + T_9 + T_{10},
\end{aligned} \tag{70}$$

Since $n_{\pm,K}n^-_{\pm,K} = (n^-_{\pm,K})^2$, $n^{k-1}_{\pm,K} \geqslant 0$, and $\rho_{\pm,K} \geqslant 0$, the first two terms in (70) can be estimated as

$$T_7 \geqslant \sum_\pm \sum_{K\in\mathcal{T}} \frac{m(K)}{\triangle t}(n^-_{\pm,K})^2, \quad T_8 \geqslant \mu \sum_\pm \sum_{K\in\mathcal{T}} \frac{m(K)}{\triangle t}(n^-_{\pm,K})^2.$$

The monotonicity of the mapping $z \mapsto z^-$ shows that T_{10} is nonnegative. By the discrete integration-by-parts formula (39), the third term in (70) becomes

$$T_9 = -D_0 \sum_\pm (1\pm p) \sum_{\sigma\in\mathcal{E}} J_{\pm,K,\sigma} D(n^-_\pm)_{K,\sigma}.$$

The sum over the boundary edges vanishes since $n^-_{\pm,K,\sigma} = 0$ for all $\sigma \in \mathcal{E}^D_{\mathrm{ext}}$. We claim that

$$-J_{\pm,K,\sigma}D(n^-_\pm)_{K,\sigma} \geqslant \frac{1}{2}\tau_\sigma DV_{K,\sigma}\big((n^-_{\pm,K,\sigma})^2 - (n^-_{\pm,K})^2\big), \quad \text{for } K\in\mathcal{T} \text{ and } \sigma\in\mathcal{E}_K, \tag{71}$$

such that

$$T_9 \geqslant \frac{D_0}{2}\sum_\pm (1\pm p)\sum_{\sigma\in\mathcal{E}} \tau_\sigma DV_{K,\sigma} D\big((n^-_\pm)^2\big)_{K,\sigma}. \tag{72}$$

To prove (71), we distinguish the cases $DV_{K,\sigma} \geqslant 0$ and $DV_{K,\sigma} \leqslant 0$. If $DV_{K,\sigma} \geqslant 0$, we apply a formulation similar to (50), leading to

$$-J_{\pm,K,\sigma}D(n^-_\pm)_{K,\sigma} = \tau_\sigma\big(DV_{K,\sigma}n_{\pm,K,\sigma} + B(DV_{K,\sigma})Dn_{\pm,K,\sigma}\big)D(n^-_\pm)_{K,\sigma}.$$

Then, using the nonnegativity of the function B, the monotonicity of the mapping $z \mapsto z^-$, and the inequality $z(z^- - y^-) \geqslant \frac{1}{2}((z^-)^2 - (y^-)^2)$, we obtain (71). If $DV_{K,\sigma} \leqslant 0$, we employ formulation (49), so that

$$-J_{\pm,K,\sigma}D(n^-_\pm)_{K,\sigma} = \tau_\sigma\big(DV_{K,\sigma}n_{\pm,K} + B(-DV_{K,\sigma})Dn_{\pm,K,\sigma}\big)D(n^-_\pm)_{K,\sigma}$$

and similar arguments lead to (71).

Applying discrete integration by parts to the right-hand side of (72) (the boundary term vanishes since the boundary data is nonnegative) and employing the discrete Poisson equation (61), we find that

$$\begin{aligned}
T_9 &\geqslant -\frac{D_0}{2}\sum_{K\in\mathcal{T}}\sum_{\sigma\in\mathcal{E}_K} \tau_\sigma DV_{K,\sigma}\big((1+p)(n^-_{+,K})^2 + (1-p)(n^-_{-,K})^2\big) \\
&= \frac{D_0}{2\lambda_D^2}\sum_{K\in\mathcal{T}} m(K)(\rho_{0,K} - C_K)\big((1+p)(n^-_{+,K})^2 + (1-p)(n^-_{-,K})^2\big) \\
&\geqslant -\frac{D_0}{2\lambda_D^2}\|C\|_\infty \sum_{K\in\mathcal{T}} m(K)\big((1+p)(n^-_{+,K})^2 + (1-p)(n^-_{-,K})^2\big).
\end{aligned}$$

Summarizing the above estimates, we conclude from (70) that

$$\left(\frac{1+\mu}{\triangle t}-\frac{D_0(1+p)}{2\lambda_D^2}\|C\|_\infty\right)\sum_{K\in\mathcal{T}}m(K)\big((n_{+,K}^-)^2+(n_{-,K}^-)^2\big)\leqslant 0.$$

By the choice of μ in (66), we deduce that

$$\sum_{K\in\mathcal{T}}m(K)\big((n_{+,K}^-)^2+(n_{-,K}^-)^2\big)\leqslant 0,$$

which implies that $n_{\pm,K}^-=0$ and hence $n_{\pm,K}\geqslant 0$ for all $K\in\mathcal{T}$.

Step 3: Upper bounds for $n_{\pm,\mathcal{T}}$. The goal is to show that $n_{\pm,K}\leqslant M^k$ for all $K\in\mathcal{T}$, where M^k is defined in Theorem 3. We multiply (68) by $(n_{\pm,K}-M^k)^+=\max\{0,n_{\pm,K}-M^k\}$, sum over all $K\in\mathcal{T}$, and add both equations:

$$\begin{aligned}
0&=\sum_\pm\sum_{K\in\mathcal{T}}\frac{m(K)}{\triangle t}\big((n_{\pm,K}-M^k)-(n_{\pm,K}^{k-1}-M^{k-1})\big)(n_{\pm,K}-M^k)^+\\
&\quad+\mu\sum_\pm\sum_{K\in\mathcal{T}}\frac{m(K)}{\triangle t}\big((n_{\pm,K}-M^k)-(\rho_{\pm,K}-M^k)\big)(n_{\pm,K}-M^k)^+\\
&\quad+\sum_\pm\sum_{K\in\mathcal{T}}\frac{m(K)}{\triangle t}(M^k-M^{k-1})(n_{\pm,K}-M^k)^+\\
&\quad+D_0\sum_\pm(1\pm p)\sum_{K\in\mathcal{T}}\sum_{\sigma\in\mathcal{E}_K}J_{\pm,K,\sigma}(n_{\pm,K}-M^k)^+\\
&\quad+\frac12\sum_\pm\sum_{K\in\mathcal{T}}m(K)\big((n_{+,K}-M^k)-(n_{-,K}-M^k)\big)(\pm(n_{\pm,K}-M^k)^+)\\
&=:T_{11}+T_{12}+T_{13}+T_{14}+T_{15}.
\end{aligned}\tag{73}$$

Using the inequality $(z-y)z^+\geqslant\frac12((z^+)^2-(y^+)^2)$, the first two terms are estimated by

$$\begin{aligned}
T_{11}&\geqslant\frac{1}{2\triangle t}\sum_\pm\sum_{K\in\mathcal{T}}m(K)\big((n_{\pm,K}-M^k)^+\big)^2,\\
T_{12}&\geqslant\frac{\mu}{2\triangle}\sum_\pm\sum_{K\in\mathcal{T}}m(K)\big((n_{\pm,K}-M^k)^+\big)^2,
\end{aligned}$$

since $n_{\pm,K}^{k-1}\leqslant M^{k-1}$ and $\rho_{\pm,K}\leqslant M^k$ by assumption. By definition of M^k, the third term T_{13} becomes

$$T_{13}=\alpha M^k\sum_\pm\sum_{K\in\mathcal{T}}m(K)(n_{\pm,K}-M^k)^+,$$

and the last term T_{15} is nonnegative.

It remains to estimate T_{14}. By discrete integration by parts (the boundary term vanishes in view of $n_{\pm,\sigma}^D\leqslant M^k$ for $\sigma\in\mathcal{E}_{\rm ext}^D$), we find that

$$T_{14}=-D_0\sum_\pm(1\pm p)\sum_{\sigma\in\mathcal{E}}J_{\pm,K,\sigma}D\big((n_\pm-M^k)^+\big)_{K,\sigma}.$$

Similarly as in Step 2, we claim that the following estimate holds:

$$\begin{aligned}
T_{14}&\geqslant D_0\sum_\pm(1\pm p)\sum_{\sigma\in\mathcal{E}}\tau_\sigma DV_{K,\sigma}D\Big(\frac12((n_\pm-M^k)^+)^2\\
&\quad+M^k(n_\pm-M^k)^+\Big)_{K,\sigma}.
\end{aligned}$$

Indeed, let first $DV_{K,\sigma} \geqslant 0$. Using the inequalities

$$D(n_\pm - M^k)_{K,\sigma} D((n_\pm - M^k)^+)_{K,\sigma} \geqslant 0$$

and

$$(n_{\pm,K,\sigma} - M^k) D((n_\pm - M^k)^+)_{K,\sigma} \geqslant \frac{1}{2} D(((n_\pm - M^k)^+)^2)_{K,\sigma} \geqslant 0,$$

it follows from (50) that

$$\begin{aligned} -J_{\pm,K,\sigma} &\geqslant \tau_\sigma DV_{K,\sigma}\big((n_{\pm,K,\sigma} - M^k) + M^k\big) D((n_\pm - M)^+)_{K,\sigma} \\ &\geqslant \tau_\sigma DV_{K,\sigma} \left(\frac{1}{2} D(((n_\pm - M^k)^+)^2)_{K,\sigma} + M^k D((n_\pm - M^k)^+)_{K,\sigma} \right). \end{aligned}$$

The proof for $DV_{K,\sigma} \leqslant 0$ is similar, employing formulation (49). Then, integrating by parts and employing the Poisson equation and $\rho_{0,K} \geqslant 0$,

$$\begin{aligned} T_{14} &\geqslant \frac{D_0}{\lambda_D^2} \sum_\pm (1 \pm p) \sum_{K\in\mathcal{T}} m(K)(\rho_{0,K} - C_K)\Big(\frac{1}{2}((n_{\pm,K} - M^k)^+)^2 \\ &\quad + M^k (n_{\pm,K} - M^k)^+ \Big) \\ &\geqslant -\frac{D_0}{\lambda_D^2} \|C\|_\infty (1+p) \sum_\pm \sum_{K\in\mathcal{T}} m(K) \Big(\frac{1}{2}((n_{\pm,K} - M^k)^+)^2 \\ &\quad + M^k (n_{\pm,K} - M^k)^+ \Big). \end{aligned}$$

Summarizing the above estimates, we infer from (73) that

$$\begin{aligned} &\left(\frac{1+\mu}{2\triangle t} - \frac{D_0}{\lambda_D^2} \|C\|_\infty (1+p) \right) \sum_\pm \sum_{K\in\mathcal{T}} m(K) \big((n_{\pm,K} - M^k)^+\big)^2 \\ &+ \left(\alpha - \frac{D_0}{\lambda_D^2} \|C\|_\infty (1+p) \right) M^k \sum_\pm \sum_{K\in\mathcal{T}} m(K)(n_{\pm,K} - M^k)^+ \leqslant 0. \end{aligned}$$

Then, choosing μ as in (66) and taking into account the definition of α, we infer that $n_{\pm,K} \leqslant M^k$ for $K \in \mathcal{T}$.

Step 4: L^∞ *bound for* $\vec{n}^k_{\perp,\mathcal{T}}$. We prove a uniform L^{2q} bound for $\vec{n}_{\perp,K} = \vec{n}_K - (\vec{n}_K \cdot \vec{m})\vec{m}$. For this, we multiply the vector version of (63) (omitting the superindex k) by $\vec{m}$ twice, and taking the difference of the equations for $\vec{n}_K$ and $(\vec{n}_K \cdot \vec{m})\vec{m}$, we obtain

$$\begin{aligned} &\frac{m(K)}{\triangle t}\big(\vec{n}_{\perp,K} - \vec{n}^{k-1}_{\perp,K} + \mu(\vec{n}_{\perp,K} - \vec{\rho}_{\perp,K})\big) + \frac{D_0}{\eta} \sum_{\sigma\in\mathcal{E}_K} \vec{J}_{\perp,K,\sigma} \qquad (74) \\ &\qquad - 2\gamma\, m(K)(\vec{n}_{\perp,K} \times \vec{m}) = -\frac{m(K)}{\tau} \vec{n}_{\perp,K}, \end{aligned}$$

where $\vec{\rho}_{\perp,K} = \vec{\rho}_K - (\vec{\rho}_K \cdot \vec{m})\vec{m}$, and $\vec{J}_{\perp,K,\sigma}$ is given by

$$\begin{aligned} \vec{J}_{\perp,K,\sigma} &= \tau_\sigma\big(-DV_{K,\sigma} \vec{n}_{\perp,K} - B(-DV_{K,\sigma}) D\vec{n}_{\perp,K,\sigma} \big) \qquad (75) \\ &= \tau_\sigma\big(-DV_{K,\sigma} \vec{n}_{\perp,K,\sigma} - B(DV_{K,\sigma}) D\vec{n}_{\perp,K,\sigma} \big). \qquad (76) \end{aligned}$$

Then, multiplying (74) by $|\vec{n}_{\perp,K}|^{2(q-1)}\vec{n}_{\perp,K}$ (where $q \in \mathbb{N}$) and summing over $K \in \mathcal{T}$, we arrive at $T_{16} + T_{17} + T_{18} + T_{19} = 0$ with

$$\begin{aligned} T_{16} &= \frac{1}{\triangle t} \sum_{K\in\mathcal{T}} m(K)(\vec{n}_{\perp,K} - \vec{n}^{k-1}_{\perp,K}) \cdot \vec{n}_{\perp,K} |\vec{n}_{\perp,K}|^{2(q-1)}, \\ T_{17} &= \frac{\mu}{\triangle t} \sum_{K\in\mathcal{T}} m(K)(\vec{n}_{\perp,K} - \vec{\rho}_{\perp,K}) \cdot \vec{n}_{\perp,K} |\vec{n}_{\perp,K}|^{2(q-1)}, \\ T_{18} &= \frac{D_0}{\eta} \sum_{K\in\mathcal{T}} \sum_{\sigma\in\mathcal{E}_K} \vec{J}_{\perp,K,\sigma} \cdot \vec{n}_{\perp,K} |\vec{n}_{\perp,K}|^{2(q-1)}, \\ T_{19} &= \sum_{K\in\mathcal{T}} m(K) |\vec{n}_{\perp,K}|^{2q}. \end{aligned}$$

The elementary inequality $|\vec{a}|^{2(q-1)}\vec{a}\cdot(\vec{a}-\vec{b}) \geqslant (|\vec{a}|^{2q}-|\vec{b}|^{2q})/(2q)$ for $\vec{a}$, $\vec{b}\in\mathbb{R}^3$ shows that

$$T_{16} \geqslant \frac{1}{2q\triangle t}\left(\sum_{K\in\mathcal{T}} m(K)|\vec{\pi}_{\perp,K}|^{2q} - \sum_{K\in\mathcal{T}} m(K)|\vec{\pi}_{\perp,K}^{k-1}|^{2q}\right),$$
$$T_{17} \geqslant \frac{\mu}{2q\triangle t}\left(\sum_{K\in\mathcal{T}} m(K)|\vec{\pi}_{\perp,K}|^{2q} - \sum_{K\in\mathcal{T}} m(K)|\vec{\rho}_{\perp,K}|^{2q}\right).$$

By discrete integration by parts (observe that $\vec{\pi}_{\perp,K,\sigma}=0$ for $\sigma\in\mathcal{E}_{ext}^{D}$),

$$T_{18} = -\frac{D_0}{\eta}\sum_{\sigma\in\mathcal{E}} \vec{J}_{\perp,K,\sigma}\cdot\left(\vec{\pi}_{\perp,K,\sigma}|\vec{\pi}_{\perp,K,\sigma}|^{2(q-1)} - \vec{\pi}_{\perp,K}|\vec{\pi}_{\perp,K}|^{2(q-1)}\right).$$

Again, we distinguish the cases $DV_{K,\sigma}\geqslant 0$ and $DV_{K,\sigma}<0$ for given $K\in\mathcal{T}$ and $\sigma\in\mathcal{E}_K$. First, let $DV_{K,\sigma}\geqslant 0$ and use formulation (76) of the numerical flux. This gives

$$\begin{aligned}
&-\vec{J}_{\perp,K,\sigma}\cdot\left(\vec{\pi}_{\perp,K,\sigma}|\vec{\pi}_{\perp,K,\sigma}|^{2(q-1)} - \vec{\pi}_{\perp,K}|\vec{\pi}_{\perp,K}|^{2(q-1)}\right)\\
&= \tau_\sigma DV_{K,\sigma}\vec{\pi}_{\perp,K,\sigma}\cdot\left(\vec{\pi}_{\perp,K,\sigma}|\vec{\pi}_{\perp,K,\sigma}|^{2(q-1)} - \vec{\pi}_{\perp,K}|\vec{\pi}_{\perp,K}|^{2(q-1)}\right)\\
&\quad + \tau_\sigma B(DV_{K,\sigma})(\vec{\pi}_{\perp,K,\sigma}-\vec{\pi}_{\perp,K})\cdot\left(\vec{\pi}_{\perp,K,\sigma}|\vec{\pi}_{\perp,K,\sigma}|^{2(q-1)}\right.\\
&\quad \left. - \vec{\pi}_{\perp,K}|\vec{\pi}_{\perp,K}|^{2(q-1)}\right).
\end{aligned}$$

Because of

$$\begin{aligned}
&\vec{a}\cdot(\vec{a}|\vec{a}|^{2(q-1)} - \vec{b}|\vec{b}|^{2(q-1)}) = |\vec{a}|^{2q} - \vec{a}\cdot\vec{b}|\vec{b}|^{2(q-1)}\\
&\geqslant |\vec{a}|^{2q} - \frac{1}{2q}|\vec{a}|^{2q} - \left(1-\frac{1}{2q}\right)|\vec{b}|^{2q}\\
&\geqslant \left(1-\frac{1}{2q}\right)(|\vec{a}|^{2q}-|\vec{b}|^{2q}) \quad \text{for all } \vec{a},\vec{b}\in\mathbb{R}^3,
\end{aligned}$$

applied to $\vec{a}=\vec{\pi}_{\perp,K,\sigma}$ and $\vec{b}=\vec{\pi}_{\perp,K}$, and the monotonicity of the mapping $\vec{a}\mapsto\vec{a}|\vec{a}|^{2(q-1)}$, we find that

$$\begin{aligned}
&-\vec{J}_{\perp,K,\sigma}\cdot\left(\vec{\pi}_{\perp,K,\sigma}|\vec{\pi}_{\perp,K,\sigma}|^{2(q-1)} - \vec{\pi}_{\perp,K}|\vec{\pi}_{\perp,K}|^{2(q-1)}\right)\\
&\qquad \geqslant \tau_\sigma\left(1-\frac{1}{2q}\right)DV_{K,\sigma}\left(|\vec{\pi}_{\perp,K,\sigma}|^{2q} - |\vec{\pi}_{\perp,K}|^{2q}\right).
\end{aligned}$$

This result still holds if $DV_{K,\sigma}<0$, thanks to formulation (75). Therefore

$$T_{18} \geqslant \frac{D_0}{\eta}\left(1-\frac{1}{2q}\right)\sum_{\sigma\in\mathcal{E}}\tau_\sigma DV_{K,\sigma}D(|\vec{\pi}_\perp|^{2q})_{K,\sigma}.$$

Using discrete integration by parts and the Poisson equation (43) leads to

$$\begin{aligned}
T_{18} &\geqslant \frac{D_0}{\eta\lambda_D^2}\left(1-\frac{1}{2q}\right)\sum_{K\in\mathcal{T}} m(K)(\rho_{0,K}-C_K)|\vec{\pi}_{\perp,K}|^{2q}\\
&\geqslant -\frac{D_0}{\eta\lambda_D^2}\|C\|_\infty\sum_{K\in\mathcal{T}} m(K)|\vec{\pi}_{\perp,K}|^{2q}.
\end{aligned}$$

Summarizing the above estimates, we obtain

$$\begin{aligned}
&\left(1+\mu+2q\triangle t\left(\frac{1}{\tau}-\frac{D_0\|C\|_\infty}{\eta\lambda_D^2}\right)\right)\sum_{K\in\mathcal{T}} m(K)|\vec{\pi}_{\perp,K}|^{2q}\\
&\leqslant \sum_{K\in\mathcal{T}} m(K)|\vec{\pi}_{\perp,K}^{k-1}|^{2q} + \mu\sum_{K\in\mathcal{T}} m(K)|\vec{\rho}_{\perp,K}|^{2q}.
\end{aligned}$$

Condition (57) on τ, the induction hypothesis $\|\vec{n}^{k-1}_{\perp,\mathcal{T}}\|_\infty \leqslant M^{k-1} \leqslant M^k$, and the fact that $\rho \in \mathcal{S}^k$ (see (67) for the definition of $\mathcal{S}^k$), such that $\|\vec{\rho}_{\perp,\mathcal{T}}\|_\infty \leqslant M^k$, imply that

$$\|\vec{n}_{\perp,\mathcal{T}}\|_{2q} \leqslant \mathrm{meas}(\Omega)^{1/(2q)} M^k \quad \text{for } q \geqslant 1.$$

Passing to the limit $q \to +\infty$, we deduce that $\|n_{\perp,\mathcal{T}}\|_\infty \leqslant M^k$.

Conclusion. In Step 1, we have proved that the mapping F^k_μ is well-defined and continuous. In Steps 2-4, we have proved that F^k_μ preserves the bounded set $\mathcal{S}^k$. Thus, the fixed-point theorem of Brouwer shows the existence of a fixed point to F^k_μ, belonging to $\mathcal{S}^k$. Let us denote this fixed point by $n^k_{\mathcal{T}} = (n^k_{0,\mathcal{T}}, \vec{n}^k_{\mathcal{T}})$. It is a solution to scheme (41)–(48) at step k and satisfies

$$0 \leqslant n^k_{\pm,K} \leqslant M^k \quad \text{and} \quad |\vec{n}^k_{\perp,K}| \leqslant M^k, \quad \text{for } K \in \mathcal{T}.$$

3.2.2 *Uniform bounds for the spin-up and spin-down densities*

In order to conclude the proof of Theorem 3, it remains to prove that the upper bounds on the spin-up and spin-down densities in fact do not depend on k. The negativity of these densities is already proved above.

We assume as induction hypothesis that $n^{k-1}_{\pm,K} \leqslant M^0$ for all $K \in \mathcal{T}$ (this property is ensured for $k = 1$ by the definition of M^0). Scheme (41)-(42) implies that

$$\frac{m(K)}{\triangle t}(n^k_{\pm,K} - n^{k-1}_{\pm,K}) + D_0(1 \pm p) \sum_{\sigma\in\mathcal{E}_K} J^k_{\pm,K,\sigma} = \mp \frac{m(K)}{2\tau}(n^k_{+,K} - n^k_{-,K}). \quad (77)$$

As in Step 3 above, we multiply (77) by $(n^k_{\pm,K} - M^0)^+$, sum over all $K \in \mathcal{T}$ and add both equations. This yields $S_1 + S_2 + S_3 = 0$, where

$$\begin{aligned}
S_1 &= \sum_\pm \sum_{K\in\mathcal{T}} \frac{m(K)}{\triangle t}\big((n^k_{\pm,K} - M^0) - (n^{k-1}_{\pm,K} - M^0)\big)(n^k_{\pm,K} - M^0)^+, \\
S_2 &= D_0 \sum_\pm (1 \pm p) \sum_{K\in\mathcal{T}} \sum_{\sigma\in\mathcal{E}_K} J^k_{\pm,K,\sigma}(n^k_{\pm,K} - M^0)^+, \\
S_3 &= \frac{1}{2\tau} \sum_{K\in\mathcal{T}} m(K)(n^k_{+,K} - n^k_{-,K}) \Big((n^k_{+,K} - M^0)^+ - (n^k_{-,K} - M^0)^+\Big).
\end{aligned}$$

It is clear that $S_3 \geqslant 0$ and, by the induction hypothesis, that

$$S_1 \geqslant \frac{1}{2\triangle t} \sum_\pm \sum_{K\in\mathcal{T}} m(K) \Big((n^k_{\pm,K} - M^0)^+\Big)^2.$$

The term S_2 is the analogue of T_{14}. Following the same ideas as in Step 3, we obtain

$$\begin{aligned}
S_2 \geqslant \frac{D_0}{\lambda_D^2} \sum_\pm (1 \pm p) \sum_{K\in\mathcal{T}} m(K)(n^k_{0,K} - C_K) \\
\times \left(\frac{1}{2}((n^k_{\pm,K} - M^0)^+)^2 + M^0(n^k_{\pm,K} - M^0)^+\right).
\end{aligned}$$

But, as $n^k_{0,K} = n^k_{+,K} + n^k_{-,K}$, the negativity of $n^k_{+,K}$ and $n^k_{-,K}$ and the definition of M^0 ensure that $n^k_{0,K} - C_K \geqslant n^k_{+,K} - M^0$ and $n^k_{0,K} - C_K \geqslant n^k_{-,K} - M^0$, leading to $S_2 \geqslant 0$. Therefore, we infer that

$$\sum_\pm \sum_{K\in\mathcal{T}} m(K) \Big((n^k_{\pm,K} - M^0)^+\Big)^2 \leqslant 0,$$

which yields the expected result.

3.3 PROOF OF THEOREM 4

Let $(n^k_{\pm,\mathcal{T}}, V^k_{\mathcal{T}})_{k\geqslant 0}$ be a solution to (43), (77) with the corresponding Dirichlet-Neumann boundary conditions. Since we have to deal with the logarithm of the densities $n^k_{\pm,K}$, which may vanish, we introduce a regularization of the discrete free energy. For $\delta > 0$, we set $n^{k,\delta}_{\pm,K} = n^k_{\pm,K} + \delta$ and define

$$\begin{aligned} E^k_\delta = \sum_{\pm}\sum_{K\in\mathcal{T}} m(K)\Big(& n^{k,\delta}_{\pm,K}(\log(n^{k,\delta}_{\pm,K}) - 1) && (78)\\ & - n^k_{\pm,K}\log\left(\frac{n^D_K}{2} + \delta\right) + \frac{n^D_K}{2}\right) && (79)\\ & + \frac{\lambda_D^2}{2}\sum_{\sigma\in\mathcal{E}} \tau_\sigma (D(V^k - V^D)_{K,\sigma})^2. \end{aligned}$$

Therefore, we have $E^k_\delta - E^{k-1}_\delta = U_1 + U_2$, where

$$\begin{aligned} U_1 &= \sum_{\pm}\sum_{K\in\mathcal{T}} m(K)\bigg(n^{k,\delta}_{\pm,K}(\log n^{k,\delta}_{\pm,K} - 1) - n^{k-1,\delta}_{\pm,K}(\log n^{k-1,\delta}_{\pm,K} - 1)\\ &\quad - (n^k_{\pm,K} - n^{k-1}_{\pm,K})\log\left(\frac{n^D_K}{2} + \delta\right)\bigg),\\ U_2 &= \frac{\lambda_D^2}{2}\sum_{\sigma\in\mathcal{E}} \tau_\sigma\big((D(V^k - V^D)_{K,\sigma})^2 - (D(V^{k-1} - V^D)_{K,\sigma})^2\big). \end{aligned}$$

The convexity of $x \mapsto x(\log x - 1)$ shows that $x(\log x - 1) - y(\log y - 1) \leqslant (x-y)\log x$ for all $x, y > 0$. Hence,

$$U_1 \leqslant \sum_{\pm}\sum_{K\in\mathcal{T}} m(K)(n^k_{\pm,K} - n^{k-1}_{\pm,K})\left(\log n^{k,\delta}_{\pm,K} - \log\left(\frac{n^D_K}{2} + \delta\right)\right).$$

Using the elementary inequality $\frac{1}{2}(x^2 - y^2) \leqslant (x-y)x$ for all $x, y \in \mathbb{R}$, integrating by parts, and employing the discrete Poisson equation (43), it follows that

$$\begin{aligned} U_2 &\leqslant \lambda_D^2 \sum_{\sigma\in\mathcal{E}} \tau_\sigma D(V^k - V^{k-1})_{K,\sigma} D(V^k - V^D)_{K,\sigma}\\ &= -\lambda_D^2 \sum_{K\in\mathcal{T}}\sum_{\sigma\in\mathcal{E}_K} \tau_\sigma D(V^k - V^{k-1})_{K,\sigma}(V^k_K - V^D_K)\\ &= \sum_{\pm}\sum_{K\in\mathcal{T}} m(K)\big(n^k_{\pm,K} - n^{k-1}_{\pm,K}\big)(V^k_K - V^D_K). \end{aligned}$$

We summarize the above inequalities and use scheme (77) to find that

$$\begin{aligned} &\frac{1}{\triangle t}(E^k_\delta - E^{k-1}_\delta)\\ &\quad\leqslant -\frac{1}{\tau}\sum_{K\in\mathcal{T}} m(K)(n^k_{+,K} - n^k_{-,K})\big(\log n^{k,\delta}_{+,K} - \log n^{k,\delta}_{-,K}\big)\\ &\qquad - \sum_{\pm} D_0(1\pm p)\sum_{K\in\mathcal{T}}\sum_{\sigma\in\mathcal{E}_K} J^k_{\pm,K,\sigma}\bigg(\log n^{k,\delta}_{\pm,K} + V^k_K\\ &\qquad - \log\left(\frac{n^D_K}{2} + \delta\right) - V^D_K\bigg). \end{aligned}$$

The first term on the right-hand side is clearly nonpositive. We apply the discrete integration-by-parts formula (39) to the second term. Then, with

the hypothesis on the boundary data (i.e. $\log(n^D/2)+V^D$ is constant in $\overline{\Omega}$ such that $DV^D_{K,\sigma} = -D(\log n^D)_{K,\sigma}$ for all $K \in \mathcal{T}$ and $\sigma \in \mathcal{E}_K$), we infer that

$$\frac{1}{\triangle t}(E^k_\delta - E^{k-1}_\delta) \leqslant \sum_{\pm} D_0(1\pm p) \sum_{\sigma\in\mathcal{E}} J^k_{\pm,K,\sigma} D(\log n^{k,\delta}_\pm + V^k)_{K,\sigma}$$
$$+ \sum_{\pm} D_0(1\pm p) \sum_{\sigma\in\mathcal{E}} J^k_{\pm,K,\sigma} D\big(\log n^D - \log(n^D+2\delta)\big)_{K,\sigma}.$$

Introducing the numerical fluxes associated to the regularized densities,

$$J^{k,\delta}_{\pm,K,\sigma} = \tau_\sigma\big(B(DV^k_{K,\sigma})n^{k,\delta}_{\pm,K} - B(-DV^k_{K,\sigma})n^{k,\delta}_{\pm,K,\sigma}\big) = J^k_{\pm,K,\sigma} - \delta\tau_\sigma DV^k_{K,\sigma},$$

we can write

$$\frac{1}{\triangle t}(E^k_\delta - E^{k-1}_\delta) \leqslant U_3 + U_4 + U_5 + U_6,$$

where

$$U_3 = \sum_{\pm} D_0(1\pm p) \sum_{\sigma\in\mathcal{E}} J^{k,\delta}_{\pm,K,\sigma} D\big(\log n^{k,\delta}_\pm + V^k\big)_{K,\sigma},$$
$$U_4 = \sum_{\pm} D_0(1\pm p) \sum_{\sigma\in\mathcal{E}} J^{k,\delta}_{\pm,K,\sigma} D(\log n^D - \log(n^D+2\delta))_{K,\sigma},$$
$$U_5 = \delta\sum_{\pm} D_0(1\pm p) \sum_{\sigma\in\mathcal{E}} \tau_\sigma DV^k_{K,\sigma} D(\log n^{k,\delta}_\pm + V^k)_{K,\sigma},$$
$$U_6 = \delta\sum_{\pm} D_0(1\pm p) \sum_{\sigma\in\mathcal{E}} \tau_\sigma DV^k_{K,\sigma} D\big(\log n^D - \log(n^D+2\delta)\big)_{K,\sigma}.$$

Now, we employ the following inequalities, which are proved in [8, Appendix A]:

$$J^{k,\delta}_{\pm,K,\sigma} D(\log n^{k,\delta}_\pm + V^k)_{K,\sigma} \leqslant -\tau_\sigma \min(n^{k,\delta}_{\pm,K}, n^{k,\delta}_{\pm,K,\sigma}) \times (D(\log n^{k,\delta}_\pm + V^k)_{K,\sigma})^2,$$
$$\big|J^{k,\delta}_{\pm,K,\sigma}\big| \leqslant \tau_\sigma \max(n^{k,\delta}_{\pm,K}, n^{k,\delta}_{\pm,K,\sigma}) \times \big|D(\log n^{k,\delta}_\pm + V^k)_{K,\sigma}\big|.$$

The first inequality yields

$$U_3 \leqslant -\sum_{\pm} D_0(1\pm p) \sum_{\sigma\in\mathcal{E}} \tau_\sigma \min(n^{k,\delta}_{\pm,K}, n^{k,\delta}_{\pm,K,\sigma})\big(D(\log n^{k,\delta}_\pm + V^k)_{K,\sigma}\big)^2,$$

while the second one, together with Young's inequality, gives $U_4 \leqslant U_{41} + U_{42}$, where

$$U_{41} = \frac{1}{4}\sum_{\pm} D_0(1\pm p) \sum_{\sigma\in\mathcal{E}} \tau_\sigma \min(n^{k,\delta}_{\pm,K}, n^{k,\delta}_{\pm,K,\sigma}) \times \big(D(\log n^{k,\delta}_\pm + V^k)_{K,\sigma}\big)^2,$$
$$U_{42} = \sum_{\pm} D_0(1\pm p) \sum_{\sigma\in\mathcal{E}} \tau_\sigma\big(\max(n^{k,\delta}_{\pm,K}, n^{k,\delta}_{\pm,K,\sigma})\big)^2 \times \frac{(D(\log n^D - \log(n^D+2\delta))_{K,\sigma})^2}{\min(n^{k,\delta}_{\pm,K}, n^{k,\delta}_{\pm,K,\sigma})},$$
$$\leqslant 2D_0\frac{(M^0+\delta)^2}{\delta}\big|\log(n^D_{\mathcal{M}}+2\delta) - \log n^D_{\mathcal{M}}\big|^2_{1,\mathcal{M}},$$

since $\min(n^{k,\delta}_{\pm,K}, n^{k,\delta}_{\pm,K,\sigma}) \geqslant \delta$ for all $K \in \mathcal{T}$ and $\sigma \in \mathcal{E}_K$. Applying Young's inequality again, we obtain $U_5 \leqslant U_{51} + U_{52}$ with

$$\begin{aligned} U_{51} &= \frac{1}{4}\sum_{\pm} D_0(1 \pm p) \sum_{\sigma\in\mathcal{E}} \tau_\sigma \min(n^{k,\delta}_{\pm,K}, n^{k,\delta}_{\pm,K,\sigma}) \\ &\quad \times \left(D(\log n^{k,\delta}_{\pm} + V^k)_{K,\sigma}\right)^2, \\ U_{52} &= \delta^2 \sum_{\pm} D_0(1 \pm p) \sum_{\sigma\in\mathcal{E}} \tau_\sigma \frac{(DV^k_{K,\sigma})^2}{\min(n^{k,\delta}_{\pm,K}, n^{k,\delta}_{\pm,K,\sigma})} \\ &\leqslant 2D\delta \sum_{\sigma\in\mathcal{E}} \tau_\sigma (DV^k_{K,\sigma})^2 \end{aligned}$$

and

$$U_6 \leqslant 2D_0\delta \left(\left| \log(n^D_{\mathcal{M}} + 2\delta) - \log n^D_{\mathcal{M}} \right|^2_{1,\mathcal{M}} + \sum_{\sigma\in\mathcal{E}} \tau_\sigma (DV^k_{K,\sigma})^2 \right).$$

Summarizing the above inequalities, we deduce that

$$\frac{1}{\triangle t}(E^k_\delta - E^{k-1}_\delta) + \frac{1}{2}\sum_{\pm} D_0(1 \pm p) \sum_{\sigma\in\mathcal{E}} \tau_\sigma \min(n^{k,\delta}_{\pm,K}, n^{k,\delta}_{\pm,K,\sigma}) \tag{80}$$

$$\times \left(D(\log n^{k,\delta}_{\pm} + V^k)_{K,\sigma}\right)^2 \tag{81}$$

$$\leqslant 4D_0\delta \sum_{\sigma\in\mathcal{E}} \tau_\sigma (DV^k_{K,\sigma})^2 + 2D_0 \left(\delta + \frac{(M^0+\delta)^2}{\delta}\right) \tag{82}$$

$$\times \left| \log(n^D_{\mathcal{M}} + 2\delta) - \log n^D_{\mathcal{M}} \right|^2_{1,\mathcal{M}}.$$

On the one hand, the term $\sum_{\sigma\in\mathcal{E}} \tau_\sigma (DV^k_{K,\sigma})^2$ does not depend on δ and is bounded (this can be seen by using scheme (43) and the L^∞ bound on $n^k_{\pm,\mathcal{T}}$). On the other hand, we rewrite

$$\begin{aligned} \left| \log(n^D_{\mathcal{M}} + 2\delta) - \log n^D_{\mathcal{M}} \right|^2_{1,\mathcal{M}} &= \left| \log\left(1 + \frac{2\delta}{n^D_{\mathcal{M}}}\right) \right|^2_{1,\mathcal{M}} \\ = \sum_{\sigma\in\mathcal{E}} \tau_\sigma \left(\log\left(1 + \frac{2\delta}{n^D_{K,\sigma}}\right) - \log\left(1 + \frac{2\delta}{n^D_K}\right) \right)^2. \end{aligned}$$

Employing the inequality $|\log y - \log x| \leqslant |y - x|/\min(x, y)$ for $x, y > 0$, and the fact that $n^D \geqslant n_* > 0$, we obtain

$$\left| \log(n^D_{\mathcal{M}} + 2\delta) - \log n^D_{\mathcal{M}} \right|^2_{1,\mathcal{M}} \leqslant \frac{4\delta^2}{n_*^2} |n^D_{\mathcal{M}}|^2_{1,\mathcal{M}}.$$

Thanks to hypothesis (54), $n^D \in H^1(\Omega)$, and Lemma 9.4 in [18], we conclude that $|n^D_{\mathcal{M}}|_{1,\mathcal{M}} \leqslant K\|n^D\|_{H^1(\Omega)}$ with K depending only on the regularity of the mesh $\mathcal{M}$. Therefore, the right-hand side in (81) tends to zero when $\delta \to 0$. Passing to the limit $\delta \to 0$ in (81) then leads to (60). This concludes the proof of Theorem 4.

3.4 NUMERICAL SIMULATIONS

As an illustration of the numerical scheme, analyzed in the previous sections, we present two-dimensional simulations of a simple double-gate ferromagnetic MESFET (metal semiconductor field-effect transistor). This device is composed of a nonmagnetic region which is sandwiched between two ferromagnetic contact regions (see Figure 8). The idea of such devices

is that the source region plays the role of a spin polarizer. The non-zero spin-orbit interaction causes the electrons to precess during the propagation through the middle channel region. At the drain contact, only those electrons with spin aligned to the drain magnetization can leave the channel and contribute to the current flow. Here, we focus on the feasibility of our numerical scheme and the verification of the properties of the numerical solution and less on the physical properties. Therefore, the physical setting considered here is strongly simplified. In particular, we just modify the standard MESFET setup by allowing for ferromagnetic regions. For a more detailed modeling, we refer e.g. to [34].

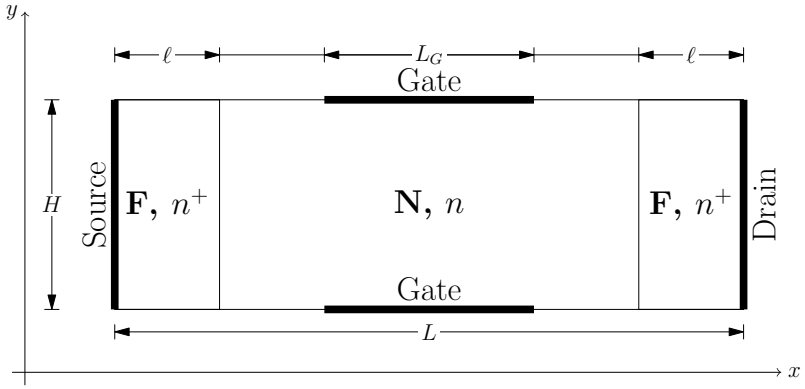

Figure 8: Geometry of a MESFET with ferromagnetic (F) source and drain regions and nonmagnetic (N) channel region.

In the following, we describe the geometry of the device in the (x, y) plane (see Figure 8). The total length is $L = 0.6\,\mu m$ and the height equals $H = 0.2\,\mu m$. The source and drain regions are highly doped with doping $C_+ = 3 \cdot 10^{23} m^{-3}$. The doping in the channel region is $C_0 = 10^{23} m^{-3}$. The length of the source and drain regions are $\ell = 0.1\,\mu m$. The gate contacts are attached at the middle of the device with a length of $L_G = 0.2\,\mu m$.

The values of the physical parameters are given in Table 1. They are similar to those used in [29] (there is a small difference in the relaxation time value). The (squared) scaled Debye length becomes $\lambda_D^2 = \varepsilon_0 \varepsilon_r U_T / (q_e C_+ L^2) \approx 1.6 \cdot 10^{-4}$. Note that condition (57) on τ is not satisfied with these physical values but it turns out that the numerical solution is still bounded (even uniformly in time). This may indicate that condition (57) on τ is technical only.

Name	Description	Value
D^*	Diffusion coefficient	$10^{-3}\,m^2 s^{-1}$
ε_r	Relative permittivity of silicon	11.7
ε_0	Permittivity of the vacuum	$8.9 \cdot 10^{-12}\,Fm^{-1}$
q_e	Elementary charge	$1.6 \cdot 10^{-10}\,C$
τ^*	Spin-flip relaxation time	$10^{-12}\,s$
U_T	Thermal voltage at room temperature	0.0026 V

Table 1: Material and model parameters.

The gate contact is considered as a Schottky contact. Usually, Robin-type boundary conditions are prescribed at a Schottky contact but also Dirichlet conditions involving the Schottky barrier height have been used to simplify the modeling [41, Section 5.1]. This simplification is possible for Schottky

contacts on n-doped materials as it is the case here. We choose the barrier potential $V_S = 0.8\,V$. The total voltage between source and gate is $V_G + V_S$, where V_G is the voltage applied at the gate. The density boundary value at the gate contact is calclulated according to [41, Formula (5.1-19)], and the potential of the closed state is taken from [29]. This gives

- at the source: $n_0 = C_+$, $\vec{n} = 0$, potential: $0\,V$,
- at the drain: $n_0 = C_+$, $\vec{n} = 0$, potential: V_D,
- at the gate:
  open state: $n_0 = 3.9 \cdot 10^{11}\,m^{-3}$, $\vec{n} = 0$, potential: V_S,
  closed state: $n_0 = 3.2 \cdot 10^{9}\,m^{-3}$, $\vec{n} = 0$, potential: $V_S + 1.2\,V$,
- for the other segments: homogeneous Neumann boundary conditions.

The magnetic field is caused by the local orientation of the electron spin in the crystal and is predetermined by the ferromagnetic properties of the material. We consider a constant magnetic field, oriented along the z-axis (perpendicular to the device). The electron spin may be also changed under the influence of the spin current, but we do not consider this effect here. In our model, $\vec{m}$ corresponds to the direction of the local magnetic field, and the parameter γ describes the intensity of the spin precession around this field. We choose $\vec{m} = 0$ in the channel region and

$$\vec{m} = \begin{cases} (0,0,1) & \text{for } x < L/3 \text{ or } x \geqslant 2L/3, \\ (0,0,0) & \text{for } L/3 \leqslant x < 2L/3. \end{cases}$$

The value for γ is taken from [36], i.e. $\gamma = \hbar/\tau$, with $\hbar$ being the reduced Planck constant. The spin polarization is nonzero only in the highly doped source and drain regions, and we take $p = 0.9$.

For the numerical discretization, we have chosen an admissible triangular mesh. Equations (5)-(11) are approximated by scheme (41)-(46), with the corresponding boundary conditions. The nonlinear system is solved at each time step by Newton's method. The time step size is $\triangle t = 0.05$. The computations are continued until a steady state is reached or, more precisely, until the difference of the solutions at two consecutive time steps in the ℓ^2 norm falls below a threshold (typically, 10^{-5}).

In Chapter 2 simulations for a one-dimensional multilayer structure are presented. Here, we consider also a multi-layer structure but for a simple MESFET model. Furthermore, we employed here a Scharfetter-Gummel discretization of the fluxes and a full Newton method, which are better adapted to large doping concentrations and smaller devices than a standard technique.

Figure 9 and Figure 10 demonstrate the steady-state density distributions in the open state. Figure 9 presents the scaled charge density n_0 and Figure 10 presents the spin density n_3 (note that $n_1 = n_2 = 0$). The densities are scaled by the doping concentration C_+, the spatial variable by the device length L. Compared to the closed state in Figure 11, the charge density is rather large in the channel region, which can be also observed in standard MESFET devices. The charge current density in the closed state is by the factor $10^5 \ldots 10^6$ smaller than in the open state. The spin density is (almost) zero in the closed state. Furthermore, the electrostatic potential for the open- and closed-state MESFET are presented in Figure 12 and Figure 13 respectively.

Current-voltage characteristics for MESFETs with and without ferromagnetic regions are shown in Figure 14. We observe that in the open state (non-positive gate potentials), the current densities in the ferromagnetic MESFET are slightly larger than in the standard device, which allows for an improved

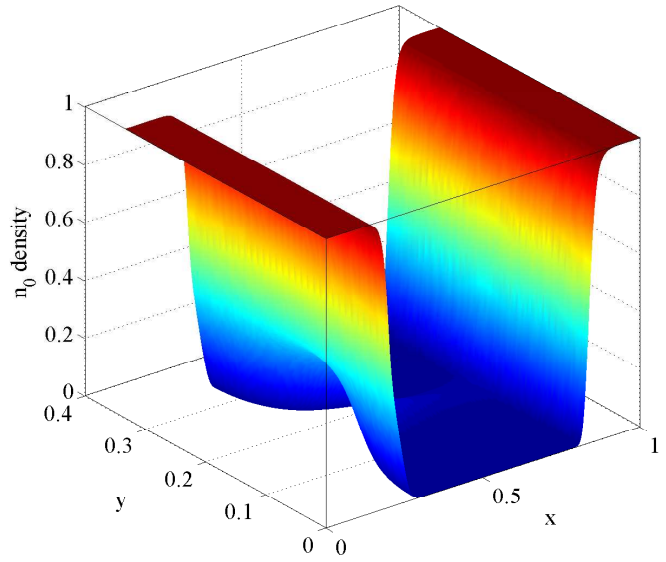

Figure 9: Scaled stationary charge density in an open-state MESFET with $V_D = -2\,V$ and $V_G = 0\,V$.

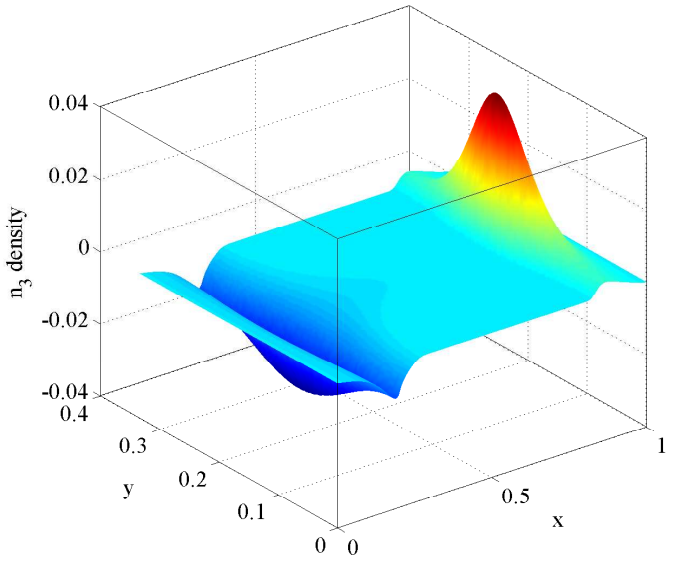

Figure 10: Scaled stationary spin density n_3 in an open-state MESFET with $V_D = -2\,V$ and $V_G = 0\,V$.

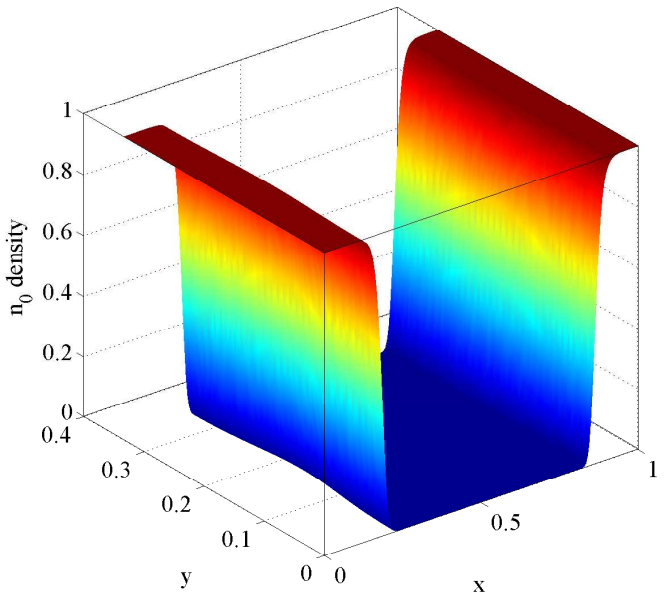

Figure 11: Scaled stationary charge density in a closed-state MESFET with $V_D = -2\,V$ and $V_G = 1.2\,V$.

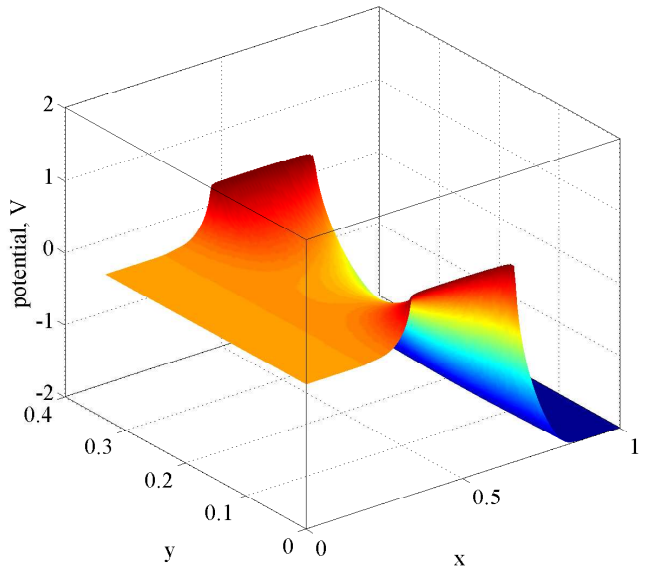

Figure 12: Electrostatic potential in a MESFET with $V_G = 0\,V$ (open state).

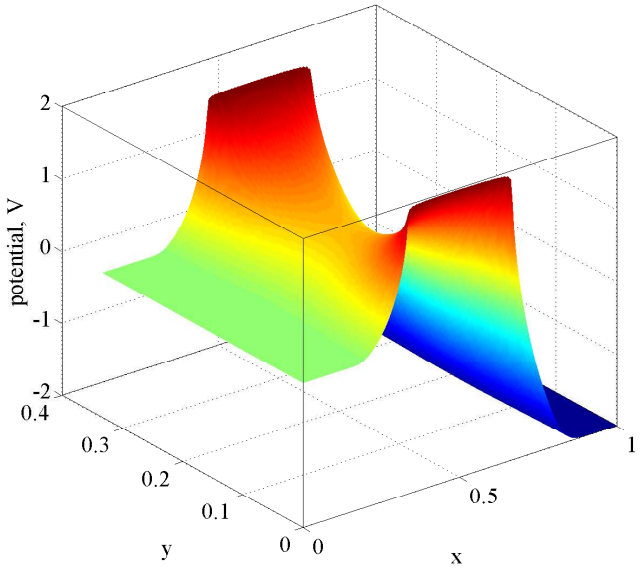

Figure 13: Electrostatic potential in a MESFET with $V_G = 1.2\,V$ (closed state).

device performance. When the transistor is closed ($V_G = 1.2\,V$), the current densities are (almost) zero for both transistor types.

In the left panel of Figure 15, we present the transient behavior of the charge density when switching from the open to the closed state ($V_D = -2\,V$; dotted line). The current values stabilize after about 1 ps. This justifies to define the numerical solution after 12 ps as the "steady-state solution". We compare these values with those computed from a standard MESFET (solid line). The stabilization in the ferromagnetic case is slightly faster which allows for faster devices.

Finally, we illustrate the free energy decay in Figure 15 (right) for various relaxation times τ. In this experiment, we have set $V_D = 0$ (source-drain voltage) and $V_G = 0$ (source-gate voltage). It turns out that the free energy decays with an exponential rate. For times larger than about 18 ps, the steady state is almost attained, and the numerical oscillations are caused by the finite machine precision. We observe that the decay is faster for smaller relaxation times which is expected. The decay rates are approximately 0.2/ps for $\tau_s = 100\,ps$, 0.4/ps for $\tau_s = 10\,ps$, and 1.7/ps for $\tau_s = 1\,ps$. The nonlinear dependence of the decay rates on τ_s may be caused by the influence of the energy dissipation.

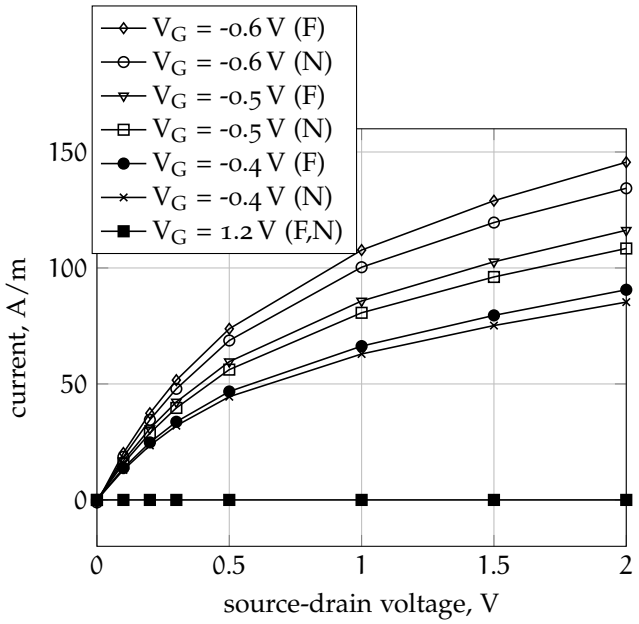

Figure 14: Current-voltage characteristics for the ferromagnetic (F) and standard (N) MESFET for various gate voltages V_G. For convenience, the source-drain voltages are given by their absolute values.

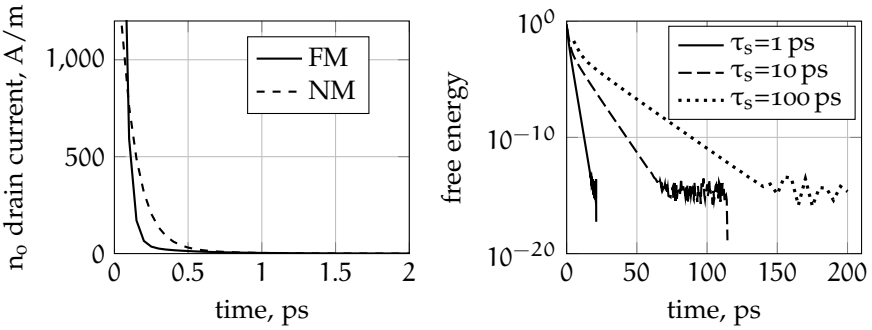

Figure 15: Left: Change of the electron drain current in the ferromagnetic (FM) and standard MESFET (NM), switching from open to closed state. Right: Semilogarithmic plot of the free energy versus time for various relaxation times.

Part III

ENERGY TRANSPORT

4 SPINORIAL ENERGY-TRANSPORT MODEL

4.1 INTRODUCTION

In the chapter we expand the described above spinorial drift-diffusion model to the spinorial energy-transport model, which besides charge and spin transport describes also the transport of energy. To this end, we reconsider the work [3]. There a spinorial energy-transport model is presented. However, the equations are not explicit and the system is difficult to analyze. We use some assumption to derive a simplified explicit version of this model.

The starting point of derivation of our energy-transport model is the spinorial Boltzmann equation for the distribution function $F(x,k,t)$ with values in the space of Hermitian 2×2 matrices,

$$\partial_t F + k\cdot\nabla_x F - \nabla_x V\cdot\nabla_k F = Q(F) + \frac{i}{2}[\vec{\Omega}\cdot\vec{\sigma}, F] + Q_{sf}(F), \tag{83}$$

where $x\in\mathbb{R}^3$ denotes the spatial variable, $k\in\mathbb{R}^3$ the wave vector, $t>0$ the time, $i=\sqrt{-1}$ the imaginary unit, and $[\cdot,\cdot]$ the commutator. The function $V(x,t)$ is the electric potential, which is usually self-consistently defined as the solution of the Poisson equation

$$-\lambda_D^2\Delta V = n_0[F] - C(x), \quad n_0[F] = \frac{1}{2}\operatorname{tr}\int_{\mathbb{R}^3} F\,dk,$$

where λ_D is the scaled Debye length, $n_0[F]$ the charge density, "tr" the trace of a matrix, and $C(x)$ the doping concentration [32]. Furthermore, $\vec{\Omega}(x,k)$ is an effective magnetic field or spin precession vector and $\vec{\sigma}=(\sigma_1,\sigma_2,\sigma_3)$ is the vector of the Pauli matrices. We choose the spin-conserving BGK-type collision operator $Q(F)=M[F]-F$, where the Maxwellian $M[F]$ is such that $Q(F)$ conserves mass and energy, and the operator $Q_{sf}(F)$ models spin-flip interactions. Details are given in Section 4.3.1.

Assuming dominant collisions and a large time scale, moment equations for the electron density $n[A,C]$ and energy density $W[A,C]$ can be derived from (83) in the diffusion limit [3], leading to

$$\begin{aligned} \partial_t n[A,C] + \operatorname{div} J_n &= F_n[\vec{\Omega},A,C],\\ \partial_t W[A,C] + \operatorname{div} J_W + J_n\cdot\nabla V &= F_W[\vec{\Omega},A,C], \quad x\in\mathbb{R}^3,\ t>0, \end{aligned} \tag{84}$$

where J_n and J_W are the particle and energy flux, respectively, and F_n, F_W are some functions; we refer to Section 4.3.1 for details. Furthermore, A and C are the Lagrange multipliers which are obtained from entropy maximization under the constraints of given mass and energy, and the electron and energy densities are the zeroth- and second-order moments

$$n[A,C] = \int_{\mathbb{R}^3} M[A,C]\,dk, \quad W[A,C] = \frac{1}{2}\int_{\mathbb{R}^3} M[A,C]|k|^2\,dk,$$

where $M[A,C]=\exp(A+C|k|^2/2)$ is the spinorial Maxwellian. Note that A and C are Hermitian matrices in $\mathbb{C}^{2\times 2}$, so $n[A,C]$ and $W[A,C]$ are Hermitian matrices too.

In contrast to the semiclassical situation, the densities cannot be expressed explicitly in terms of the Lagrange multipliers because of the matrix structure. In order to obtain explicit equations, we need to impose simplifying

assumptions on A and C. Our strategy is to formulate first the variables in terms of the Pauli basis,

$$A = a_0\sigma_0 + \vec{a}\cdot\vec{\sigma}, \quad C = c_0\sigma_0 + \vec{c}\cdot\vec{\sigma},$$

where σ_0 is the unit matrix and $a_0, c_0 \in \mathbb{R}$, $\vec{a}, \vec{c} \in \mathbb{R}^3$. The densities may be expanded in this basis as well, $n[A,C] = n_0\sigma_0 + \vec{n}\cdot\vec{\sigma}$, $W[A,C] = W_0\sigma_0 + \vec{W}\cdot\vec{\sigma}$, and the Maxwellian becomes

$$M[A,C] = e^{a_0+c_0|k|^2/2}\bigg(\cosh|\vec{b}(k)|\sigma_0 + \frac{\sinh|\vec{b}(k)|}{|\vec{b}(k)|}\vec{b}(k)\cdot\vec{\sigma}\bigg), \tag{85}$$
$$\vec{b}(k) := \vec{a} + \vec{c}\frac{|k|^2}{2}.$$

The formulation of the energy-transport model (84) in terms of the Pauli components $(a_0,\vec{a})$, $(c_0,\vec{c})$ still leads to nonexplicit equations, so we impose some conditions. We derive the explicit model by assuming $\vec{c} = 0$. Moreover, we compute the entropy (free energy) and the entropy production, thus providing not only the monotonicity of the entropy but also gradient estimates. One more result is the numerical solution: we discretize the one-dimensional equations using a semi-implicit Euler finite-volume scheme and illustrate the effect of the temperature on two multilayer structures.

The chapter is organized as follows. The main results are detailed in Section 4.2. The derivation of the general energy-transport model from the spinorial Boltzmann equation is recalled in Section 4.3.1 and the general model is formulated in terms of the Pauli components in Section 4.3.2. In Section 4.4, the simplified energy-transport model is derived. The entropy structure is investigated in Section 4.5. Some numerical experiments are performed in Section 4.6.

4.2 MAIN RESULTS

4.2.1 *Derivation of an explicit spin energy-transport model*

We derive an explicit version of (84) under the simplifying assumption $\vec{c} = 0$.

If the Lagrange multiplier C is interpreted as a "temperature" tensor, it might be reasonable to suppose that the "spin" part $\vec{c}$ is much smaller than the non-vanishing trace part c_0, which motivates the simplification $\vec{c} = 0$. This allows us to write three of the eight scalar moments $(n_0,\vec{n})$ and $(W_0,\vec{W})$ in terms of the remaining moments, leading to equations for five moments. We choose the moments $(n_0,\vec{n},W_0)$, leading to the system (see Section 4.4)

$$\partial_t n_0 + \operatorname{div} J_n = 0, \quad J_n = -\big(\nabla(n_0T) + n_0\nabla V\big), \tag{86}$$
$$\frac{3}{2}\partial_t(n_0T) + \operatorname{div} J_W + J_n\cdot\nabla V = 0, \quad J_W = -\frac{5}{2}\big(\nabla(n_0T^2) + n_0T\nabla V\big), \tag{87}$$
$$\partial_t\vec{n} - \sum_{j=1}^{3}\partial_{x_j}\big(\partial_{x_j}(\vec{n}T) + \vec{n}\partial_{x_j}V\big) + \vec{\Omega}_e\times\vec{n} = -\frac{\vec{n}}{\tau_{sf}}, \quad x\in\mathbb{R}^3,\ t>0, \tag{88}$$

where $T = 2W_0/(3n_0)$ is interpreted as the electron temperature, $\partial_{x_j} = \partial/\partial x_j$, $\vec{\Omega}_e$ is the even part of the effective field (with respect to k), and $\tau_{sf} > 0$ is the spin-flip relaxation time. In this model, $(n_0, \frac{3}{2}n_0T_0)$ solves the semiclassical energy-transport equations, and the spin-vector density $\vec{n}$

solves a drift-diffusion-type equation, which is coupled to the equations for $(n_0, \frac{3}{2}n_0T_0)$ via T only. Our numerical experiments indicate that this coupling is rather weak.

Motivated from [36], we may include a polarization matrix P in the definition of the collision operator $Q(F)$. We choose $Q(F) = P^{1/2}(M[F] - F)P^{1/2}$, where the direction of $P = \sigma_0 + p\vec{\Omega}\cdot\vec{\sigma}$ in spin space is the local magnetization $\vec{\Omega}$ and $p \in [0,1)$ represents the spin polarization of the scattering rates. This operator conserves spin, mass, and (in contrast to the operators in [36]) energy. The corresponding spin energy-transport model (still under the assumption $\vec{c} = 0$) becomes (see Remark 5)

$$\partial_t n_0 + \operatorname{div} j_n = 0, \quad j_n = \eta^{-2}\big(J_n - p\vec{\Omega}\cdot\vec{J}_n\big), \tag{89}$$

$$\frac{3}{2}\partial_t(n_0T) + \operatorname{div} j_W + j_n\cdot\nabla V = 0, \quad j_W = \eta^{-2}\big(J_W - p\vec{\Omega}\cdot\vec{J}_W\big), \tag{90}$$

$$\partial_t\vec{n} + \operatorname{div}\vec{j} + \vec{\Omega}_e\times\vec{n} = -\frac{\vec{n}}{\tau_{sf}}, \quad x\in\mathbb{R}^3,\ t>0, \tag{91}$$

where $\eta = \sqrt{1-p^2}$, J_n, J_W are as above, and

$$\vec{J}_n = -\big(\nabla(\vec{n}T) + \vec{n}\nabla V\big), \quad \vec{J}_W = -\frac{5}{2}\big(\nabla(\vec{n}T^2) + \vec{n}\nabla V\big),$$
$$\vec{j} = \eta^{-2}\big((1-\eta)(\vec{J}_n\cdot\vec{\Omega})\vec{\Omega} + \eta\vec{J}_n - p\vec{\Omega}J_n\big).$$

Note that we recover the model (86)-(88) if $p = 0$. We compare both models numerically in Section 4.6. It turns out that the polarization matrix P leads to a stronger mixing of the spin density components, and the heat flux effects causes a smoothing of these components.

Remark 4. The equations (89) and (91) of the spinorial energy-transport model coincide except for a small detail with the equations (5) and (6) from the lowest-order moment drift-diffusion system considered in Part II. This small detail is the difference in the coefficients in front of the cross-diffusion terms. The reason of this difference lays in the representation of density matrix in the Pauli basis. In Part II we use a rather physical approach of [36] and we have:

$$N = \frac{1}{2}n_0\sigma_0 + \vec{n}\cdot\vec{\sigma}$$

whereas in this chapter we represent the density matrix N ($n[A, C]$) like in [46]:

$$N = n_0\sigma_0 + \vec{n}\cdot\vec{\sigma}.$$

Respectively in the first case $n_0 = \operatorname{tr}(N)$ and in the second one: $n_0 = \frac{1}{2}\operatorname{tr}(N)$. By the second approach we automatically have symmetric diffusion matrix, whereas the charge density n_0 is a half of the physical charge density. In our study this difference is rather technical and we do not pay attention to it any more. □

4.2.2 *Entropy inequalities*

We prove that there exists an entropy (or free energy) which is nonincreasing in time along solutions to the corresponding equations. To simplify the computations, we neglect electric effects, i.e., the potential V is assumed to be constant (also see Remark 6 for the general situation).

The kinetic entropy of the general spin model (84) is given by

$$H = \int_{\mathbb{R}^3}\int_{\mathbb{R}^3} \operatorname{tr}(M\log M)\,dk\,dx, \tag{92}$$

where the Maxwellian is defined by (85) and "tr" denotes the trace of a matrix. It was shown in [3, Theorem 2.2] that the entropy is nonincreasing along

solutions to (84). Our aim is to quantify the entropy production $-dH/dt$ which provides gradient estimates. To this end, we insert the simplifying Maxwellians in (92) and compute explicit expressions for the entropy:

$$H = \int_{\mathbb{R}^3} \left(n_+ \log(n_+ T_+^{-3/2}) + n_- \log(n_- T_-^{-3/2})\right) dx, \tag{93}$$

and the corresponding entropy inequality reads as (see Proposition 7)

$$\frac{dH}{dt} + 4\int_{\mathbb{R}^3} \left(|\nabla\sqrt{n_+ T}|^2 + |\nabla\sqrt{n_- T}|^2 + 5n_0|\nabla\sqrt{T}|^2\right) dx \leqslant 0.$$

4.3 A GENERAL ENERGY-TRANSPORT MODEL FOR SPIN TRANSPORT

4.3.1 *Derivation from the spinorial Boltzmann equation*

We sketch briefly the derivation of the general energy-transport model (84) from the spinorial Boltzmann transport equation (83). Details are given in [3]. We consider the Boltzmann equation in the diffusion scaling,

$$\partial_t F_\varepsilon + \frac{1}{\varepsilon}\left(k\cdot\nabla_x F_\varepsilon - \nabla_x V\cdot\nabla_k F_\varepsilon\right) = \frac{1}{\varepsilon^2} Q(F_\varepsilon) + \frac{i}{2}[\vec{\Omega}_\varepsilon(x,k)\cdot\vec{\sigma}, F_\varepsilon] + Q_{sf}(F_\varepsilon), \tag{94}$$

The parameter $\varepsilon > 0$ is the scaled mean free path and is supposed to be small. We have assumed the parabolic-band approximation such that the mean velocity equals $v(k) = k$.

The last term in (94) represents the spin-flip interactions which are specified in (110) below. The commutator $[\cdot,\cdot]$ on the right-hand side of (94) can be rigorously derived from the Schrödinger equation with spin-orbit Hamiltonian in the semiclassical limit [28, Chapter 1]. The term models a precession effect around the effective field [3].

The first term on the right-hand side of (94) models collisions that conserve mass and energy. For simplicity, we employ the BGK-type operator (named after Bhatnagar, Gross, and Krook) $Q(F) = M[F] - F$, where the Maxwellian $M[F]$ associated to F has the same mass and energy as F,

$$\int_{\mathbb{R}^3} M[F]dk = \int_{\mathbb{R}^3} F dk, \quad \frac{1}{2}\int_{\mathbb{R}^3} M[F]|k|^2 dk = \frac{1}{2}\int_{\mathbb{R}^3} F|k|^2 dk. \tag{95}$$

The Maxwellian is constructed from entropy maximization under the constraints of given mass and energy, which yields, in case of Maxwell-Boltzmann statistics, the existence of Lagrange multipliers $A(x,t)$ and $C(x,t)$ such that [3]

$$M[F](x,k,t) = \exp\left(A(x,t) + C(x,t)\frac{|k|^2}{2}\right),$$

where exp is the matrix exponential and A, C are Hermitian 2×2 matrices satisfying (95).

The space of Hermitian 2×2 matrices can be spanned by the unit matrix σ_0 and the Pauli matrices $\vec{\sigma} = (\sigma_1,\sigma_2,\sigma_3)$,

$$\sigma_0 = \begin{pmatrix} 1 & 0 \\ 0 & 1 \end{pmatrix}, \quad \sigma_1 = \begin{pmatrix} 0 & 1 \\ 1 & 0 \end{pmatrix}, \quad \sigma_2 = \begin{pmatrix} 0 & -i \\ i & 0 \end{pmatrix}, \quad \sigma_3 = \begin{pmatrix} 1 & 0 \\ 0 & -1 \end{pmatrix}.$$

Accordingly, we may write $A = a_0 + \vec{a}\cdot\vec{\sigma}$ and $C = c_0 + \vec{c}\cdot\vec{\sigma}$, where a_0, $c_0 \in \mathbb{R}$, $\vec{a} = (a_1,a_2,a_3)$, $\vec{c} = (c_1,c_2,c_3) \in \mathbb{R}^3$, and $\vec{a}\cdot\vec{\sigma} = \sum_{j=1}^3 a_j\sigma_j$. The coefficients in the Pauli basis are computed from $a_0 = \frac{1}{2}\operatorname{tr}(A)$, $\vec{a} = \frac{1}{2}(\vec{\sigma}A)$,

and similarly for c_0, $\vec{c}$; see, e.g., [36]. The matrix exponential can be also expanded in the Pauli matrix, giving $M[F] = M_0\sigma_0 + \vec{M}\cdot\vec{\sigma}$, where

$$\begin{aligned} M_0 &= e^{a_0+c_0|k|^2/2}\cosh\left|\vec{a}+\vec{c}\frac{|k|^2}{2}\right|, \\ \vec{M} &= e^{a_0+c_0|k|^2/2}\frac{\sinh|\vec{a}+\vec{c}|k|^2/2|}{|\vec{a}+\vec{c}|k|^2/2|}\left(\vec{a}+\vec{c}\frac{|k|^2}{2}\right). \end{aligned} \tag{96}$$

It is shown in [3, Theorem 3.1] that F_ε converges formally to $M := M[A,C] = \exp(A + C|k|^2/2)$ as $\varepsilon\to 0$, where (A,C) are solutions to the following spin energy-transport system for the electron density $n(x,t)$ and energy density $W(x,t)$, which are related to (A,C) via the moment equations

$$n = \int_{\mathbb{R}^3} M[A,C]\,dk, \quad W = \frac{1}{2}\int_{\mathbb{R}^3} M[A,C]|k|^2\,dk.$$

The general energy-transport equations read as [3, Theorem 3.1]

$$\begin{aligned} \partial_t n + \operatorname{div}_x J_n &= \frac{i}{2}\int_{\mathbb{R}^3}\left[\vec{\Omega}_{ET}\cdot\vec{\sigma}, M\right]dk \\ &\quad -\frac{1}{4}\int_{\mathbb{R}^3}\left[\vec{\Omega}_o\cdot\vec{\sigma},[\vec{\Omega}_o\cdot\vec{\sigma},M]\right]dk + \int_{\mathbb{R}^3} Q_{sf}(M)\,dk, \end{aligned} \tag{97}$$

$$\begin{aligned} \partial_t W + \operatorname{div}_x J_W + J_n\cdot\nabla_x V &= \frac{i}{2}\int_{\mathbb{R}^3}\left[\vec{\Omega}_o\cdot\vec{\sigma},M\right]\frac{|k|^2}{2}dk \\ &\quad -\frac{1}{4}\int_{\mathbb{R}^3}\left[\vec{\Omega}_o\cdot\vec{\sigma},[\vec{\Omega}_o\cdot\vec{\sigma},M]\right]\frac{|k|^2}{2}dk + \frac{1}{2}\int_{\mathbb{R}^3} Q_{sf}(M)|k|^2\,dk, \end{aligned} \tag{98}$$

where the effective field $\vec{\Omega}_{ET}$ is defined by

$$\vec{\Omega}_{ET} = (k\cdot\nabla_x - \nabla_x V\cdot\nabla_k)\vec{\Omega}_o + \vec{\Omega}_e, \tag{99}$$

and $\vec{\Omega}_o$ and $\vec{\Omega}_e$ are the odd and even parts of $\vec{\Omega}$ (with respect to k), respectively. The tensor-valued fluxes are defined by

$$\begin{aligned} J_n &= -\operatorname{div}_x\Pi - n\nabla_x V + \Pi_{\Omega_o}, \\ J_W &= -\operatorname{div}_x Q - (W\sigma_0+\Pi)\nabla_x V + Q_{\Omega_o}, \end{aligned} \tag{100}$$

and the tensors $\Pi = (\Pi^{j\ell})$, $Q = (Q^{j\ell})$ with $\Pi^{j\ell}$, $Q^{j\ell}\in\mathbb{C}^{2\times 2}$ and $\Pi_{\Omega_o} = (\Pi^j_{\Omega_o})$, $Q_{\Omega_o} = (Q^j_{\Omega_o})$ with $\Pi^j_{\Omega_o}$, $Q^j_{\Omega_o}\in\mathbb{C}^{2\times 2}$ are given by the moments

$$\begin{aligned} \Pi^{j\ell} &= \int_{\mathbb{R}^3} k_j k_\ell M\,dk, & Q^{j\ell} &= \frac{1}{2}\int_{\mathbb{R}^3} k_j k_\ell |k|^2 M\,dk, \\ \Pi^j_{\Omega_o} &= i\int_{\mathbb{R}^3}\left[\vec{\Omega}_o\cdot\vec{\sigma},M\right]k_j\,dk, & Q^j_{\Omega_o} &= \frac{i}{2}\int_{\mathbb{R}^3}\left[\vec{\Omega}_o\cdot\vec{\sigma},M\right]k_j|k|^2\,dk, \end{aligned}$$

where $j,\ell = 1,2,3$. The first two terms on the right-hand sides of (97) and (98) are due to spinor effects; they vanish in the classical energy-transport model. The last term on the left-hand side of (98) is the Joule heating and it is also present in the classical model. The last terms in (97)-(98) express the moments of the spin-flip interactions.

4.3.2 *Formulation in the Pauli basis*

In order to derive the simplified spin energy-transport model in explicit form, it is convenient to formulate (97)-(98) in the Pauli basis. Recall that $n = n_0\sigma_0 + \vec{n}\cdot\vec{\sigma}$ and $W = W_0\sigma_0 + \vec{W}\cdot\vec{\sigma}$. Furthermore, we expand

$$\begin{aligned} \int_{\mathbb{R}^3} Q_{sf}(M)\,dk &= Q_{sf,n,0}\sigma_0 + \vec{Q}_{sf,n}\cdot\vec{\sigma}, \\ \frac{1}{2}\int_{\mathbb{R}^3} Q_{sf}(M)|k|^2\,dk &= Q_{sf,W,0}\sigma_0 + \vec{Q}_{sf,W}\cdot\vec{\sigma}. \end{aligned} \tag{101}$$

Lemma 5 (Energy-transport model in Pauli components). *Equations* (97)-(98) *can be written in the Pauli components* $(n_0, \vec{n})$ *and* $(W_0, \vec{W})$ *as*

$$\partial_t n_0 - \operatorname{div}_x\left(\frac{2}{3}\nabla_x W_0 + n_0\nabla_x V\right) = Q_{sf,n,0}, \tag{102}$$

$$\begin{aligned}\partial_t \vec{n} &- \sum_{j=1}^3 \partial_{x_j}\left(\frac{2}{3}\partial_{x_j}\vec{W} + \vec{n}\partial_{x_j}V + 2\int_{\mathbb{R}^3}(\vec{\Omega}_o\times\vec{M})k_j\,dk\right) \\ &+ \sum_{j=1}^3\int_{\mathbb{R}^3}\partial_{x_j}(\vec{\Omega}_o\times\vec{M})k_j\,dk + \sum_{j=1}^3\partial_{x_j}V\int_{\mathbb{R}^3}\partial_{k_j}(\vec{\Omega}_o\times\vec{M})\,dk \\ &+ \int_{\mathbb{R}^3}\vec{\Omega}_e\times\vec{M}\,dk + \int_{\mathbb{R}^3}\left(|\vec{\Omega}_o|^2 - \vec{\Omega}_o\otimes\vec{\Omega}_o\right)\cdot\vec{M}\,dk = \vec{Q}_{sf,n},\end{aligned} \tag{103}$$

$$\begin{aligned}\partial_t W_0 &- \operatorname{div}_x\left(\frac{1}{6}\int_{\mathbb{R}^3}\nabla_x M_0|k|^4\,dk + \frac{5}{3}W_0\nabla_x V\right) \\ &- \left(\frac{2}{3}\nabla_x W_0 + n_0\nabla_x V\right)\cdot\nabla_x V = Q_{sf,W,0},\end{aligned} \tag{104}$$

$$\begin{aligned}\partial_t \vec{W} &- \sum_{j=1}^3\left\{\partial_{x_j}\left(\frac{1}{6}\partial_{x_j}\int_{\mathbb{R}^3}\vec{M}|k|^4\,dk + \frac{5}{3}\vec{W}\partial_{x_j}V\right.\right. \\ &+ \left.\int_{\mathbb{R}^3}(\vec{\Omega}_o\times\vec{M})k_j|k|^2\,dk\right) \\ &+ \left.\left(\frac{2}{3}\partial_{x_j}\vec{W} + \vec{n}\partial_{x_j}V + 2\int_{\mathbb{R}^3}(\vec{\Omega}_o\times\vec{M})k_j\,dk\right)\partial_{x_j}V\right\} \\ &+ \frac{1}{2}\sum_{j=1}^3\partial_{x_j}\int_{\mathbb{R}^3}(\vec{\Omega}_o\times\vec{M})k_j|k|^2\,dk \\ &+ \frac{1}{2}\sum_{j=1}^3\partial_{x_j}V\int_{\mathbb{R}^3}\partial_{k_j}(\vec{\Omega}_o\times\vec{M})|k|^2\,dk + \frac{1}{2}\int_{\mathbb{R}^3}(\vec{\Omega}_e\times\vec{M})|k|^2\,dk \\ &+ \int_{\mathbb{R}^3}\left(|\vec{\Omega}_o|^2 - \vec{\Omega}_o\otimes\vec{\Omega}_o\right)\cdot\vec{M}|k|^2\,dk = \vec{Q}_{sf,W},\end{aligned} \tag{105}$$

where $\partial_{x_j} = \partial/\partial x_j$, $\partial_{k_j} = \partial/\partial k_j$.

Proof. We reformulate (97)-(98) in terms of the Pauli coefficients. For this, set $J_n = (J^j_n)_{j=1,2,3}$, $J_W = (J^j_W)_{j=1,2,3}$ and $J^j_n = J^j_{n,0}\sigma_0 + \vec{J}_n\cdot\vec{\sigma}$, $J^j_W = J^j_{W,0}\sigma_0 + \vec{J}_W\cdot\vec{\sigma}$. We obtain

$$\partial_t n_0 + \sum_{j=1}^3\partial_{x_j}J^j_{n,0} = Q_{sf,n,0}, \tag{106}$$

$$\begin{aligned}\partial_t\vec{n} &+ \sum_{j=1}^3\partial_{x_j}\vec{J}^j_n + \int_{\mathbb{R}^3}\vec{\Omega}_{ET}\times\vec{M}\,dk \\ &+ \int_{\mathbb{R}^3}\left(|\vec{\Omega}_o|^2 - \vec{\Omega}_o\otimes\vec{\Omega}_o\right)\cdot\vec{M}\,dk = \vec{Q}_{sf,n},\end{aligned} \tag{107}$$

$$\partial_t W_0 + \sum_{j=1}^3\left(\partial_{x_j}J^j_{W,0} + J^j_{n,0}\partial_{x_j}V\right) = Q_{sf,W,0}, \tag{108}$$

$$\begin{aligned}\partial_t\vec{W} &+ \sum_{j=1}^3\left(\partial_{x_j}\vec{J}^j_W + \vec{J}^j_n\partial_{x_j}V\right) + \int_{\mathbb{R}^3}(\vec{\Omega}_{ET}\times\vec{M})|k|^2\,dk \\ &+ \frac{1}{2}\int_{\mathbb{R}^3}\left(|\vec{\Omega}_o|^2 - \vec{\Omega}_o\otimes\vec{\Omega}_o\right)\cdot\vec{M}|k|^2\,dk = \vec{Q}_{sf,W}.\end{aligned} \tag{109}$$

Let us expand the integrals involving $\vec{\Omega}_{ET}$ and the fluxes. Let $\phi(k) = 1$ or $\phi(k) = |k|^2/2$. Then, recalling definition (99) for $\vec{\Omega}_{ET}$,

$$\begin{aligned}
&\int_{\mathbb{R}^3} (\vec{\Omega}_{ET} \times \vec{M})\phi(k)\,dk \\
&\quad = \int_{\mathbb{R}^3} \big(k \cdot \nabla_x - \nabla_x V \cdot \nabla_k\big)(\vec{\Omega}_o \times \vec{M})\phi(k)\,dk \\
&\quad + \int_{\mathbb{R}^3} (\vec{\Omega}_e \times \vec{M})\phi(k)\,dk = \sum_{j=1}^3 \partial_{x_j} \int_{\mathbb{R}^3} (\vec{\Omega}_o \times \vec{M}) k_j \phi(k)\,dk \\
&\quad - \sum_{j=1}^3 \partial_{x_j} V \int_{\mathbb{R}^3} (\partial_{k_j} \vec{\Omega}_o \times \vec{M})\phi(k)\,dk + \int_{\mathbb{R}^3} (\vec{\Omega}_e \times \vec{M})\phi(k)\,dk.
\end{aligned}$$

Inserting these expressions into the evolution equations for $\vec{n}$ and $\vec{W}$, we recover the integrals in the second and third line of (103), and the last integral in the third line of (105).

It remains to compute the fluxes (100). First, we calculate

$$\Pi^{j\ell} = \frac{1}{3}\int_{\mathbb{R}^3} M|k|^2\,dk\delta_{j\ell} = \frac{2}{3}W\delta_{j\ell}, \quad Q^{j\ell} = \frac{1}{6}\int_{\mathbb{R}^3} M|k|^4\,dk\delta_{j\ell}.$$

Furthermore, using the formula $[\vec{u}\cdot\vec{\sigma}, \vec{v}\cdot\vec{\sigma}] = 2i(\vec{u}\times\vec{v})\cdot\vec{\sigma}$ for $\vec{u}, \vec{v} \in \mathbb{R}^3$, we find that $\Pi_{\Omega_o} = \Pi_{\Omega_o,0}\sigma_0 + \vec{\Pi}_{\Omega_o}\cdot\vec{\sigma}$ with $\Pi_{\Omega_o,0} = 0$ and $\vec{\Pi}_{\Omega_o} = -2\int_{\mathbb{R}^3}(\vec{\Omega}_o \times \vec{M})k\,dk$. Therefore,

$$\begin{aligned}
J^j_{n,0} &= -\sum_{\ell=1}^3 \partial_{x_\ell}\Pi^{j\ell}_0 - n_0\partial_{x_j}V + \Pi^j_{\Omega_o,0} = -\frac{2}{3}\partial_{x_j}W_0 - n_0\partial_{x_j}V, \\
\vec{J}^j_n &= -\sum_{\ell=1}^3 \partial_{x_\ell}\vec{\Pi}^{j\ell} - \vec{n}\partial_{x_j}V + \vec{\Pi}^j_{\Omega_o} = -\frac{2}{3}\partial_{x_j}\vec{W} - \vec{n}\partial_{x_j}V \\
&\quad - 2\int_{\mathbb{R}^3}(\vec{\Omega}_o \times \vec{M})k_j\,dk.
\end{aligned}$$

Expanding $Q_{\Omega_o} = Q_{\Omega_o,0}\sigma_0 + \vec{Q}_{\Omega_o}\cdot\vec{\sigma}$ with $Q_{\Omega_o,0} = 0$ and $\vec{Q}_{\Omega_o} = -\int_{\mathbb{R}^3}(\vec{\Omega}_o \times \vec{M})k|k|^2\,dk$, it follows that

$$\begin{aligned}
J^j_{W,0} &= -\sum_{\ell=1}^3 \big(\partial_{x_\ell}Q^{j\ell}_0 + (W_0\delta_{j\ell} + \Pi^{j\ell}_0)\partial_{x_\ell}V\big) + Q^j_{\Omega_o,0} \\
&= -\frac{1}{6}\partial_{x_j}\int_{\mathbb{R}^3} M_0|k|^4\,dk - \frac{5}{3}W_0\partial_{x_j}V, \\
\vec{J}^j_W &= -\sum_{\ell=1}^3 \big(\partial_{x_\ell}\vec{Q}^{j\ell} + (\vec{W}\delta_{j\ell} + \vec{\Pi}^{j\ell})\partial_{x_\ell}V\big) + \vec{Q}^j_{\Omega_o} \\
&= -\frac{1}{6}\partial_{x_j}\int_{\mathbb{R}^3} \vec{M}|k|^4\,dk - \frac{5}{3}\vec{W}\partial_{x_j}V - \int_{\mathbb{R}^3}(\vec{\Omega}_o \times \vec{M})k_j|k|^2\,dk.
\end{aligned}$$

Inserting these expressions into (106)-(109) gives (102)-(105). □

4.4 SIMPLIFIED SPIN ENERGY-TRANSPORT EQUATIONS

In this section, we derive the explicit model. We assume for simplicity that the odd part of the magnetization vanishes, $\vec{\Omega}_o = 0$, and that the even part $\vec{\Omega}_e$ depends on x only. Moreover, we suppose that the spin-flip interactions are modeled by the relaxation-time operator

$$Q_{sf}(M) := -\frac{1}{\tau_{sf}}\left(M - \frac{1}{2}\operatorname{tr}(M)\sigma_0\right) = -\frac{1}{\tau_{sf}}\vec{M}\cdot\vec{\sigma}, \tag{110}$$

where $\tau_{sf} > 0$ is the average time between two subsequent spin-flip collisions, and we recall that $M = M_0\sigma_0 + \vec{M}\cdot\vec{\sigma}$. In particular, with the notation of (101),

$$Q_{sf,n,0} = 0, \quad \vec{Q}_{sf,n} = -\frac{\vec{n}}{\tau_{sf}}, \quad Q_{sf,W,0} = 0, \quad \vec{Q}_{sf,W} = -\frac{\vec{W}}{\tau_{sf}}.$$

Then system (102)-(105) reduces to

$$\partial_t n_0 - \operatorname{div}\left(\frac{2}{3}\nabla W_0 + n_0\nabla V\right) = 0, \tag{111}$$

$$\partial_t \vec{n} - \sum_{j=1}^{3}\partial_{x_j}\left(\frac{2}{3}\partial_{x_j}\vec{W} + \vec{n}\partial_{x_j}V\right) + \vec{\Omega}_e\times\vec{n} = -\frac{\vec{n}}{\tau_{sf}}, \tag{112}$$

$$\begin{aligned}\partial_t W_0 - \operatorname{div}&\left(\frac{1}{6}\nabla\int_{\mathbb{R}^3} M_0|k|^2\,dk + \frac{5}{3}W_0\nabla V\right)\\ &-\left(\frac{2}{3}\nabla W_0 + n_0\nabla V\right)\cdot\nabla V = 0,\end{aligned} \tag{113}$$

$$\begin{aligned}\partial_t\vec{W} - \sum_{j=1}^{3}&\left\{\partial_{x_j}\left(\frac{1}{6}\partial_{x_j}\int_{\mathbb{R}^3}\vec{M}|k|^4\,dk + \frac{5}{3}\vec{W}\partial_{x_j}V\right)\right.\\ &\left.+\left(\frac{2}{3}\partial_{x_j}\vec{W} + \vec{n}\partial_{x_j}V\right)\partial_{x_j}V\right\} + \vec{\Omega}_e\times\vec{W} = -\frac{\vec{W}}{\tau_{sf}}.\end{aligned} \tag{114}$$

Given $(n_0, \vec{n}, W_0)$, we define the spin-up/spin-down densities $n_\pm$ and the temperature T by

$$n_\pm = n_0 \pm |\vec{n}|, \quad W_0 = \frac{3}{2}n_0 T. \tag{115}$$

We also introduce the Gaussian with standard deviation $\theta > 0$,

$$g_\theta(k) = (2\pi\theta)^{-3/2}\exp\left(-\frac{|k|^2}{2\theta}\right), \tag{116}$$

whose moments are given by

$$\int_{\mathbb{R}^3} g_\theta(k)\begin{pmatrix}1\\ |k|^2/2\\ |k|^4/6\end{pmatrix}dk = \begin{pmatrix}1\\ 3\theta/2\\ 5\theta^2/2\end{pmatrix}. \tag{117}$$

Theorem 6 (Spin energy-transport model with $\vec{c} = 0$)**.** *For $\vec{c} = 0$, system (111)-(114) can be written in the variables $(n_0, T, \vec{n})$ as (86)-(88).*

Proof. Under the assumption $\vec{c} = 0$, the higher-order moments in (113)-(114) can be computed explicitly. Indeed, the Pauli expansion of the Maxwellian (96) simplifies to

$$M_0 = e^{a_0 + c_0|k|^2/2}\cosh|\vec{a}|, \quad \vec{M} = e^{a_0+c_0|k|^2/2}\sinh|\vec{a}|\frac{\vec{a}}{|\vec{a}|}.$$

Observe that $c_0 < 0$ is necessary to ensure the integrability of M_0 and $\vec{M}$. The above expressions can be reformulated by introducing the new Lagrange multipliers

$$\kappa_\pm := \left(\frac{2\pi}{-c_0}\right)^{3/2} e^{a_0\pm|\vec{a}|}, \quad \theta := -\frac{1}{c_0}, \quad \vec{\gamma} := \frac{\vec{a}}{|\vec{a}|}.$$

Then $M_0 = \frac{1}{2}(\kappa_+ + \kappa_-)g_\theta(k)$, $\vec{M} = \frac{1}{2}(\kappa_+ - \kappa_-)g_\theta(k)\vec{\gamma}$, where g_θ is defined in (116). As a consequence, we have

$$n_0 = \int_{\mathbb{R}^3} M_0 dk = \frac{1}{2}(\kappa_+ + \kappa_-), \quad \vec{n} = \int_{\mathbb{R}^3} \vec{M} dk = \frac{1}{2}(\kappa_+ - \kappa_-)\vec{\gamma},$$
$$W_0 = \frac{1}{2}\int_{\mathbb{R}^3} M_0|k|^2 dk = \frac{3}{4}\theta(\kappa_+ + \kappa_-),$$

and we infer from (115) that $\kappa_\pm = n_\pm$, $\vec{\gamma} = \vec{n}/|\vec{n}|$, and $\theta = T$. Then the Pauli coefficients become $M_0 = n_0 g_T(k)$, $\vec{M} = \vec{n} g_T(k)$ and

$$\vec{W} = \frac{1}{2}\int_{\mathbb{R}^3} \vec{M}|k|^2 dk = \frac{3}{2}\vec{n}T, \quad \frac{1}{6}\int_{\mathbb{R}^3} M_0|k|^4 dk = \frac{5}{2}n_0 T^2.$$

Inserting these expressions into (111)-(114) shows the result. □

Remark 5. The derivation of model (89)-(91) is similar to that one in [3], therefore we sketch it only. The Maxwellian is here given by

$$M[F](k) = (2\pi\theta[F])^{-3/2} e^{-|k|^2/(2\theta[F])} \int_{\mathbb{R}^3} F(k')dk',$$
$$\text{where } \theta[F] = \frac{1}{3}\frac{\int_{\mathbb{R}^3} \operatorname{tr}(PF(k))|k|^2 dk}{\int_{\mathbb{R}^3} \operatorname{tr}(PF(k))dk}.$$

The formal limit $\varepsilon \to 0$ in (94) gives $Q(F^0) = 0$, where $F^0 = \lim_{\varepsilon\to 0} F_\varepsilon$, showing that $F^0 = M[F^0]$. Next, we perform a Hilbert expansion $F_\varepsilon = M[F] + \varepsilon F^1 + O(\varepsilon^2)$ and assume that F^1 is odd with respect to k. Since 1, $|k|^2/2$ are even functions, F^1 does not contribute to the moments $n = \int_{\mathbb{R}^3} F dk$, $W = \frac{1}{2}\int_{\mathbb{R}^3} F|k|^2 dk$. It holds that $W = \frac{3}{2}nT$, where $T := \theta[F^0]$. After a computation which is similar to the derivation of the semiclassical energy-transport equations, we obtain the moment equations

$$\partial_t n + \operatorname{div} G_n + i[n, \vec{\Omega}\cdot\vec{\sigma}] = \frac{1}{2}\operatorname{tr}(n) - n,$$
$$G_n = -P^{-1/2}\big(\nabla(nT) + n\nabla V\big)P^{-1/2},$$
$$\frac{3}{2}\partial_t(nT) + \operatorname{div} G_W + G_n\cdot\nabla V = 0,$$
$$G_W = -\frac{5}{3}P^{-1/2}\big(\nabla(nT^2) + nT\nabla V\big)P^{-1/2}.$$

In order to formulate these equations in the Pauli components, we observe that for any 2×2 Hermitian matrix $A = a_0\sigma_0 + \vec{a}\cdot\vec{\sigma}$, it holds that $P^{1/2}AP^{1/2} = b_0\sigma_0 + \vec{b}\cdot\vec{\sigma}$, where

$$\begin{pmatrix} b_0 \\ \vec{b}\end{pmatrix} = \eta^{-2}\begin{pmatrix} 1 & -p\vec{\Omega}^\top \\ -p\vec{\Omega} & (1-\eta)\vec{\Omega}\otimes\vec{\Omega} + \eta\sigma_0\end{pmatrix}\begin{pmatrix} a_0 \\ \vec{a}\end{pmatrix}, \quad \eta = \sqrt{1-p^2}.$$

We omit the calulcation and only note that this leads to (89)-(91). □

4.5 ENTROPY STRUCTURE

In this section, we investigate the entropy structure of the spin energy-transport equations derived in the previous section. Recall that the entropy of the general model is given by

$$H = \int_{\mathbb{R}^3}\int_{\mathbb{R}^3} \operatorname{tr}(M\log M)dkdx,$$

where $M = M_0\sigma_0 + \vec{M}\cdot\vec{\sigma}$ is the Maxwellian. We introduce $M_\pm = M_0 \pm |\vec{M}|$ and $P_\pm = \frac{1}{2}(\sigma_0 \pm (\vec{M}/|\vec{M}|)\cdot\vec{\sigma})$. Then (P_+, P_-) is a set of complete orthogonal

projections since $P_\pm^2 = P_\pm$, $P_+P_- = 0$, and $P_+ + P_- = \sigma_0$. Therefore, for any function $f : \mathbb{R} \to \mathbb{R}$,

$$\begin{aligned} f(M) &= f(M_+)P_+ + f(M_-)P_- \\ &= \frac{1}{2}\big(f(M_+) + f(M_-)\big)\sigma_0 + \frac{1}{2}\big(f(M_+) - f(M_-)\big)\frac{\vec{M}}{|\vec{M}|}\cdot\vec{\sigma}. \end{aligned}$$

In particular, since the Pauli matrices are traceless,

$$H = \frac{1}{2}\int_{\mathbb{R}^3}\int_{\mathbb{R}^3}(M_+\log M_+ + M_-\log M_-)\,dk\,dx. \tag{118}$$

We wish to explore the entropy structure of the model (86)-(88) ($\vec{c} = 0$), neglecting the electric field:

$$\begin{aligned} \partial_t n_0 = \Delta(n_0 T), \quad \frac{3}{2}\partial_t(n_0 T) = \frac{5}{2}\Delta(n_0 T^2), \\ \partial_t \vec{n} = \Delta(\vec{n}T) - \vec{\Omega}_e\times\vec{n} - \frac{\vec{n}}{\tau_{sf}}, \end{aligned} \tag{119}$$

where $x \in \mathbb{R}^3$, $t > 0$. We claim that the entropy is given by (93). Indeed, since $\vec{c} = 0$ by assumption, $M = g_T(k)(n_0\sigma_0 + \vec{n}\cdot\vec{\sigma})$, where $g_T(k)$ is defined in (116) (see the proof of Theorem 6). Then $M_\pm = g_T(k)n_\pm$ and (118) shows that

$$\begin{aligned} H &= \frac{1}{2}\int_{\mathbb{R}^3}\int_{\mathbb{R}^3} g_T(k)\big(n_+\log(n_+ g_T(k)) + n_-\log(n_- g_T(k))\big)\,dx\,dk \\ &= \frac{1}{2}\int_{\mathbb{R}^3}(n_+\log n_+ + n_-\log n_-)\,dx \\ &\quad + \int_{\mathbb{R}^3}(n_+ + n_-)\int_{\mathbb{R}^3} g_T(k)\log g_T(k)\,dk\,dx \\ &= \frac{1}{2}\int_{\mathbb{R}^3}(n_+\log n_+ + n_-\log n_-)\,dx \\ &\quad - \int_{\mathbb{R}^3}(n_+ + n_-)\left(\frac{3}{2} + \frac{3}{2}\log(2\pi T)\right)dx. \end{aligned}$$

Thus, since $\int_{\mathbb{R}^3}(n_+ + n_-)\,dx$ is constant in time, we find that, up to a constant,

$$H = \int_{\mathbb{R}^3}\big(n_+\log(n_+T^{-3/2}) + n_-\log(n_-T^{-3/2})\big)\,dx,$$

which is exactly (93). Recall that $n_\pm = n_0 \pm |\vec{n}|$.

Proposition 7 (Entropy inequality for system (119))**.** *The entropy* (93)*, considered as a function of time, is nonincreasing along (smooth) solutions* $(n_0, T, \vec{n})$ *to* (119)*, and*

$$\begin{aligned} &\frac{dH}{dt} + 4\int_{\mathbb{R}^3}\big(|\nabla\sqrt{n_+T}|^2 + |\nabla\sqrt{n_-T}|^2\big)\,dx + 20\int_{\mathbb{R}^3} n_0|\nabla\sqrt{T}|^2\big)\,dx \\ &+ \frac{1}{2}\int_{\mathbb{R}^3}(n_+ - n_-)(\log n_+ - \log n_-)\left(\frac{1}{\tau_{sf}} + T\left|\nabla\frac{\vec{n}}{|\vec{n}|}\right|^2\right)dx = 0. \end{aligned} \tag{120}$$

Proof. We compute

$$\begin{aligned}
\frac{dH}{dt} &= \int_{\mathbb{R}^3} \sum_{s=\pm} \left(\log(n_s T^{-3/2}) \partial_t n_s - \frac{3}{2} \frac{1}{T} \partial_t (n_s T) \right) dx \\
&= \int_{\mathbb{R}^3} \Big(\log\left((n_0 + |\vec{n}|) T^{-3/2}\right) \partial_t (n_0 + |\vec{n}|) - \frac{3}{2} \frac{1}{T} \partial_t (n_0 T + |\vec{n}| T) \\
&\quad + \log\left((n_0 - |\vec{n}|) T^{-3/2}\right) \partial_t (n_0 - |\vec{n}|) - \frac{3}{2} \frac{1}{T} \partial_t (n_0 T - |\vec{n}| T) \Big) dx \\
&= \int_{\mathbb{R}^3} \Big\{ \log\left(\frac{n_0^2 - |\vec{n}|^2}{T^3} \right) \partial_t n_0 + \log\left(\frac{n_0 + |\vec{n}|}{n_0 - |\vec{n}|} \right) \frac{\vec{n}}{|\vec{n}|} \cdot \partial_t \vec{n} \qquad (121) \\
&\quad - \frac{2}{T} \partial_t \left(\frac{3}{2} n_0 T \right) \Big\} dx. \qquad (122)
\end{aligned}$$

Inserting (86) in the first term and integrating by parts, we find that

$$\int_{\mathbb{R}^3} \log\left(\frac{n_0^2 - |\vec{n}|^2}{T^3} \right) \partial_t n_0 \, dx = - \int_{\mathbb{R}^3} \nabla \log\left(\frac{n_0^2 - |\vec{n}|^2}{T^3} \right) \cdot \nabla (n_0 T) dx.$$

Furthermore, using (88) in the second term on the right-hand side of (122) and integrating by parts gives

$$\begin{aligned}
&\int_{\mathbb{R}^3} \log\left(\frac{n_0 + |\vec{n}|}{n_0 - |\vec{n}|} \right) \frac{\vec{n}}{|\vec{n}|} \cdot \partial_t \vec{n} \, dx \\
&\quad = - \int_{\mathbb{R}^3} \nabla \Big(\log\left(\frac{n_0 + |\vec{n}|}{n_0 - |\vec{n}|} \right) \Big) \frac{\vec{n}}{|\vec{n}|} \cdot \nabla (\vec{n} T) dx \\
&\qquad - \int_{\mathbb{R}^3} \log\left(\frac{n_0 + |\vec{n}|}{n_0 - |\vec{n}|} \right) \nabla \frac{\vec{n}}{|\vec{n}|} \cdot \nabla (\vec{n} T) dx \\
&\qquad - \frac{1}{\tau_{sf}} \int_{\mathbb{R}^3} |\vec{n}| \log\left(\frac{n_0 + |\vec{n}|}{n_0 - |\vec{n}|} \right) dx.
\end{aligned}$$

Since $\nabla \vec{n} \cdot \vec{n} = 0$ and

$$\begin{aligned}
\nabla \frac{\vec{n}}{|\vec{n}|} \cdot \nabla (\vec{n} T) &= \nabla \frac{\vec{n}}{|\vec{n}|} \cdot \nabla \left(|\vec{n}| T \frac{\vec{n}}{|\vec{n}|} \right) = |\vec{n}| T \left| \nabla \frac{\vec{n}}{|\vec{n}|} \right|^2, \\
\frac{\vec{n}}{|\vec{n}|} \cdot \nabla (\vec{n} T) &= \frac{\vec{n}}{|\vec{n}|} \cdot (T \vec{n} + \vec{n} \nabla T) = T \nabla |\vec{n}| + |\vec{n}| \nabla T = \nabla (|\vec{n}| T),
\end{aligned}$$

it follows that

$$\begin{aligned}
&\int_{\mathbb{R}^3} \log\left(\frac{n_0 + |\vec{n}|}{n_0 - |\vec{n}|} \right) \frac{\vec{n}}{|\vec{n}|} \cdot \partial_t \vec{n} \, dx = - \int_{\mathbb{R}^3} \log\left(\frac{n_0 + |\vec{n}|}{n_0 - |\vec{n}|} \right) \cdot \nabla (|\vec{n}| T) dx \\
&- \int_{\mathbb{R}^3} \log\left(\frac{n_0 + |\vec{n}|}{n_0 - |\vec{n}|} \right) |\vec{n}| T \left| \nabla \frac{\vec{n}}{|\vec{n}|} \right|^2 dx - \frac{1}{\tau_{sf}} \int_{\mathbb{R}^3} |\vec{n}| \log\left(\frac{n_0 + |\vec{n}|}{n_0 - |\vec{n}|} \right) dx.
\end{aligned}$$

Finally, we employ (87) to reformulate the last term on the right-hand side of (122):

$$\begin{aligned}
&- \int_{\mathbb{R}^3} \frac{2}{T} \partial_t \left(\frac{3}{2} n_0 T \right) dx = 5 \int_{\mathbb{R}^3} \nabla \frac{1}{T} \cdot \nabla (n_0 T^2) dx \\
&\quad = -5 \int_{\mathbb{R}^3} \nabla \log T \cdot \nabla (n_0 T) dx - 5 \int_{\mathbb{R}^3} \frac{n_0}{T} |\nabla T|^2 dx.
\end{aligned}$$

Summarizing these expressions, we have

$$\begin{aligned}\frac{dH}{dt} &= -\int_{\mathbb{R}^3}\left\{\nabla\log\left(\frac{n_0^2-|\vec{n}|^2}{T^3}\right)\cdot\nabla(n_0T)\right.\\ &\quad+\nabla\log\left(\frac{n_0+|\vec{n}|}{n_0-|\vec{n}|}\right)\cdot\nabla(|\vec{n}|T)\\ &\quad\left.+5\nabla\log T\cdot\nabla(n_0T)+5\frac{n_0}{T}|\nabla T|^2\right\}dx\\ &\quad-\int_{\mathbb{R}^3}\left\{\log\left(\frac{n_0+|\vec{n}|}{n_0-|\vec{n}|}\right)|\vec{n}|T\left|\nabla\frac{\vec{n}}{|\vec{n}|}\right|^2\right.\\ &\quad\left.+\frac{1}{\tau_{sf}}|\vec{n}|\log\left(\frac{n_0+|\vec{n}|}{n_0-|\vec{n}|}\right)\right\}dx\\ &= I_1+I_2.\end{aligned}$$

The integrals in I_2 correspond, up to the minus sign, the second and third integrals in (120). It remains to show that I_1 corresponds to the first integral in (120), up to the sign. Indeed, since $\log(n_0^2-|\vec{n}|^2)=\log n_+ + \log n_-$ and $\log((n_0+|\vec{n}|)/(n_0-|\vec{n}|))=\log n_+ - \log n_-$, we have

$$\begin{aligned}I_1 &= -\int_{\mathbb{R}^3}\nabla\log(n_0^2-|\vec{n}|^2)\cdot\nabla(n_0T)dx\\ &\quad-\int_{\mathbb{R}^3}\nabla\log\left(\frac{n_0+|\vec{n}|}{n_0-|\vec{n}|}\right)\cdot\nabla(|\vec{n}|T)dx-2\int_{\mathbb{R}^3}\nabla\log T\cdot\nabla(n_0T)dx\\ &= -\int_{\mathbb{R}^3}\big(\nabla\log n_+\cdot\nabla(n_+T)+\nabla\log n_-\cdot\nabla(n_-T)\\ &\quad+\nabla\log T\cdot\nabla(n_+T+n_-T)\big)dx\\ &= -\int_{\mathbb{R}^3}\big(\nabla\log(n_+T)\cdot\nabla(n_+T)+\nabla\log(n_-T)\cdot\nabla(n_-T)\big)dx.\end{aligned}$$

This ends the proof. □

Remark 6. When system (86)-(88) includes the electric field, a computation similar to the proof of Proposition 7 shows that the entropy-production identity reads as

$$\begin{aligned}&\frac{dH}{dt}+\int_{\mathbb{R}^3}\left(\frac{|\nabla(n_+T)+n_+T\nabla V|^2}{n_+T}+\frac{|\nabla(n_-T)+n_-T\nabla V|^2}{n_-T}\right)dx\\ &+10\int_{\mathbb{R}^3}(n_++n_-)|\nabla\sqrt{T}|^2\big)dx\\ &+\frac{1}{2}\int_{\mathbb{R}^3}(n_+-n_-)(\log n_+-\log n_-)\left(\frac{1}{\tau_{sf}}+T\left|\nabla\frac{\vec{n}}{|\vec{n}|}\right|^2\right)dx=0.\end{aligned}$$

Thus, the presence of the electric field complicates the existence of a priori bounds. □

4.6 NUMERICAL EXPERIMENTS

We perform some numerical simulations using the model (89)-(91) with the spin polarization matrix, We consider, as in [36], three- and five-layer structures that consist of alternating nonmagnetic and ferromagnetic layers. Multilayer structures are promising for applications in micro-sensor and high-frequency devices. In this work, they serve to illustrate the solution behavior rather than to model practical devices.

4.6.1 *Numerical scheme*

We solve equations (89)-(91) on the finite interval $[0,1]$ which is divided in m equal subintervals K of length $\triangle x = 1/m$. The finite-volume method is employed and the generic unknown u_K is an approximation of the integral $\int_K u dx$. The difference quotient $Du_{K,\sigma}/(\triangle x) := (u_{K,\sigma} - u_K)/(\triangle x)$ approximates the gradient of u in the subinterval K, where $u_{K,\sigma}$ is the value in the neighboring element K' such that $\overline{K} \cap \overline{K'} = \{\sigma\}$. Then the flux $J_u = -(\nabla(uT) + u\nabla V)$ through the point σ can be approximated by

$$J_{u,K,\sigma} = -\frac{1}{\triangle x}\left(D(uT)_{K,\sigma} + \frac{1}{2}(u_K + u_{K,\sigma})DV_{K,\sigma}\right). \tag{123}$$

Special care has to be taken for the discretization of the Joule heating term $\mathcal{J}_n \cdot \nabla V$. We suggest to approximate it according to [10, 15]

$$\int_K \mathcal{J}_n \cdot \nabla V dx \approx \frac{1}{2\triangle x}\sum_\sigma \triangle x \mathcal{J}_{n,K,\sigma} DV_{K,\sigma},$$

where the sum is (here and in the following) over the two end points of the interval K. The values C_K, $\vec{\Omega}_K$, p_K are given by the integrals of $C(x)$, $\vec{\Omega}(x)$, $p(x)$ over K, respectively, and the values $\vec{\Omega}_\sigma$, p_σ are the arithmetic averages of $\vec{\Omega}$, p in the neighboring subintervals of the intersecting point σ, respectively. Finally, we set $\eta_\sigma = \sqrt{1-p_\sigma^2}$.

The stationary solution is computed as the limit $t_k = k\triangle t \to \infty$ from the implicit Euler finite-volume discretization of (89)-(91). We solve first the Poisson equation for the electric potential V^k with the charge density from the previous time step $k-1$, solve then the moment equations for $(n_0^k, W_0^k, \vec{n}^k)$, and update finally the temperature. Given $(n_{0,K}^{k-1}, \vec{n}_K^{k-1}, T_K^{k-1})$ and $W_{0,K}^{k-1} = \frac{3}{2} n_{0,K}^{k-1} T_K^{k-1}$, the numerical scheme reads as

$$\begin{aligned}
&-\frac{\lambda_D^2}{\triangle x}\sum_\sigma DV_{K,\sigma}^k = \triangle x(n_{0,K}^{k-1} - C_K),\\
&\frac{\triangle x}{\triangle t}(n_{0,K}^k - n_{0,K}^{k-1}) + \sum_\sigma \mathcal{J}_{n,K,\sigma}^k = 0,\\
&\frac{\triangle x}{\triangle t}(W_{0,K}^k - W_{0,K}^{k-1}) + \sum_\sigma \mathcal{J}_{W,K,\sigma}^k + \frac{1}{2\triangle x}\sum_\sigma \triangle x \mathcal{J}_{n,K,\sigma}^k DV_{K,\sigma}^k = 0,\\
&\frac{\triangle x}{\triangle t}(\vec{n}_K^k - \vec{n}_K^{k-1}) + \sum_\sigma \vec{\mathcal{J}}_{K,\sigma}^k + \gamma\triangle x(\vec{\Omega}_K \times \vec{n}_K^k) = -\frac{\triangle x}{\tau_{sf}}\vec{n}_K^k,\\
&T_K^k = \frac{2}{3}\frac{W_{0,K}^k}{n_{0,K}^k},
\end{aligned}$$

and the discrete fluxes are defined by

$$\begin{aligned}
\mathcal{J}_{n,K,\sigma}^k &= -D_0\eta_\sigma^{-2}(J_{n,K,\sigma}^k - p_\sigma\vec{\Omega}_\sigma \cdot \vec{J}_{n,K,\sigma}^k),\\
\mathcal{J}_{W,K,\sigma}^k &= -\frac{5}{3}D_0\eta_\sigma^{-2}(J_{W,K,\sigma}^k - p\vec{\Omega}_\sigma \cdot \vec{J}_{W,K,\sigma}),\\
\vec{\mathcal{J}}_{K,\sigma}^k &= -D_0\eta_\sigma^{-2}(-p_\sigma\vec{\Omega}_\sigma J_{n,K,\sigma}^k + (1-\eta_\sigma)\vec{\Omega}_\sigma \otimes \vec{\Omega}_\sigma \cdot \vec{J}_{n,K,\sigma}^k\\
&\quad + \eta_\sigma \vec{J}_{n,k,\sigma}^k),
\end{aligned}$$

and the fluxes $J_{n,K,\sigma}^k$, $\mathcal{J}_{W,K,\sigma}^k$, and $\vec{J}_{K,\sigma}^k$ are discretized according to (123) with the exception that the temperature and the densities in the drift term are explicit, i.e.

$$J_{u,K,\sigma}^k = -\frac{1}{\triangle x}\left(D(u^k T^{k-1})_{K,\sigma} + \frac{1}{2}(u_K^{k-1} + u_{K,\sigma}^{k-1})DV_{K,\sigma}^k\right).$$

Note that we have introduced the scaled diffusion coefficient D_0 and the parameter γ, which come from the scaling of the equations. The values are $D_0 \approx 6.9 \cdot 10^{-4}$ and $\gamma = 4$. The scaled Debye length equals $\lambda_D \approx 1.2 \cdot 10^{-4}$. We have chosen the (scaled) boundary conditions $n_0 = 1$, $\vec{n} = 0$, and $V = V_D$ at $x = 0, 1$ with $V_D(0) = 0$ and $V_D(1) = U/U_T$. Here, $U_T = 0.026\,V$ is the thermal voltage at room temperature.

The discrete linear system is solved for each time step k until the maximum norm of the difference between two consecutive solutions is smaller than a predefined threshold ($10^{-8} \dots 10^{-10}$). This solution is considered as a steady state. The numerical parameters are $\triangle x = 0.003$, $\triangle t = 5 \cdot 10^{-4} \dots 10^{-3}$, and the (unscaled) physical parameters are $D = 10^{-3}\,m^2 s^{-1}$ (diffusion coefficient), $\tau_{sf} = 10^{-12}\,s$, and $U = -1\,V$ (applied bias).

4.6.2 *Three-layer structure*

As the first numerical experiment, we consider a three-layer structure which consists of a nonmagnetic layer sandwiched between two ferromagnetic layers; see Figure 16. This structure may be regarded as a diode with ferromagnetic source and drain regions. The length of the diode is $L = 1.2\,\mu m$, the ferromagnetic layers have length $\ell = 0.2\,\mu m$, and the doping concentrations are $C = 10^{23}\,m^{-3}$ in the highly doped regions and $C = 4 \cdot 10^{20}\,m^{-3}$ in the lowly doped region.

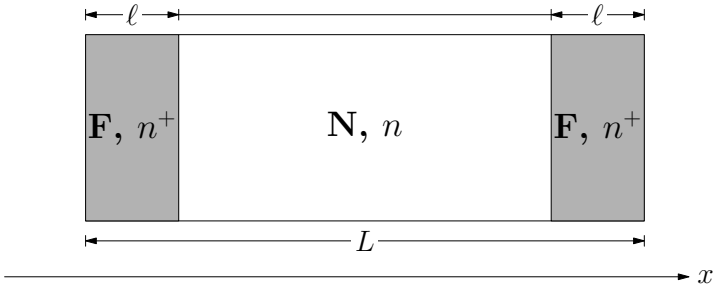

Figure 16: Geometry of the three-layer structure with ferromagnetic (**F**) highly doped (n^+) source and drain regions and nonmagnetic (**N**) lowly doped (n) channel region.

The local magnetization in the side regions is aligned with the z-axis (orthogonal to the diode), $\vec{\Omega}(x) = (0, 0, 1)^\top$ for $x \in [0, \ell] \cup [L - \ell, L]$ and $\vec{\Omega}(x) = 0$ else. The polarization in the ferromagnetic regions equals $p = 0.66$.

Figure 17 and Figure 18 show the stationary charge density n_0 and the spin density $\vec{n} = (0, 0, n_3)$ respectively, compared with the solution to the corresponding spinorial drift-diffusion model (with constant temperature). As expected, the charge densities are similar with some small differences close to the junction of the drain region. The spin component n_3 exhibits some peaks around the junctions which can be explained by the discontinuity of $p(x)$ (and hence $\eta(x)$) at the junctions [36, Sec. 8.1], [45]. The peaks are smaller in the energy-transport model which may be due to thermal diffusion.

The temperature for different values of the polarization p is illustrated in Figure 19. The case $p = 0$ corresponds to a nonmagnetic diode. The temperature maximum increases with p but the temperature decreases with p in the drain region. Possibly, higher values of p lead to stronger heat fluxes increasing the temperature in the channel region.

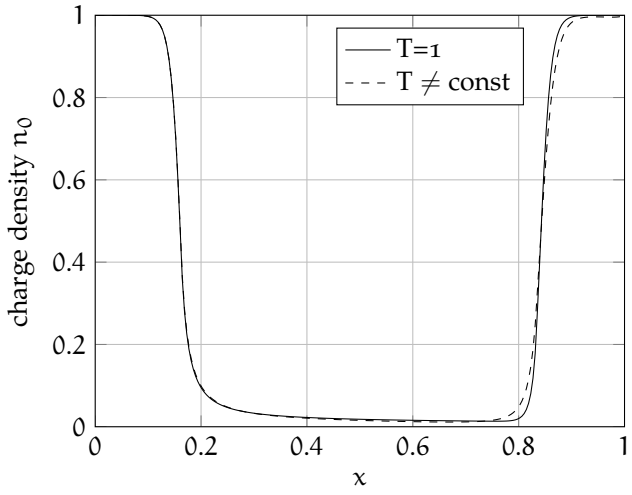

Figure 17: Charge density n_0 in the three-layer structure computed from the spin energy-transport model ($T \neq$ const.) and from the corresponding spin drift-diffusion model ($T = 1$).

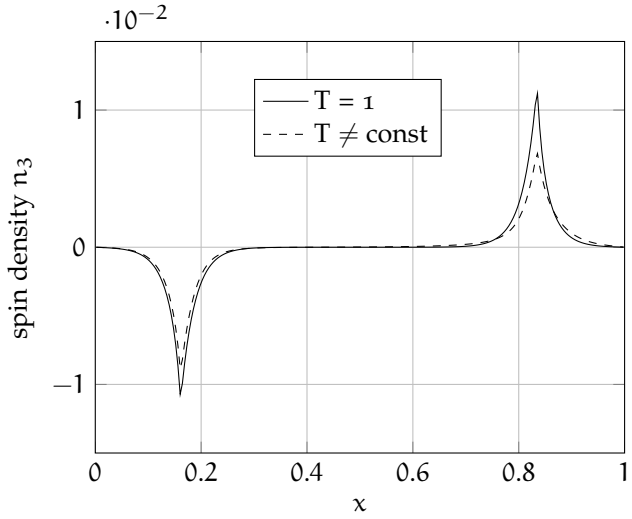

Figure 18: Spin density n_3 in the three-layer structure computed from the spin energy-transport model ($T \neq$ const.) and from the corresponding spin drift-diffusion model ($T = 1$).

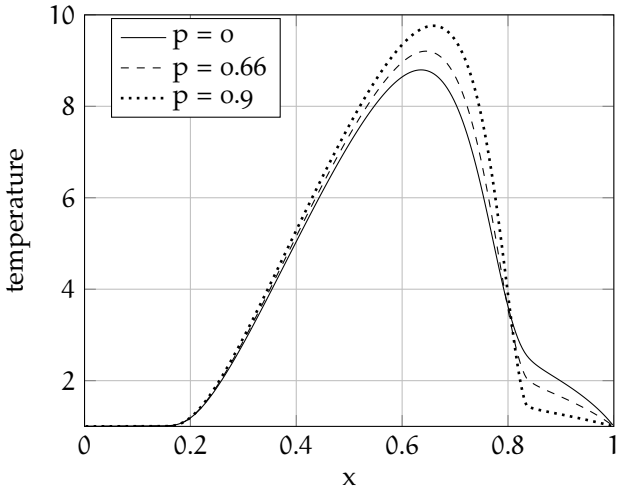

Figure 19: Temperature in the three-layer structure for various polarizations p.

4.6.3 *Five-layer structure*

The five-lyer structure is composed of two ferromagnetic layers sandwiched between two nonmagnetic layers and separated by a thin nonmagnetic layer in the middle of the structure; see Figure 20. The choice of the lengths L and ℓ and of the doping concentrations is as in Subsection 4.6.2. The middle region has the thickness $d = L/21 \approx 60\,\mathrm{nm}$. Again we take $p = 0.66$. The local magnetization is different in the two layers: $\vec{\Omega}(x) = (0,0,1)^\top$ for $x \in [L/6, 10L/21]$, $\vec{\Omega}(x) = (0,1,0)^\top$ for $x \in [11L/21, 5L/6]$, and $\vec{\Omega}(x) = 0$ else.

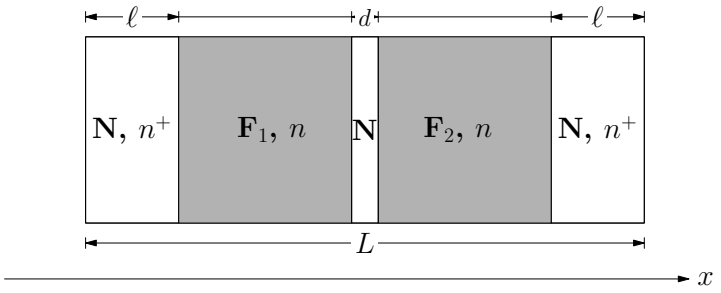

Figure 20: Geometry of the five-layer structure with ferromagnetic ($\mathbf{F}_1$, $\mathbf{F}_2$) lowly doped (n) regions and nonmagnetic ($\mathbf{N}$) regions. The source and drain regions are highly doped (n^*), while the middle region is lowly doped.

The effect of the temperature is now stronger than in the three-layer structure. The charge density n_0 is presented in Figure 21. The interplay of the charge and spin densities in the nonmagnetic middle region causes a small hump in n_0 and a more significant increase before the drain junction, compared to Figure 17. The hump is larger when the electric potential is a linear function and the temperature is constant; see Figure 3 in [36].

In contrast to the three-layer structure, all components of the spin vector density are nonzero. However, the component n_1 is relatively small. We present the remaining components n_2 and n_3 in Figure 22. The temperature causes a significant smoothing of the peaks between the magnetic/nonmagnetic junctions.

Figure 23 shows the comparison of the temperature distributions for different values of the polarization p. The temperature maximum decreases

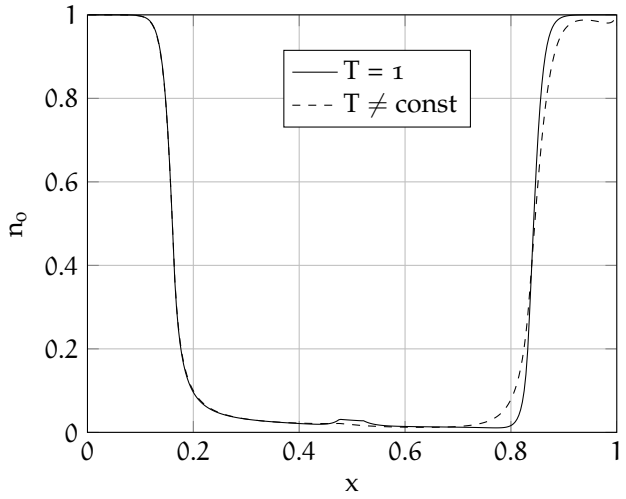

Figure 21: Charge density n_0 in the five-layer structure.

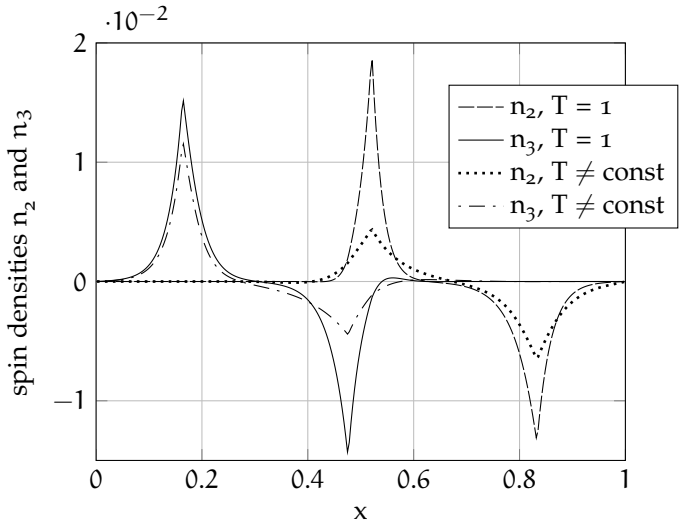

Figure 22: Spin density components n_2 and n_3 in the five-layer structure computed from the spin energy-transport model (T ≠ const.) and from the corresponding spin drift-diffusion model (T = 1).

with p, opposite to the situation in the three-layer structure. We observe that the polarization strongly influences the temperature. When $p = 0$, we obtain the same curve as in Figure 19 since this describes the same nonmagnetic diode.

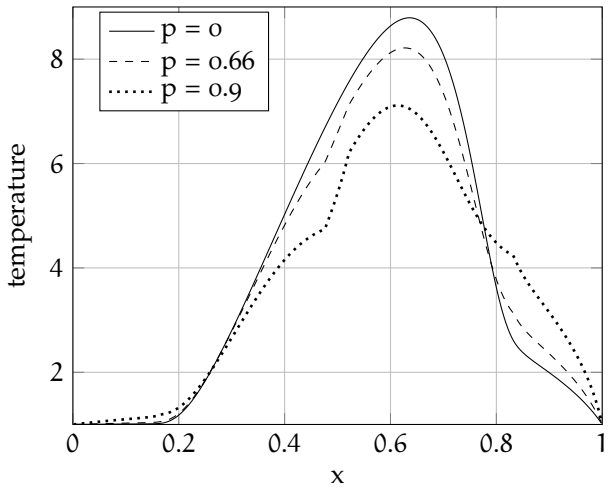

Figure 23: Temperature T in the five-layer structure for various polarizations p.

Part IV

OUTLINE & OUTLOOK

This study complements the existing research on macroscopic spinorial models. The spinorial drift-diffusion and energy-transport models are investigated in this work. The second model is the extension of the first one. Both of them describe charge and spin currents in semiconductor. The second one additionally considers the transport of energy. Both models are nonlinear and fully coupled. Thus, the level of complexity of the models is relatively high. To accomplish the analysis some assumptions on the physical parameters are necessary (e.g. constant magnitization, or diffusion coefficient). The main results of the study are the proofs of existence of bounded solutions (both continuous and discrete) for the drift-diffusion model and the derivation of the spinorial energy-transport model, as well as entropy inequalities for both systems. A part of the work is devoted to implementation of numerical solutions of the systems, which is not trivial by so complicated models.

One of the big further steps of the study could be an inclusion of the Landau-Lifshitz-Gilbert equation (LLG) to obtain a wider framework describing spin effects in semiconductors with self-consistently given magnetization. That could be especially interesting for modelling of realistic devices exploiting ferromagnetic semiconductors. The other option could be the consideration of the spin-orbit coupling. In this study we neglect it to simplify the models. Though, the thorough modelling of spin-orbit interaction could significantly help the investigation of the spin transistor.

[1] N. Ben Abdallah and P. Degond. "On a hierarchy of macroscopic models for semiconductors." In: *J. Math. Phys.* 37 (1996), pp. 3308–3333.

[2] N. Ben Abdallah, P. Degond, and S. Génieys. "An energy-transport model for semiconductors derived from the Boltzmann equation." In: *J. Stat. Phys.* 84 (1996), pp. 205–231.

[3] N. Ben Abdallah and R. El Hajj. *On hierarchy of macroscopic models for semiconductor spintronics*.

[4] C. Abert, M. Ruggeri, F. Bruckner, C. Vogler, D. Praetorius G. Hrkac, and D. Suess. *A three-dimensional spin-diffusion model for micromagnetics*.

[5] C. Abert, G. Hrkac, M. Page, D. Praetorius, M. Ruggeri, and D. Suess. "Spin-polarized transport in ferromagnetic multilayers: An unconditionally convergent FEM integrator." In: *Computers Math. Appl.* 68 (2014), pp. 639–654.

[6] S. Bandyopadhyay and M. Cahay. "Reexamination of some spintronic field-effect device concepts." In: *Appl. Phys. Lett.* 85 (2004), pp. 1433–1435.

[7] L. Barletti and F. Méhats. "Quantum drift-diffusion modeling of spin transport in nanostructures." In: *J. Math. Phys.* 51 (2010), 053304, 20 pp.

[8] M. Bessemoulin-Chatard, C. Chainais-Hillairet, and M.-H. Vignal. "Study of a finite volume scheme for the drift-diffusion system. Asymptotic behavior in the quasi-neutral regime." In: *SIAM J. Numer. Anal.* 52-4 (2014), pp. 1666–1691.

[9] A. Bournel, V. Delmouly, P. Dollfus, G. Tremblay, and P. Hesto. "Theoretical and experimental considerations on the spin field effect transistor." In: *Physica E* 10 (2001), pp. 86–90.

[10] C. Chainais-Hillairet. "Discrete duality finite volume schemes for two dimensional drift-diffusion and energy-transport models." In: *Int. J. Numer. Meth. Fluids* 59 (2009), pp. 239–257.

[11] M. Chatard. "Asymptotic behavior of the Scharfetter-Gummel scheme for the drift-diffusion model." In: *Springer Proc. Math.* 4 (2011). Proceedings of the conference "Finite Volumes for Complex Applications. VI. Problems and Perspectives", pp. 235–243.

[12] D. Chen, E. Kan, U. Ravaioli, C. Shu, and R. Dutton. "An improved energy transport model including nonparabolicity and non-Maxwellian distribution effects." In: *IEEE Electr. Device Letters* 13 (1992), pp. 26–28.

[13] L. Chen and L. Hsiao. "The solution of Lyumkis energy transport model in semiconductor science." In: *Math. Meth. Appl. Sci.* 26 (2003), pp. 1421–1433.

[14] S. Datta and B. Das. "Electronic analog of the electrooptic modulator." In: *Appl. Phys. Lett.* 56 (1990), pp. 665–667.

[15] K. Domelevo and P. Omnés. "A finite volume method for the Laplace equation on almost arbitrary two-dimensionalgrids." In: *Math. Model. Num. Analysis* 39 (2005), pp. 1203–1249.

[16] M. I. Dyakonov, ed. *Spin Physics in Semiconductors*. Berlin: Springer-Verlag, 2008.

[17] L. C. Evans. *Partial differential equations*. Graduate Studies in Mathematics, Vol. 19. Providence, R.I: American Math. Society, 2010.

[18] R. Eymard, T. Gallouët, and R. Herbin. *Finite volume methods*. Ed. by P. G. Ciarlet and J. L. Lions. North-Holland.

[19] J. Fabian, A. Matos-Abiague, C. Ertler, P. Stano, and I. Žutić. "Semiconductor spintronics." In: *Acta Phys. Slovava* 57 (2007), pp. 565–907.

[20] D. Fedorov, P. Zahn, M. Gradhand, and I. Mertig. "First-principles calculations of spin relaxation times of conduction electrons in Cu with nonmagnetic impurities." In: *Phys. Rev. B* 77 (2008), 092406, 4 pp.

[21] H. Gajewski and K. Gärtner. "On the discretization of van Roosbroeck's equations with magnetic field." In: *Z. Angew. Math. Mech.* 76 (1996), pp. 247–264.

[22] H. Gajewski and K. Gröger. "On the basic equations for carrier transport in semiconductors." In: *J. Math. Anal. Appl.* 113 (1986), pp. 12–35.

[23] K. Gärtner and A. Glitzky. "Existence of bounded steady state solutions to spin-polarized drift-diffusion systems." In: *SIAM J. Math. Anal.* 41 (2010), pp. 2489–2513.

[24] D. Gilbarg and N. S. Trudinger. *Elliptic Partial Differential Equations of Second Order*. Grundlehren der Mathematischen Wissenschaften, Vol. 224. Berlin: Springer-Verlag, 1983.

[25] A. Glitzky. "Analysis of a spin-polarized drift-diffusion model." In: *Adv. Math. Sci. Appl.* 18 (2008), pp. 401–427.

[26] A. Glitzky. "Uniform exponential decay of the free energy for Voronoi finite volume discretized reaction-diffusion systems." In: *Math. Nachr.* 284 (2011), pp. 2159–2174.

[27] R. El Hajj. "Diffusion models for spin transport derived from the spinor Boltzmann equation." In: *Commun. Math. Sci.* 12 (2014), pp. 565–592.

[28] R. El Hajj. *Etude mathématique et numérique de modèles de transport: application à la spintronique*. France: PhD thesis, Université Paul Sabatier, 2008.

[29] S. Holst, A. Jüngel, and P. Pietra. "An adaptive mixed scheme for energy-transport simulations of field-effect transistors." In: *SIAM J. Sci. Comp.* 25 (2004), pp. 1698–1716.

[30] A.M. Il'in. "A difference scheme for a differential equation with a small parameter affecting the highest derivative." In: *Mat. Zametki* 6 (1969). (in Russian), pp. 237–248.

[31] J. Jerome. *Analysis of Charge Transport. A Mathematical Study of Semiconductor Devices*. Berlin: Springer, 1996.

[32] A. Jüngel. *Transport Equations for Semiconductors*. Lecture Notes in Physics 773. Berlin: Springer, 2009.

[33] L. D. Landau and E. M. Lifshitz. *Quantum mechanics: Non-relativistic theory. Vol. 3*. Course of theoretical physics. U.K.: Pergamon press, 1977.

[34] T. Low, M. Lundstrom, and D. Nikonov. "Modeling of spin metal-oxide-semiconductor field-effect transistor: A nonequilibrium Green's function approach with spin relaxation." In: *J. Appl. Phys.* 104 (2008), 094511, 10 pp.

[35] Y. Pershin, S. Saikin, and V. Privman. "Semiclassical transport models for semiconductor spintronics." In: *Electrochem. Soc. Proc.* 2004-13 (2005), pp. 183–205.

[36] S. Possanner and C. Negulescu. "Diffusion limit of a generalized matrix Boltzmann equation for spin-polarized transport." In: *Kinetic Related Models* 4 (2011), pp. 1159–1191.

[37] F. Poupaud. "Diffusion approximation of the linear semiconductor Boltzmann equation: analysis of boundary layers." In: *Asympt. Anal.* 4 (1991), pp. 293–317.

[38] M. Ruggeri, C. Abert, G. Hrkac, D. Süss, and D. Praetorius. "Coupling of dynamical micromagnetism and a stationary spin drift-diffusion equation: A step towards a fully self-consistent spintronics framework." In: *Physica B: Condensed Matter* 486 (2016), pp. 88 –91.

[39] S. Saikin. "A drift-diffusion model for spin-polarized transport in a two-dimensional non-degenerate electron gas controlled by spin–orbit interaction." In: *J. of Phys.: Condensed Matter* 16 (2004), 5071–5081.

[40] D.I. Scharfetter and H.K. Gummel. "Large-signal analysis of a silicon Read diode oscillator." In: *IEEE Trans. Electron Dev.* ED-16 (1969), pp. 64–77.

[41] S. Selberherr. *Analysis and Simulation of Semiconductor Devices*. Vienna: Springer, 1984.

[42] H. Spohn. "Entropy production for quantum dynamical semigroups." In: *J. Math. Phys.* 19 (1978), pp. 1227–1230.

[43] S. Sugahara and M. Tanaka. "A spin metal-oxide-semiconductor field-effect transistor using half-metallic-ferromagnet contacts for the source and drain." In: *Appl. Phys. Lett.* 84 (2004), pp. 2307–2309.

[44] G. Troianiello. *Elliptic Differential Equations and Obstacle Problems*. New York: Plenum Press, 1987.

[45] T. Valet and A. Fert. "Theory of the perpendicular magnetoresistance in magnetic multilayers." In: *Phys. Rev. B* 48 (1993), pp. 7099–7113.

[46] N. Zamponi. "Analysis of a drift-diffusion model with velocity saturation for spin-polarized transport in semiconductors." In: *J. Math. Anal. Appl.* 420 (2014), pp. 1167–1181.

[47] N. Zamponi and A. Jüngel. "Two spinorial drift-diffusion models for quantum electron transport in graphene." In: *Commun. Math. Sci.* 11 (2013), pp. 927–950.

[48] E. Zeidler. *Nonlinear Functional Analysis and its Applications*. Vol. Vol. II/A. New York: Springer, 1990.

[49] I. Žutić, J. Fabian, and S. Das Sarma. "Spin-polarized transport in inhomogeneous magnetic semiconductors: theory of magnetic/nonmagnetic p-n junctions." In: *Phys. Rev. Lett.* 88 (2002), 066603, 4 pp.

[50] I. Žutić, J. Fabian, and S. Das Sarma. "Spintronics: Fundamentals and applications." In: *Rev. Modern Phys.* 76 (2004), pp. 323–410.